RESPONSE OF RETINAL GANGLION CELLS TO STRETCH INJURY IN THE OPTIC NERVE OF THE ADULT GUINEA PIG

By

MD. NAZRUL ISLAM, M.B.B.S.: M. Phil.

Thesis submitted in candidature for the degree of Master of Science (Medical Science) in the Faculty of Medicine, University of Glasgow.

Department of Anatomy
University of Glasgow

August, 1992

ProQuest LLC.
789 East Eisenhower Parkway
P.O. Box 1346
Ann Arbor, MI 48106 – 1346

بِسْمِ اللّٰهِ الرَّحْمٰنِ الرَّحِيْمِ

IN THE NAME OF ALLAH

THE MOST BENEFICENT AND MERCIFUL

DEDICATION

This thesis is dedicated to the memory of my parents.

Md. Abdur Rahman
Shabida Khatoon
(late)

ACKNOWLEDGEMENT

I am grateful to Dr A.P. Payne, Acting Head of Anatomy Department for allowing me to carry out this research in the Department and for his constant encouragement. I would also like to thank Dr Payne for his considerable assistance in the statistical analyses.

I am thankful to my supervisor, Dr W.L. Maxwell, for his keen interest, patience, support, guidance and constructive criticism throughout the period of my research.

I thank all the technical staff for their help and assistance. In particular, I am indebted to Mr O. Reid, Mr R. Kerr, Mr J. McGadey and Mrs C. Watt for their valuable assistance with TEM and SEM; Mr A. Lockhart for histological work; Ms. M. Hughes and Mrs C. Crossan for their help in photographic and artistic work. Thanks are due to Mrs L. Peedle for taking pains in typing the thesis.

Finally, I thank Dr N. Latif and Dr A. Taher for their wonderful companionship throughout the period of study.

Special thanks to my wife Umme-Kulsum and my children Nasrina Parvin, Mussan-na Akhtar and Najmus Shakib for their patience, love and moral support.

I am grateful to Professor L E Thibault, Department of Bio-Engineering, University of Pennsylvania, Philadelphia, U.S.A. for the construction of the stretch injury apparatus provided in a Head Injury Grant from the National Institutes of Health held jointly by the

Universities of Pennsylvania and Glasgow. All animal procedures conformed to current United States Public Health Service standards and were approved by (1) the University of Pennsylvania Institutional Animal Care and Use Committee and (2) the Home Office.

I am grateful to the World Health Organization (WHO) for granting me this scholarship and the Government of Bangladesh for allowing me to proceed to my research on deputation.

Dr MD. Nazrul Islam

CONTENTS

ABSTRACT

An established model for axonal injury in the optic nerve of the adult guinea pig (Gennarelli et al., 1989) has allowed analysis of the response of the ganglion cell to stretch injury. Six adult guinea pigs, two in each survival group, were killed at 3, 7 and 14 days after stretch injury. Retinas were processed for light microscopy and transmission/scanning electron microscopy. A morphometric study was carried out on the TEM micrographs. Retinas from the left eye were used as control material.

Central chromatolysis occurs in about one third of the ganglion cells three days after injury. The majority of the injured ganglion cells demonstrate degenerative changes at seven days after injury. At 14 days after injury, severely degenerative and dying ganglion cells are noted. These cells have grossly mis-shapen nuclei, disappearance of cytoplasmic organelles and the occurrence of dense bodies in their cytoplasm, with focal aggregation of chromatin in the nuclei. These changes are indicative of necrobiosis of these cells. Small ganglion cells do not demonstrate any morphological changes.

However, at 7 and 14 days after injury, a noble and exciting morphological change indicative of a regenerative response occurs in a few ganglion cells. These morphological changes are the assumption of an irregular

nuclear profile, enlarged vacuolated nucleolus and, in addition, the occurrence of discrete Nissl bodies in the cytoplasm. These changes are comparable to those documented in regenerative neurons of the facial and hypoglossal nuclei (Jones & Lavelle, 1986; Hall & Borke, 1988) after axotomy.

Proliferation of Müller cell and astrocyte processes and microglial cells is found at 7 and 14 days after stretch injury. Phagocytic activity of the microglial cells is noted.

After comparative study it can be concluded that the time course of chromatolysis is longer in stretch injury than in either crush or transection of the optic nerve. That the level of injury is less severe than in the latter two models of axonal injury, and that this lesser injury allows the demonstration of an attempted regenerative response by a number of retinal ganglion cells.

INTRODUCTION

Axonal damage has now been identified as a primary response of neurons in models of diffuse brain injury and traumatic injury to the head in human beings (Adams et al., 1982a, 1982b); Barron, 1982; Gennarelli et al., 1982; Povlishock et al., 1983; Povlishock, 1986; Erb and Povlishock, 1988; Maxwell et al., 1991a). Axonal damage is manifested as the diffuse formation of axonal swellings, within two to six hours after injury (Maxwell et al., 1991a), scattered throughout the neuraxis in multiple foci. Later, Wallerian degeneration occurs in the distal part of the axons and abortive growth regeneration in the proximal part (Povlishock, 1986).

Both in mild (Povlishock et al., 1983) and severe (Erb and Povlishock, 1988) injury to the brain, documented swelling of the axons has been described one hour after injury (Povlishock, 1983). This axonal perturbation leads to secondary axotomy which first occurs 6-12 hours after mild traumatic injury (Povlishock et al., 1983). Whereas in severe injury to the brain, the time course for axonal separation following the formation of reactive swellings (Povlishock, 1983) is reduced to 2 to 4 hours (Erb & Povlishock, 1988).

Maxwell et al. (1991a) demonstrated that the initial site of axonal damage in stretch injury to the optic nerve is the node of Ranvier. Formation of nodal blebs 15 mins after axonal injury, loss of subaxolemma density, aggregation of vesicular profiles within the nodal blebs

secondary axotomy within 24-72 hours after primary insult (Maxwell et al., 1991a).

The whole brain presents several limitations in study of the neuronal response to axonal injury to the CNS. In the brain, it is very difficult to precisely determine the origin, direction of travel and terminations of axons that have been injured. The optic nerve provides a convenient model to study responses to central (intrinsic) axonal injury since the optic nerve is an accessible and isolated bundle of central, myelinated nerve fibres.

RETINA:

The visual system consists of the retina, optic nerves, optic chiasma, optic tracts, lateral geniculate bodies, geniculo-calcarine radiations and visual cortex. The retina and optic nerve are derivatives of the forebrain. Consequently, their morphology and physiology are very much like that of the brain. The retina is connected to the brain by the optic nerve through the optic chiasma and optic tracts.

The retina was named by Rujos of Ephesus (110 AD) because of its functional appearance as a net to hold the vitreous humor. The retina is a very thin, delicate transparent tissue which lines the inner eye and is attached to the choroid through its pigment epithelium. The thickness of the human retina is 0.18 mm at the equator, 0.10 mm at the ora-serrata and 0.56 mm near the optic disc (Hogan et al., 1971). The optic disc lies nasal

to the posterior pole of the retina. The central posterior part of the retina is termed the area centralis. A nasotemporal band within the retina having a particularly high density of ganglion cells is known as the visual streak (Provis, 1979).

The visual streak of the guinea pig lies inferior to the optic disc (Choudhury, 1978) whereas, in the retina of the cat (Felis domesticus) the visual streak lies within the area centralis (Provis, 1979).

BLOOD SUPPLY OF THE RETINA:

The retina is unique in having the highest oxygen consumption per unit weight of any tissue. In the human being, the outer third of the retina is nourished by the choroidal circulation, the inner two thirds receives nutrition from the retinal circulation and a small amount probably receives from the vitreous in the human retina (Hogan et al., 1971).

In the guinea pig, the central part of the retina close to the optic disc is vascularized whereas the peripheral part is non-vascularized (Schnitzer, 1988).

RETINAL LAYERS:

The retina consists of ten well defined layers (Barr & Kiernan, 1988). These are (from external to internal: Figures 2,3).

1) Pigment epithelium layer
2) Rod and cone layer

3) Outer limiting membrane
4) Outer nuclear layer
5) Outer plexiform layer
6) Inner nuclear layer
7) Inner plexiform layer
8) Ganglion cell layer
9) Nerve fibre layer and
10) Inner limiting membrane.

The rods and cones are the sensory receptors. There are three neurons in the visual pathway. The first of these neurons is the bipolar cell, the cell body of which lies in the inner nuclear layer. The second neuron is the ganglion cell of the ganglion cell layer. The third neuron extends from the lateral geniculate body to the visual cortex. The axons of the ganglion cells form the nerve fibre layer of the retina, optic nerve, optic chiasma and optic tracts.

THE GANGLION CELL LAYER:

The ganglion cell layer consists of ganglion cells, neuroglial cells and glial processes. This retinal layer is situated external to the nerve fibre layer and internal to the inner plexiform layer. Throughout most of the retina ganglion cells form a layer one cell thick, but on the temporal side of the disc, they form a double layer of cells in the retina of the human being (Hogan et al., 1971). In the macular region the cells increase to eight to ten layers.

There are various types of ganglion cells. Variations among the ganglion cells are based on somal size, degree of arborization and spread of their dendritic processes into the bipolar synaptic field

CLASSIFICATIONS OF THE GANGLION CELLS:

Different authors have classified the ganglion cells of the retina in different ways depending on either the dendritic arborization (Boycott and Dowling, 1969), dendritic field size and diameter (Boycott and Wassle, 1974) or cell diameters (Hughes, 1975). Boycott and Wassle (1974) classified the ganglion cells of the cat retina into α (23-38μm), β (11-29μm) and γ (8-18μm) nodal mode, depending on dendritic field sizes and diameters. Hughes (1975) classified them by their diameters into large (more than 20 μm), medium (12-20 μm) and small sized (7-12 μm) ganglion cells.

According to Hughes (1981) the percentage distribution of the different ganglion cell types in the cat's retina is 4% (α nodal mode), 39% (β nodal mode) and 57% (γ nodal mode).

However, the classification of the ganglion cell based on cellular diameter or sizes (Boycott & Wassle, 1974; Stone & Fukada, 1974; Hughes, 1975) are not suitable criteria in the study of the injured ganglion cells since there is a possibility that degeneration and atrophy of injured cells results in their being classified as cells from within lower size groups.

Boycott and Dowling (1969) classified the ganglion cells on the basis of silver impregnation staining. It is not possible by TEM to differentiate the different types of ganglion cells that can be seen with the light microscope by silver impregnation.

Barron et al. (1986) studied the response of the retinal ganglion cell of the rat to crush injury of the optic nerve. They classified the ganglion cells of the retina in a straightforward manner into either ganglion cells (90%) or small neurons (10%) on qualitative evidence of the cells.

The small neurons have a thin rim of cytoplasm around the round or oval nucleus. The nucleoli are small. Their cytoplasm is relatively electron dense and contains only a very few organelles.

The ganglion cells are larger. The nucleus is about half of the cell size. It has a prominent nucleolus. The cytoplasm contains abundant Nissl substances and other organelles. The larger ganglion cells have a large nucleus and abundant cytoplasmic organelles. These can easily be differentiated from the small neurons in which the nucleus is surrounded by a thin rim of cytoplasm containing few organelles.

In this study I therefore decided to use the classification of the ganglion cells of the retina developed by Barron et al (1986).

STRUCTURAL CHARACTERISTICS OF RETINAL GANGLION CELLS:

The retinal ganglion cells are multipolar and vary in size and shape. The cells are rounded, elongated or polygonal in shape. The nucleus is round or oval and quite large. It takes up half or more of the cell volume and is usually eccentric in position in the majority of cells. The nucleus contains a single prominent nucleolus but occasionally two may be present. They have an abundant cytoplasm. The cytoplasm contains cluster-like aggregates of many short, randomly oriented cisternae of rough ER.

Under the light microscope, these clusters are visualized as the Nissl substances. The Nissl substances may be more abundant in the peripheral cytoplasm, but can be distributed throughout the cytoplasm. Ultrastructurally, free ribosomes are also numerous in the cytoplasm which contains much smooth ER as well. The prominent Golgi-apparatus lies near the nucleus and mitochondria are scattered throughout the cytoplasm. It also contains high concentrations of neurofilaments. The cytoplasmic face of the nucleus is mildly scalloped. (Provis, 1979).

NUCLEOLUS: (Review: Goessens, 1984)

The nucleus of the retinal ganglion cell bears a prominent nucleolus. The nucleolus consists of a fibrillar component, the fibrillar centres, a granular component, the nucleolar interstices (vacuoles), the nucleolar associated chromatin and nucleolar matrix.

The fibrillar component:

The fibrillar component forms the electron-opaque reticular structure of the nucleolus, termed as nucleolonemal strands. These dense fibrillar components contain RNA and DNA.

Fibrillar centres:

The lighter fibrous material which often appears as small spheres surrounded by and intimately associated with the fibrillar components. This electron-lucent material enclosed by the fibrillar component is now generally termed the fibrillar centres. The fibrillar centres are composed of protein and a small amount of DNA.

The granular component:

The granular component is formed of loosely packed granules approximately 15 nm in diameter which closely resemble cytoplasmic ribosomes. They are situated around the fibrillar component or along and between the strands of fibrillar components. Sometimes there is an accumulation of the granular material forming the intranucleolar body (INB). The granules are composed of ribonucleoprotein.

The nucleolar interstices:

Nucleoli frequently contain more or less spherical light areas of lower density than the nucleolar surrounding mass. They have been referred to as nucleolar interstices. The nucleolar interstices play a role in the storage and transportation of ribosomal precursors.

The nucleolar associated chromatin:

The body of the nucleolus is surrounded by a layer of condensed chromatin of variable thickness. Cytochemical analysis has demonstrated the presence of DNA in the nucleolar associated chromatin (Goessens, 1984).

Nucleolar matrix:

In addition to the above mentioned nucleolar component there is also a residual fibrillar meshwork. This residual nucleolar structure retaining the size and shape of the original nucleolus is called the nucleolar matrix. The fibrillar meshwork of the nucleolus is made of an insoluble protein structure representing a skeletal meshwork specific to the nucleolus (Scheer et al., 1982).

DISPLACED AMACRINE CELLS IN THE GANGLION CELL LAYER:

The amacrine cells are present in the inner nuclear layer of the retina. Some cells of the ganglionic layer have the structural appearance of amacrine cells of the inner nuclear layer. These cells of the ganglionic layer are called displaced amacrine cells. Cajal gave the amacrine cell its name because he believed that it did not have an axon. Although generally considered to be axonless, there are documented examples of amacrine cells with an axon (Catsicas et al., 1987; Dacey, 1989).

Earlier studies of the ganglion cell layer of the rat retina have demonstrated that there is a population of small neurons which survive optic nerve section and do not label with HRP following injection into the subcortical visual centres or the optic nerve. (Bunt et al., 1974;

Cowey & Perry, 1979; Perry, 1981). Now, it is established that 38%, 50% and 80% respectively, of all neuronal profiles in the ganglion cell layers of rabbit (Hughes, 1985), rat (Perry, 1981) and cat (Wong & Hughes, 1987) are displaced amacrine cells.

HRP injected into either the superior colliculus or optic nerve fills two thirds of the neurons in the γ nodal mode ganglion cells of the retina of the cat (Hughes, 1981). Those cells of the γ-mode which are unlabelled by HRP are displaced amacrine cells (Hughes, 1981). It is concluded that γ-nodal mode profiles of the ganglionic cells of the retina includes the displaced amacrine cells (Hughes, 1981).

MORPHOLOGY OF THE DISPLACED AMACRINE CELLS:

Amacrine cells of the ganglionic layer are of small size, 8-10 μm in diameter. The cell body is flask-shaped. The great majority of the cells possess an eccentric, cup-shaped nucleus. The nucleoplasm is often penetrated by long invaginations of the nuclear wall originating at the boundary of the cytoplasmic cup (Hughes & Vaney, 1980; Vaney et al., 1981). These processes are filled with dark cytoplasm and appear in many cells to point towards the nucleolus (Vaney et al., 1981). The cytoplasm of these neurons is well provided with basophilic Nissl granules.

NEUROGLIA OF THE RETINA:

The neuroglia of the retina form two major groups:

macroglia and microglia. In the retina the macroglia consist of astrocytes and Müller cells. The neuroglia, except for the microglia, differentiate from glioblasts of the neuroectoderm. Microglia may be derived from mesoderm (Schnitzer, 1989).

Microglia:

The microglia are small, densely staining cells with rounded nucleus which contains prominent clumps of hetrochromatin. It has a thin rim of cytoplasm around the nucleus. The cytoplasm of the microglia contains lysosomes lipofuscin granules, Golgi-apparatus, mitochondria and long narrow cisternae of rough surfaced endoplasmic reticulum (Kohno et al., 1982). Microglia cells are found in the retina from the day of birth in the rabbit (Schnitzer, 1989). Owing to the relation found between developing microglia and blood vessels, a vascular origin has been proposed for the retinal microglial cell (Boya et al., 1987). In the adult animal, the microglia are found in the nerve fibre layer, ganglion cell layer and a few in the inner plexiform layer (Kohno et al., 1982; Schnitzer, 1989).

The function of the microglia in a normal retina of the adult animal is not known. The microglia contain both the machinery necessary for metabolic activity as well as the energy source, glycogen.

The major function of microglia within the ganglion cell and inner plexiform layers of the lesioned retina is to remove the debris produced after degradation of neurons

(Miller & Oberdorfer, 1981; Thanos, 1991). They are comparable to the classical 'gitter' cells when they are activated and their cytoplasm becomes filled with debris.

Schnitzer and Scherer (1990) observed an increased number of microglial cells in the retina within a few days after sectioning the rabbit's optic nerve. They demonstrated a small number of mitotic figures of microglial cells on Nissl stained whole mounts. This observation suggests that some microglial cells present in the retina are capable of proliferating.

Astrocyte:

The shape of the astrocytes is stellate in the outermost region of the retina, elongate in the central part of the retina with the majority of astroglial processes aligned in parallel with the ganglion cell axons (Karschin et al., 1986). The morphology of the stellate shaped retinal astrocyte resembles that of fibrous rather than protoplasmic astrocytes (Karschin et al., 1986; Stone & Dreher, 1987). The cytoplasm of the cells is rich in glial intermediate filaments. The cell body of the retinal astrocyte lies in the nerve fibre layer (Karschin et al., 1986; Schnitzer and Karschin, 1986). But the processes of the astroglia also spread in the ganglion cell layer and inner plexiform layer.

The long slender astrocyte processes form an interconnected honeycomb-like scaffolding between vessels and nerve fibres. This network lies parallel to the

internal limiting membrane and perpendicular to the Müller cell processes. In the normal retina astrocytes invest the nerve fibres and blood vessels but they do not invest neuronal somas (Stone & Dreher, 1987).

In the retinal response to injury astrocytic processes proliferate to fill any space in the surrounding tissue that is left vacant by destruction of neural cells (Barron et al., 1986). Their fibres tend to be arranged in parallel bundles, so they can provide support to the tissue of the retina. However, it was observed in both mouse and rat retinae that lesions do not affect the distribution of retinal astrocytes at all (Allcut et al., 1984; Baker and Perry, 1985).

Müller cell:

In 1851, Heinrich Müller, a German anatomist, described the radial glia (Müller cell) of the retina. The Müller cells, the largest cells in the retina, extend all the way from the external to the internal limiting membrane. Fine horizontal processes extend laterally in the two plexiform layers and through the nerve fibre layer. The nucleus of the Müller cells is located at any level within the inner nuclear layer. Müller cell nuclei are round or oval in shape and are appended to the sides of the radial trunks. The trunk of the Müller cell process begins to broaden into the vitread endfoot. Müller cells individually wrap neurons in the ganglion cell layer (Dreher et al., 1988; Robinson & Dreher, 1990).

Müller cells maintain the tissue structure of the

retina. It has been suggested that Müller cells provide neurons with nutrients such as glycogen, particularly in avascular retinae (Ripps and Witkovsky, 1985; Newman, 1986). In response to the injury to the optic nerve, the end feet of Müller cells are hypertrophied 7 days post-operatively (Barron et al., 1986). Microglia and Müller cell cytoplasm actively phagocytose degenerating ganglion cell bodies and their optic fibres following lesions in the retina in neonatal rats (Miller and Oberdorfer, 1981).

AXON REACTION:

The response of the neuronal soma to axonal injury, crucial to axonal repair, is known as the axon reaction. The nature of the axon reaction varies according to the class of the neuron affected. There are two major classes of neurons: intrinsic and extrinsic. In the intrinsic neurons, the cell body and its processes are located within the central nervous system (CNS). Whereas the extrinsic neurons are located in whole or in part outside the CNS (Review: Lieberman, 1971).

Extrinsic neurons exhibit the axon reaction and regenerative responses after axotomy dependent upon the severity of the injury to the axons and the distance of the site of injury from the cell body (Nissl, 1894, cited by Lieberman, 1971; Meyer, 1901; Review: Lieberman, 1971; Review: Barron, 1983; Hall & Borke, 1988).

The complex changes in the histological appearance of axotomized nerve cell bodies was first called Primare Reizung (Primary irritation) by Nissl (1894, cited by Lieberman, 1971), chromatolysis by Marinesco (1896, cited by Lieberman, 1971), and axonal reaction by Meyer (1901). Over the years, a large number of studies have confirmed that chromatolysis, nuclear eccentricity and cell swelling are consistent features of the axon reaction in extrinsic neurons that regenerate after injury (Review: Barron, 1983).

There is a large amount of literature describing the

axon reaction in a wide variety of intrinsic neurons (Review: Barron, 1983) including retinal ganglion cells in mammals (Barron et al., 1986). But there is no published information for any somal regenerative response by intrinsic neurons in the mammals.

CELL SIZE IN AXON REACTION:

An increase in the somal volume is a consistent feature during the axon reaction in mammalian peripheral or extrinsic regenerating neurons (Review: Lieberman, 1971). Hall & Borke (1988) carried out a morphometric study of axotomized neurons of the hypoglossal nucleus of the rat. They observed a significant increase (21%) in the size of the axotomized regenerating neurons.

Whereas extrinsic neurons often enlarge after axotomy or retain remarkably stable configurations (Review: Barron, 1983), the cell bodies of the intrinsic neurons usually undergo atrophy (Fry & Cowan, 1972; Kalil & Schneider, 1975; Macchi et al., 1975; Barron et al., 1976, 1977; Egan et al., 1977; Loewy & Schader, 1977; Barron et al., 1986).

Transient enlargement of axotomized central neurons was observed by Barron et al. (1977) and Egan et al., (1977). Barron et al. (1986) studied the response of the retinal ganglion cell in the rat after crush injury to the optic nerve. They observed a highly significant decrease in the somal area over the course of their experiment. They also observed somal atrophy followed by a highly

significant degree of cytoplasmic shrinkage.

CHROMATOLYSIS:

Chromatolysis is the most conspicuous morphological change of the neuronal soma in response to axotomy. Chromatolysis (Chroma-Color; lysis-loosing) is the disintegration, redistribution and apparent disappearance from the cell body of cytoplasmic Nissl substances (Review: Lieberman, 1971). The process of gradual spread of Nissl body disintegration from the centre towards the periphery of the neuron is known as central chromatolysis.

In central neurons, chromatolysis, in the strict sense lysis of Nissl bodies, is an early indication of the axon reaction (Review: Barron, 1983). Large rubral neurons and Betz cells of the cat may actually exhibit a typical central chromatolysis following lateral funiculotomy (Barron et al., 1977; Egan et al., 1977). The latter authors also observed perinuclear 'capping' in these central neurons. Classical central chromatolysis has been observed in a wide variety of central neurons of different mammalian species (Review: Lieberman, 1971; Review: Barron, 1983). Such types of axon reaction have been described in the neurons of Clarke's nucleus after spinocerebellar tractotomy, in large pyramidal cells of the cerebral cortex after interruption of pyramidal fibres, in neurons of the red nucleus after interruption of descending efferents (Review: Lieberman, 1971) and in retinal ganglion cells after crush injury to the optic nerve (Barron et al., 1986).

However, Misantone et al. (1984) and Allcutt et al. (1984) did not observe classical chromatolysis in retinal ganglion cells of the rat after optic nerve crush. Barron et al. (1986) provided a detailed analysis of chromatolytic changes in retinal ganglion cells after crush to the optic nerve of the rat. Gennarelli et al. (1989) have provided evidence for possible chromatolysis after stretch injury in the guinea pig optic nerve. But the latter authors have provided no detailed information concerning the neuronal somal response to stretch injury, or provided a time course for that response or any numerical data concerning the number of injured cells.

Chromatolysis (TEM observations):

The first electron microscopic study of axotomized neurons was done by Hartmann (1954). He paid attention principally to mitochondrial changes and made no observation relevant to the phenomenon of chromatolysis. However, Causey & Hoffman (1955) reported a loss of granular ER and suggested that this was the ultrastructural basis of chromatolysis. This view has received considerable support in subsequent electron microscopic studies of neurons which show central chromatolysis by light microscopy (Review: Lieberman, 1971). Nissl bodies of light microscopy comprise concentrations of rough ER with flattened cisternae with poly-ribosomal complexes lying apparently free in the intercisternal cytoplasmic matrix (Review: Lieberman, 1971). In chromatolytic

neurons, there is a disintegration of the Nissl bodies and this is characterized by disorganization of ordered cisternal arrays. There is an apparent decrease in the amount of the rough ER, and a dispersion of the persisting rough ER and of free polyribosomes toward the cellular periphery (Review: Lieberman, 1971; Review: Barron, 1983). Severe depletion of rough ER may be found in the degenerating neurons that have either electron-dense or abnormally electron-lucent cytoplasm (Review: Barron, 1983).

The axon reaction of intrinsic neurons that die or atrophy is frequently accompanied by disaggregation and dispersal of cytoplasmic polyribosomal clusters, and loss of rough ER (Review: Barron, 1983). Dying neurons are depleted, often grossly, of all ER components and may have electron-dense or electron-lucent cytoplasm (Review: Barron, 1983).

Conversely, during recovery of injured extrinsic neurons, clusters of free ribosomes increase (Review: Barron et al., 1983).

Concentration of Nissl substances around the nucleus of axotomized extrinsic regenerating neurons (nuclear caps) has been observed by many light microscopists (Review: Lieberman, 1971) and are correlated with the peri-nuclear concentration of rough ER and ribosomes visualised by transmission electron microscopy (Review: Barron, 1983).

Change in smooth ER:

An increased amount of smooth ER occurs in extrinsic

neurons early during the axon reaction (Review: Lieberman, 1971; Hall & Borke, 1988) and atrophying central neurons (Barron et al., 1967). It has been suggested that increased smooth ER is formed by detachment of ribosomes from the granular ER (Review: Lieberman, 1971; Hall & Borke, 1988) perhaps due to disruptive forces or enhanced metabolism as measured in gold-fish retinal ganglion cells (Whitnall & Graftstein, 1983).

NUCLEAR ECCENTRICITY IN AXON REACTION:

Nuclear eccentricity is observed after early chromatolytic changes in both motor and sensory extrinsic neurons (Review: Lieberman, 1971). At the later stages of the axon reaction, nuclei again became centrally located at about the same time that the normal Nissl pattern is recovered (Barron & Tuncbay, 1962) or shortly thereafter (Review: Lieberman, 1971). The significance of nuclear displacement is not understood.

NUCLEAR SIZE AND SHAPE IN AXON REACTION:

Increased nuclear volume is to be expected in the regenerating extrinsic neurons because of the anabolic nature of the response to axotomy, and has been described by several authors (Review: Lieberman, 1971).

However, Barron (1983) reported that actively regenerating neurons 10-30 days post-operatively in feline cervical motor neurons of the adult cat had smaller nuclei than normal (20% decrease in cross-sectional area).

Aldkogius et al. (1980) also observed a reduction in nuclear sizes in neurons of the dorsal vagal motor nucleus after vagotomy. Conversely, some researchers have found no alteration in nuclear size of chromatolyzed peripheral neurons (Review: Lieberman, 1971). Hall & Borke (1988) studied regenerating neurons of the hypoglossal nucleus after axotomy. They did not find any significant variation of nuclear volume following axotomy.

There are very limited quantitative observations on changes in nuclear size in axotomized intrinsic neurons. Barron et al. (1976, 1977) found a measurable nuclear atrophy in feline rubral neurons within one week of cervical rubrospinal tractotomy. Barron et al. (1977) observed a mean decrease in nuclear area of 48% 60 days post-operatively. Loewy & Schader (1977) reported that nuclear areas of Clarke's column neurons were reduced by 35 - 60% of normal 100 days after axotomy. On the contrary, Barron et al. (1986) found no significant differences of nuclear areas of the retinal ganglion cell after crush injury to the optic nerve in the rat.

Increased folding of the nuclear membrane of axotomized extrinsic neurons, particularly of the aspect facing into the cytocentrum has been described by many authors (Review: Lieberman, 1971). Regenerating neurons of the hypoglossal nucleus had irregular nuclear profiles (Hall & Borke, 1988). Murray & Forman (1971) described similar nuclear features in the regenerating retinal ganglion cell of the goldfish retina.

The indentation of the nuclear envelope by narrow channels of cytoplasm is a prominent feature of the axon reaction in some extrinsic regenerating neurons. The enlarged nucleo-cytoplasmic interface is related to enhanced neuronal metabolism and increased nucleo-cytoplasmic interchange (Review: Lieberman, 1971; Hall & Borke, 1988).

However, severe nuclear indentations were also observed in advanced degenerating neurons and degenerating retinal ganglion cells of the adult rat after crush injury to the optic nerve (Barron et al., 1986).

NUCLEOLAR CHANGE IN AXON REACTION:

The nucleolus is the most sensitive indicator of changes in the functional state of a cell and an increase in the nucleolar volume is one of the earliest events of the axon reaction (Review: Lieberman, 1971). Jones & Lavelle (1986) provided quantitative data on nucleolar enlargement of regenerating facial motor neurons of the adult hamster after sectioning of the facial nerve. They observed a significant and dramatic increase in nucleolar volume in axotomized neurons relative to control neurons. Hall & Borke (1988) demonstrated a highly significant increase of nucleolar fractional volume (%), [nucleolar cross-sectional area/nuclear cross-sectional area] x 100, in the hypoglossal motor neurons of the rat after axotomy of the hypoglossal nerve. Nucleolar enlargement has also been reported in extrinsic regenerating neurons by other

authors (Watson, 1965, 1970; Aldkogius et al., 1980).

Vacuolization of the nucleolus has been shown to be a consistent feature of nucleolar enlargement after injury in regenerating extrinsic neurons. (Review: Lieberman, 1971; Jones & Lavelle, 1986; Hall & Borke, 1988). A similar nucleolar response to axotomy has been documented in the retinal ganglion cell of the goldfish (Murray & Grafstein, 1969; Whitnall & Grafstein, 1982, 1983).

A correlation between nucleolar vacuolization and increased nuclear activity have been made (Johnsson, 1969). An acceleration of ribosomal RNA and subsequent protein synthesis has been correlated with nucleolar enlargement and vacuolization in general (Goessens, 1984) and among regenerating neurons (Watson, 1965; Murray & Grafstein, 1969; Whitnall & Grafstein, 1982, 1983) in particular.

However, nucleolar enlargement and metabolic activation are not ubiquitous among regenerating neurons. Spinal motor neurons of the cat demonstrate neither nucleolar enlargement nor heightened nucleolar metabolism following axotomy (Cova & Barron, 1981).

Barron et al. (1977) found nucleolar atrophy in feline rubral neurons within 14 days of axotomy, and at earlier post-operative time in kittens (Barron et al., 1976).

Nucleoli may no longer be discernible in dying cells (Barron et al., 1973), or the nucleolus may be transformed into an amorphous mass of granular material (Raisman, 1973).

Golgi apparatus, mitochondria, lysosomes and neurofilaments do not show any conclusive changes under examination by transmission electron microscope during the axon reaction (Review: Lieberman, 1971; Review: Barron, 1983, Barron et al., 1986).

DIFFERENCE OF RESPONSE OF THE RETINAL GANGLION CELL TO TRANSECTION, CRUSH OR STRETCH INJURY TO THE OPTIC NERVE:

Grafstein & Ingoglia (1982) transected intracranially the optic nerve in adult mice. They observed a 20% loss in the ganglion cell population accompanied by a reduction in cell size of 25% at 3 days post-lesion. Misantone et al. (1984) observed shrinkage among 90% of retinal ganglion cell (from 74 μm^2 to 42 μm^2) by 11 days following crush injury to the optic nerve of adult rats. Comparing the neural responses following crush injury to the optic nerve with the response to nerve transection (Grafstein & Ingoglia, 1982; Richardson et al., 1982), Misantone et al. (1984) concluded that nerve transection has more rapid and severe consequences than crush injury.

About 80% of the large and medium-sized ganglion cells degenerate by 10 days following optic nerve crush in adult mice (Allcutt et al. 1984).

Barron et al (1986) observed advanced degenerative changes in the retinal ganglion cells of adult rats by 3 days following crush injury to the optic nerve and profiles of dead cells regularly from 14 days.

Stretch injury to the optic nerve:

A new model for axonal injury, utilizing stretch injury to the optic nerve of the adult guinea pig has been developed (Gennarelli et al., 1989). This model produces an injury by mechanisms similar to those that cause diffuse axonal/brain injury in human beings. The amount of stretch

and the rate of stretch are controlled separately. The deformations of the optic nerve occurring in stretch injury are comparable to those in the human brain when head motion causes axonal injury (Gennarelli et al., 1989). Transection of the optic nerve produces complete axotomy of all optic nerve fibres as well as disruption of all blood vessels in the nerve. In crush injury of the optic nerve, most of the axons are transected and blood vessels are damaged to a variable degree. In stretch injury of the optic nerve, with the new model (Gennarelli et al., 1989), 17% of the axons are injured. Although Gennarelli et al. (1989) reported the absence of vascular injury in the optic nerve or retina to stretch injury to the optic nerve, Maxwell et al. (1991b) documented wide spread endothelial changes in the microvasculature of the optic nerve to stretch injury. The principal site of axonal damage is the node of Ranvier and secondary axotomy occurs 24 to 72 hours after primary insult (Maxwell et al., 1991a).

A small amount of evidence for the retinal ganglion cell response to stretch injury to the optic nerve was provided by Gennarelli et al. (1989). They observed some retinal ganglion cells with eccentric nuclei and dispersion of rough endoplasmic reticulum but others were normal or nearly normal in appearance. These changes were consistent with the central chromatolysis seen in light microscopy. Gennarelli et al. (1989) also studied glucose utilization/metabolism of the retina. They observed multiple patches of increased glucose utilization rather

than the expected homogeneous appearance of the normal retina. The magnitude of increase in glucose metabolism in these areas measured 13% compared to nearby areas of apparently normal metabolism. They speculated that these areas represent increased metabolic activity in ganglion cells of injured axons and are correlated with increased metabolic activity during central chromatolysis.

The current literature and a comparison of the retinal ganglion cell response to axonal injury is summarized in the table below.

Comparison of available literature and responses of retinal ganglion cells to injury.

Author	Type of injury to optic nerve	Animal type	Chromatolysis	Other Changes
1. Grafstein & Ingoglia (1982)	Sectioning	Mouse	No	20% neuronal loss to 3 dpl & 25% decrease in size in same period.
2. Allcutt et al. (1984)	Crush	Mouse	No	80% loss of large and medium size ganglion cell by 10 dpl.
3. Misantone et al. (1984)	Crush	Rat	No	Temporary shrinkage of of 90% cell by 11 dpl and degenerating cell rarely noted.
4. Barron et al. (1986)	Crush	Rat	+ve 3rd dpl	35% neuronal loss in 3-7 dpl then progressed slowly.
5. Gennarelli et al. (1989)	Stretch	Guinea Pig	+ve (dpl not mentioned.	Glucose utilization was increased following injury.

Dpl = Days post lesion.

AIM OF THE STUDY:

A new model for axonal injury, utilizing stretch injury to the optic nerve (Gennarelli et al., 1989) results in a less severe injury than transection or crush. The purpose of this study is to characterize morphologically and structurally the somal response of retinal ganglion cells after stretch injury to axons, in the adult guinea pig optic nerve.

The aims of the present study are:-

1. to determine whether classical chromatolysis occurs in retinal ganglion cells after axonal injury.
2. to observe the time course of the response of the injured cells.
3. to determine whether there is any regeneration response.

MATERIALS AND METHODS

MATERIALS:

Six adult Albino Hartly guinea pigs weighing 700g (range 650-750g) were taken for this study. Two animals within each survival group were killed at 3, 7 and 14 days after stretch injury to the right optic nerve. The left eyes were taken as controls. The retinas from both eyes were processed for transmission electron microscopy (TEM).

BIOMECHANICS AND INJURY APPARATUS: (Figure 1)

The injury apparatus is custom-designed to deliver reproducible and measurable amounts of elongation or tensile strain to the optic nerve of the guinea pig. The anaesthetized animal's head is placed between the ear canal pins in the head holder of the apparatus (Figure 1).

The two free ends of a sling of umbilical tape placed behind and around the globe, were attached to the force transducer on the apparatus. The head holder has three degrees of freedom of motion so that one can align the transducer sling, and optic nerve along the axis of the optic canal. The angulations to achieve this alignment are 30^{o} laterally and 20^{o} above the intraorbital line (Gennarelli et al., 1989). Precise alignment is necessary to pull the nerve exactly axial to the optic canal. This prevents bending of the nerve around the lip of the canal and prevents undesirable localized injury. The apparatus is provided with a pulse generator operated via the trigger on the control box which can be set to deliver a desired but controlled amount of displacement of the cylinder,

sling and optic nerve. This displacement occurs as the pulse generator activates the solenoid piston that is connected via the metal bar (Figure 1) to both the displacement transducer (DT) and force transducer (Figure 1). The force and time history of the injury event is recorded on a storage oscilloscope. A permanent record of the oscilloscope trace is recorded on Polaroid film.

METHODS:

SURGICAL PROCEDURES FOR OPTIC NERVE STRETCH INJURY:

The animals were deeply anaesthetized with intramuscular ketamine (50 mg/kg^{-1}) and xylazine (3 mg/kg^{-1}). The right eyelids were infiltrated with 1% xylocaine containing epinephrine. The lids were retracted with 4-0 silk sutures. A lateral canthotomy was performed. A 360^{o} opening of the conjunctiva was performed peripheral to the limbus, including the extraocular muscles. The globe was retracted temporally. The optic nerve was dissected free from any attachments. A sling was fashioned from sterile umbilical tape. Once the sling had been moistened with isotonic saline, it was placed over the globe and positioned firmly against the posterior pole of the globe so that the optic nerve ran through the slit. Then the animal was secured in the stereotaxic head holder.

The free end of the sling was finally attached to the injury apparatus as described earlier. The line of force applied to the optic nerve was exactly in line with the longitudinal axis of the optic canal, 30^{o} lateral and 20^{o} above the intraorbital line (Gennarelli et al., 1989).

This regulation alignment minimizes secondary causes of injury brought about by bending of the nerve around the tip of the optic canal.

The same initial amount of force (35-40g pre-load) was placed on each nerve so as to nullify anatomical slack which normally allows for free movement of the eyeball. A displacement of 5 mm was then applied by a pulse generator activation of the solenoid which provided a force ranging between 119.5g and 142.5g, which when added to the 30-40g of pre-load, gave a total force of 155-180g over periods ranging from 19 to 21 ms (Gennarelli et al., 1989). At this force level, there were no instances of optic nerve avulsion or of traumatic vascular injury which resulted in tearing of blood vessels in the optic nerve or retina. Throughout the operation the eye was moistened with isotonic saline and xylocaine at frequent intervals.

Immediately following injury, the sling was carefully removed and the canthal incision was closed with 4-0 silk sutures. Chloramphenicol (0.5% w/v) eye drops were administered to the lesioned eye to prevent infection. The animals were examined at regular time intervals after injury. In all cases, they resumed normal feeding and motor behaviour. No evidence of post-operative infection was observed.

FIXATION PROCEDURES:

The animals were terminally anaesthetized, at 3, 7 and 14 days after injury, with ketamine, xylazine and

pentobarbital (30 mg/kg^{-1}).

The previous tarsoraphy and canthotomy were reopened and the globe was temporarily retracted. The globes were opened on the equators. The retina and the orbit were flooded with 3% glutaraldehyde and 1% paraformaldehyde in 0.1M phosphate buffer (pH 7.2) for 10 min.

Then, after transcardiac perfusion with normal saline for 60s, the descending aorta was clamped and the animal's head was perfused with 3% glutaraldehyde and 1% paraformldehyde in 0.1M phosphate buffer for 30 min. One hour later the globes, optic nerves, chiasm and optic tract were removed and stored in fixative at $5^{o}C$ for 24 hours. Then the specimens were stored in fixatives at room temperature.

TISSUE COLLECTION:

The eye ball was washed with 0.1M phosphate buffer overnight and cut into four quadrants. The retina and attached choroid was separated from the sclera carefully under the dissecting microscope in a Petri dish containing phosphate buffer. The retinal pieces were transferred onto a glass slide. A retinal strip of 2 mm width was taken 2 mm eccentric to the optic disc and cut into blocks (0.5 - $1mm^2$) with the help of the dissecting microscope and a sheet of transparent graph paper which was laid between the light source of the microscope and the glass slide. The blocks were left in a labelled container containing buffer and then processed for TEM.

Blocks were collected at the above sites since the cellular density of the ganglionic layer at 2-4 mm from the optic disc is more or less uniform in the guinea pig retina (Boycott & Wassle, 1974; Choudhury, 1978).

TISSUE PROCESSING FOR TEM:

Retinal blocks were post-fixed in 1% osmium tetroxide (OsO_4) in 0.1M phosphate buffer for one hour. After rinsing with buffer and distilled water, tissue blocks were stained in 2% aqueous uranyl acetate en bloc for one hour, dehydrated through ascending concentrations of acetone and embedded in Durcupan resin.

DURCUPAN EMBEDDING:

Due to the thinness of the retina, the time allowed in each step was shorter than usual. A brief account of the embedding procedure is given here:-

Wash in Phosphate buffer	(overnight)
Post-fix in buffered osmium tetroxide	1 hour
Rinse in corresponding buffer 2 changes	10 min. each
Rinse in distilled water 2 changes	
Stain with 2% aqueous uranyl acetate	1 hour
Rinse in distilled water (one change)	
Dehydration through 50%, 70%, 90% acetone	15 min. each
100% acetone (3 changes)	15 min. each
Acetone/Resin (3:1)	1 hour
Acetone/Resin (1:1)	1 hour
Acetone/Resin (1:3)	1 hour

Pure Resin (3 changes)	1.5 hours each
Embedding in fresh Durcupan resin in hot oven (56°C) in between cover slips under weight	48 hours

DURCUPAN RESIN:

Durcupan embedding medium is a kind of epoxy resin developed by Staubli (1960, cited by Glauert, 1965). Although the recipe suggested by Staubli (1960) has been modified several times, these modifications are basically similar to the original mixture which contains Durcupan resin, a hardener, an accelerator and a plasticizer.

The formula of Durcupan resin used for the present embedding medium was:

Durcupan	10g
DDSA	10g
DMP 30	0.39g
Dibutyl phthalate	0.39g

Flattening of the retinal blocks:

Only a few ganglion cells for study were obtained in sections cut in the radial axis of the retina. First attempts to cut a tangential section through the ganglion cell layer did not provide a high number of ganglion cells due to the normal curvature of the retina. I attempted to flatten the retina between glass slides under weight in a Petri-dish containing phosphate buffer as described by Wassle et al., (1975). But the flattened retinal blocks became recurved again after osmication and dehydration.

In a final approach, retinal blocks were flattened during embedding in resin. The retinal blocks were embedded between two coverslips which were placed between two rubber sheets under weight (200-300g) and left under pressure in an oven at 56°C for 48 hours. Then the attached pair of coverslips were separated with a razor blade. The tissue remained attached with one of the coverslips. The tissue was transferred from the coverslip to the resin blank with rapid Araldite. It was found easier to transfer the tissue from the coverslip to the resin block when embedding in Durcupan resin rather than Araldite.

SEMITHIN SECTION:

Blocks were trimmed and sectioned with a Porter Blum Ultra Microtome (MT-2). For tangential sections, the block face and glass knife should be aligned properly with help of the knife shadow on the block. The block face may be either a vitreous surface of the retina or choroidal surface. As the ganglion cell layer is only one cell thickness, continuous monitoring was needed.

The first 3-4 semithin sections (1μ thickness) were cut and checked either for the nerve fibre layer, or choroidal blood vessels, pigmented epithelium or rods and cones. These observations gave a guideline for further sectioning for the ganglion cell layer. Semithin sections of 1μm thickness were cut tangentially through the ganglion cell layer. With the aid of the hot plate, the sections

were stretched and dried on glass slides before staining with 1% Azure Blue.

LIGHT MICROSCOPIC PHOTOGRAPHY:

Photographs were taken from different areas of the semithin sections, stained with Azure blue, at a magnification of 25 x 12.5 with a Leitz-Vario-Orthomat light microscope. The prints were of 9.5" x 7.0" size and total magnification was 625.

Quantitative analysis of the different populations of cells in the ganglion cell layer of the control and experimental retinae were studied from these photomontages.

THIN SECTION:

A specific area of interest on the block was further trimmed. Serial thin sections (silver and gold colours) were cut on glass knives and floated on the surface of a water bath using a Reichert-Jung Ultracut ultramicrotome. The thin sections were stretched with chloroform vapour and collected on 300 mesh copper grids. These grids were air-dried prior to staining.

STAINING:

As the tissue blocks were stained with 2% aqueous uranyl acetate for 1 hr after osmication, the thin sections on copper grids were stained only with lead citrate for 4 minutes. After rinsing in distilled water for 2 min, grids were air dried in a dust-free area and examined in a Jeol-100S transmission electron microscope.

TEM PHOTOGRAPHY:

Only cells of the ganglionic layer cut through the nucleolus were examined and photographed. Photographs were taken at a magnification of 2.8, 7.0, 14.0 and 21.0 thousands times for each of the cell soma, cytoplasm, nucleus and cytoplasmic details respectively. The prints were double the size of the negatives and were used for morphometric and qualitative studies.

MORPHOMETRIC STUDIES:

The cross-sectional areas (μm^2) of the cell bodies, nuclei and nucleoli were measured with the help of the MOP-AMO2 computer. The mean area (μm^2) was calculated for each of the following cell groups:-

a) control ganglion cells,
b) chromatolytic ganglion cells three days after injury,
c) degenerating ganglion cells at seven and fourteen days after injury,
d) regenerating ganglion cells at seven and fourteen days after injury, and
e) small neurons three, seven and fourteen days after injury.

A one way analysis of variance was carried out using the **Statgraphics** program (Statistical Graphics Corporation) on IBM computer to determine whether changes in these values were of statistical significance within 95% confidence limits. In addition, the nucleolar fractional area (%) was estimated using the following formula:

Nucleolar fractional area

$$= \frac{\text{Nucleolar cross-sectional area}}{\text{Nuclear cross-sectional area}} \times 100$$

= %,

for all of the cell nuclei included within the quantitative analysis.

SCANNING ELECTRON MICROSCOPY (SEM):

Scanning electron microscopy gives scientists a powerful research tool in gaining a rapid appreciation of the gross form of the tissues and of single cell. Although the resolution of the SEM does not match that of TEM, the results in many cases are informative.

In this study, vibrotome sections of 200μ thickness were cut along the radial axis of the retina (2-4 mm from the optic disc). The tissues fixed for TEM were also used in SEM.

Processing procedure used for SEM:

Fixation and dehydration:

1.	Retinal sections post-fixed with buffered 1% osmic acid	30 min.
2.	Transfer to phosphate buffer (pH 7.4)	30 min.
3.	Dehydration through 50% acetone	30 min.
4.	Dehydration through absolute acetone 3 changes	30 min. each

Critical Point Drying:

1. Arrange specimens in baskets and place in the boat which is filled with acetone.
2. Place boat inside the chamber and seal door tightly.

3. Open inner valve and fill chamber with liquid carbon dioxide.
4. Open outlet valve and run off acetone whilst keeping chamber filled with CO_2 for approximately 4 mins.
5. Close all valves here for 15-20 mins, ensuring that the CO_2 level is above the level of the boat.
6. Flush chamber contents (liquid CO_2/acetone) with fresh CO_2 for 1 min and leave for a further 10 min.
7. Flush chamber once more for one minute to get rid of any remaining acetone. Drop level of liquid CO_2 to below the level of the boat. This is important as an excessive build-up of pressure will blow the valve.
8. Switch on heater and leave until temperature reaches $35^{o}C$.
9. The CO_2 inside the chamber is now gaseous. Open outlet valve to release gas slowly until pressure inside the chamber is zero.
10. Remove specimens and mount on stubs using double sided Sellotape.

Sputter coating:

Specimens are coated with Gold to provide conduction in order to minimise any 'charging' artefact from the electron beam in the microscope. This is done in a Polaron sputter coater.

Specimens are now ready for SEM screening. The specimens were examined with a JEOL JSM-T300 scanning electron microscope and photographs taken.

RESULTS

LIGHT MICROSCOPY

CONTROL RETINA:

Cells of the ganglionic layer of the control retina were counted and grouped according to the criteria developed by Barron et al. (1986) from the photomontages of tangentially cut semithin sections (1μm thickness). Only cells cut through the nucleus were counted. The percentage of the ganglionic cells, small neurons and glial cells is 69%, 29.5% and 1.5% respectively.

Ganglion cells:

The average diameters of the ganglion cells were calculated from the photomontage. The diameter, in these cells, ranges from 13-26 μm. The ganglion cell has a large nucleus usually eccenteric in position (Figure 4). The nucleus contains one or, occasionally, two prominent nucleoli (Figure 4). Although the nucleoli are usually located centrally in the nucleus, marginally placed nucleoli are not uncommon (Figure 4). The nuclear outline is regular or scalloped on the cytoplasmic face of the nucleus (Figure 4). The cytoplasm contains clumps of the Nissl substances.

Small Neurons:

The average diameter of the small neurons ranges from 8 to 11 μm. They have a relatively large nucleus containing a prominent nucleolus (Figure 4). The nucleus is surrounded by a thin rim of cytoplasm. The small neurons are darker than the ganglion cells when stained using Azure blue.

Glial Cells:

Only the cell body of the microglia is found in the ganglionic layer. In the control retina, they are very few in number (1.5%). The diameter of the glial nucleus ranges from 5.0 to 6.5 μm. They have characteristic clumps of heterochromatin in their nucleus (Figure 4). Müller cell processes fill the gaps between the cells of the ganglion layer. Astrocytic processes are not resolvable by light microscopy.

EXPERIMENTAL RETINA:-

Three days post trauma:

Central chromatolysis occurs in about one third of the ganglion cells on the third day after stretch injury to the optic nerve. Nissl substances assume a peripheral position leaving a central pale area in the cytoplasm close to the eccentric nucleus (Figure 5). There is a clear line of demarcation between the chromatolytic and non-chromatolytic zone of the cytoplasm in injured ganglion cells (Figure 5). Small neurons do not show central chromatolysis (Figure 5). The glial cells also do not show any changes.

Seven days post-trauma:

Seven days after injury central chromatolysis is widespread in injured ganglion cells (Figure 6). The proportion of chromatolytic ganglion cells increases in comparison to three days after injury. Conversely, the size of most of the chromatolytic ganglion cells is reduced in comparison to the ganglion cells in both the control and at the third day after injury. A few of the larger sized

injured ganglion cells contain an eccentric nucleus with an irregular nuclear profile. The nucleus contains a prominent nucleolus. Small neurons and glial cells do not show any changes.

Fourteen days post-trauma:

Chromatolytic ganglion cells are still present 14 days after stretch injury to the optic nerve (Figures 7,8). A high number of pyknotic cells are seen at this survival (Figure 7). The proportion of the ganglion cells decreases dramatically in comparison to controls and shorter survival periods. A few ganglion cells possess a nucleus of irregular profiles which contain a prominent nucleolus.

Small neurons do not show any changes. The microglial cells are now found more frequently in the sections. On a few occasions two microglia are found lying very closely suggesting proliferation of these cells (Figure 8).

ELECTRON MICROSCOPIC OBSERVATION

CONTROL RETINA:

Ganglion cell:

Ultrastructural observations were made on photomontages prepared from forty ganglion cells from the control retina. In each cell, the nucleus contained a nucleolus, and all cells were examined at equal magnification.

The ganglion cell has a large eccentric nucleus which is usually round or oval in shape. The cytoplasmic face of the nucleus may be scalloped or may have deep indentations orientated towards the nucleolus (Figures 9,10,11).

The nucleus of the ganglion cell contains one or two nucleoli (Figures 9,10). A typical nucleolus contains all of the nucleolar components. The nucleolonemal strands, the dense fibrillar materials, enclose the nucleolar vacuoles (Figure 36). Light fibrillar centres and granular material are present within the nucleolonemal strands. Large clumps of 'nucleolar associated chromatin' are also present in relation to the nucleolus (Figure 36).

The cytoplasm of the normal ganglion cells contains prominent clumps of rough/granular endoplasmic reticulum and polyribosomes which constitute the Nissl bodies of light microscopy. Nissl bodies comprise concentrations of rough ER with flattened cisternae elongate or short, and arranged in parallel or whorl-like, with polyribosomal clusters lying in the cisternal cytoplasmic matrix (Figures

15,16). The Nissl bodies of the ganglion cells are usually distributed away from the nuclear envelope.

Long or short granular ER, other than Nissl bodies, are also present in the cytoplasm. Free polyribosomal clusters are distributed in the cytoplasm.

The normal ganglion cell has a well developed Golgi-apparatus which are generally situated close to the nucleus or occasionally near the cell periphery (Figures 12,13). The Golgi-apparatus comprises a series of stacks of parallel agranular cisternae associated with vesicles of different sizes (Figure 14).

The mitochondria of the ganglion cells are round, oval or elongate in shape. The mitochondrial matrix is often electronlucent. Mitochondria are distributed throughout the cytoplasm with an increased density close to the nucleus. Dense bodies and/or lysosomes are observed in the cytoplasm (Figures 12,13). The ganglion cell has numerous neurofilaments in the cytoplasm (Figures 11,13).

Small neurons:

The small neurons are smaller and darker than ganglion cells. The nuclei are round or oval in shape. The nucleus contains a prominent nucleolus and is surrounded by a thin rim of cytoplasm containing very few organelles. Granular ER or polyribosomes are scattered in the cytoplasm (Figures 17,18).

Glial cells:

The microglia are the small dark glial cells of the ganglionic layer of the retina (Figure 41). The number of

microglia is very few in the normal retina (1.5%). The nucleus contains characteristic clumps of hetero-chromatin. The cytoplasm contains a good amount of large mitochondria and elongated granular endoplasmic reticulum.

The radially oriented Müller cell processes are cut in cross-section in tangential sections of the ganglionic layer of the retina and give the appearance of dark, round areas around the cells of the ganglionic layer. The Müller cell processes are more electron dense than the astrocytic processes which are arranged perpendicular to the Müller cell processes. The cell bodies of the Müller cells are situated in the inner nuclear layer of the retina. The Müller cell processes ensheath the ganglionic cells and then expand to form the inner limiting membrane of the retina.

The cell bodies of the astrocytes are situated in the nerve fibre layer of the retina. The astrocytic cell processes usually form a network around the nerve fibre of the retina and are orientated parallel to the inner limiting membrane. Astrocyte processes are rarely seen in the ganglionic layer of the normal retina. The cytoplasm of the cell body and processes contains numerous intermediate filaments (Figures 40,41).

ELECTRON MICROSCOPY:

EXPERIMENTAL RETINA:

TEM photographs of 250 ganglion cells containing a discrete nucleolus from the three experimental groups were

examined qualitatively and morphometrically.

Three days post trauma:

Ganglion cells: In about one third of the ganglion cells, the rough ER is disorganized and peripherally located reflecting the central chromatolysis noted by light microscopy (Figures 19,20). The compact parallel arrays or whorl pattern of the rough ER of the control cells is lost. Mitochondria and dense bodies accumulate in the central clear zone of the cytoplasm (Figure 20). Neurofilaments become more visible in this clear part of the cytoplasm. There is no obvious ultrastructural change of the Golgi-apparatus. In the chromatolytic ganglion cells the nucleus is consistently eccentric and the cytoplasmic face of the nucleus is often irregular. The ultrastructure of the nucleolus is mostly comparable to that in the control (Figures 36, 37).

No ultrastructural change is found in the small neurons and glial cells at three days after injury.

Seven days post trauma:

The chromatolysis becomes widespread throughout the cytoplasm in most of the injured ganglion cells 7 days after stretch injury to the axons. The amount of rough ER and polyribosomes is reduced in comparison to that in ganglion cells of the control or the third day after injury (Figures 21,22,24,25). Conversely, the amount of smooth ER is increased in comparison to the control ganglion cells (Figure 26). No significant alterations occur in the

mitochondria. These advanced chromatolytic cells degenerate to form atrophied ganglion cells. The nuclei of the degenerating ganglion cells become extremely eccentric, mis-shapen and distorted by deep furrows (Figure 24).

A few ganglion cells demonstrating early chromatolysis are still present, having peripheral margination of the Nissl substances and an eccentric nucleus (Figure 23).

On the other hand, a new variety of reactive ganglion cell occurs at seven days post trauma, demonstrating an irregular profile to the nucleus which contains an enlarged, vacuolated nucleolus and a discrete amount of Nissl substance in the cytoplasm (Figure 27). These ganglion cells are comparable to the regenerating neurons of the facial nucleus (Jone and Lavelle, 1986) and hypoglossal nucleus (Hall and Borke, 1988) after axotomy. I suggest that these ganglion cells are regenerating ganglion cells.

The distinguishing features of a regenerating ganglion cell are a ruffled nucleus which contains an enlarged vacuolar nucleolus (Figures 27,38). Rough ER and polyribosomes are found in the nuclear identations and abutted to the nuclear membrane (Figure 28), and are comparable to the 'perinuclear cap' (Review: Lieberman, 1971) of light microscopy (Figure 28).

The nucleolus of the regenerating ganglion cells has loosened and less electron dense nucleolonemal strands, and

an increased amount of nucleolar vacuoles. The general appearance of the nucleolus becomes granular. The nucleolar associated chromatin is distributed around the nucleolus (Figure 38). In contrast, the nuclei of the degenerating ganglion cells contain focal aggregations of chromatin and marginally displaced nucleoli (Figure 29).

The cytoplasm of the regenerating ganglion cells contains discrete Nissl substances (Figure 27). The amount of smooth ER and free polyribosomes increase in these cells in comparison to the controls (Figure 29). A prominent Golgi-apparatus and normal mitochondria are present in these cells.

Glial cells:

The number of microglia in the sections is similar to that of the control. But there is proliferation of Müller cell and astrocytic cell processes. (Figure 42).

Fourteen days post trauma:

In this survival group, chromatolytic ganglion cells degenerate further and present the features of dying cells. The degenerating ganglion cells showing an electron dense cytoplasm, and a severely mis-shapen nucleus containing focal aggregation of chromatin (Figures 30, 31, 32) indicative of necrobiosis of these cells. The atrophied, degenerative ganglion cells are also surrounded by a proliferation of Müller cell and astrocyte processes (Figure 32). Typical nucleoli are not discernible in the degenerating cell nuclei. Some of the degenerating ganglion

cells present a severe form of apoptosis: disappearance of most of the cytoplasmic organelles leaving an electron-lucent cytoplasm (Figure 30), indicative of dying cells (Review: Lieberman, 1971).

Ganglion cells which I suggest are regenerating, are still found at fourteen days after injury. The regenerating ganglion cells have an irregular profile to nucleus. The nucleus contains an enlarged, vacuolated nucleolus (Figures 34, 39) as described earlier. The granular ER has reformed to be arranged in parallel stacks (Figures 34, 35). Free polyribosomes and mitochondria are distributed throughout the cytoplasm.

Small neurons still do not demonstrate any changes.

Glial cells:

Microglia:- Microglia are found more frequently 14 days after injury in comparison to the control and earlier survival groups. Occasionally, pairs of microglia are found in this group (Figure 8). A few enlarged microglia are found loaded with cellular debris and lipid inclusions in the cytoplasm (Figure 45).

Astrocyte and Müller cell processes:- There is marked proliferation of astrocyte and Müller cell processes which fill the gaps left by degenerated ganglion cells. (Figure 44).

MORPHOMETRIC STUDY:

The morphometric analysis of the cross-sectional area of the cell soma, the nucleus, the nucleolus and the nucleolar fractional area within the nucleus was done using the MOP-computer on TEM micrographs. Only cells within the ganglion cell layer containing a discrete nucleolus were considered.

Somal cross-sectional area:

The somal cross-sectional area of the control ganglion cell is 149.24 $\pm$ 6.48 μm^2. At three days after injury, the somal cross-sectional area of the chromatolytic ganglion cells increases to 199.50 $\pm$ 8.50 μm^2. At seven days survival, the somal cross-sectional area of the degenerating ganglion cells decreases progressively at day 7 (109.00 $\pm$ 3.00 μm^2) and at day 14 (98.00 $\pm$ 8.00 um^2) after injury (Figure 52).

Conversely, the somal cross-sectional areas of the regenerating ganglion cells increases at 7 days to 234.00 $\pm$ 22.00 and 14 days to 230.50 $\pm$ 16.50 um^2. Analysis of variance (F) demonstrates a highly significant variance over the groups ($F = 25.421$, df 5 x 8, $p = 0.0001$). Individual comparisons using confidence intervals demonstrates that soma size in **regenerating** ganglion cells at 7 and 14 days after injury is significantly greater than soma size in controls ($p < 0.05$). This is not the case in **degenerating** ganglion cells which, by 14 days after operation, were significantly smaller than controls ($p < 0.05$) (Figure 52). Analysis of variance of the cross-

sectional area of the small neurons in the control group and at 3, 7 and 14 days after injury do not show any significant changes (Figure 56).

Nuclear cross-sectional area:

There is an increase in nuclear cross-sectional area of the chromatolytic ganglion cells (85.00 ± 1.00 μm^2) at 3 days after injury when compared with control values (66.0 ± 3.24 μm^2). Whereas, in the degenerating ganglion cells, the nuclear sizes decrease progressively at day 7 (48.50 ± 2.50 μm^2) and day 14 (40.50 ± 6.50 um^2) after injury (Figure 53). Analysis of variance (F = 8.68, df 5 x 8, p = 0.0043) demonstrates that there is no significant difference in nuclear area between control and chromatolytic or regenerating ganglion cells. However, there is a significant reduction of nuclear area in **degenerating** ganglion cells at 14 days after injury ($p < 0.05$) (Figure 53). There is no significant change in nuclear area of small neurons between the control or any experimental group (Figure 57).

Nucleolar area and fractional area:

The average nucleolar area of the control ganglion cells is 1.70 ± 0.11 um^2, and increases to 3.77 ± 0.17 μm^2 in the chromatolytic ganglion cells on the third day after injury. There is no significant change in the nucleolar area in the **degenerating** ganglion cells at either 7 or 14 days after injury (Figure 54). But analysis of variance (F) demonstrates a highly significant variance over the

groups ($F = 13.83$, df 5 x 8, $p < 0.005$). Individual intergroup comparisons using confidence intervals demonstrates that nucleolar area in **regenerating** ganglion cells at 7 and 14 days is significantly greater than in controls ($p < 0.05$) (Figure 54). In addition, intergroup comparison using confidence intervals demonstrates a highly significant variance in nucleolar fractional area in **regenerating** ganglion cells, but not in degenerating or chromatolytic ganglion cells (Figure 55).

Nucleolar areas and nucleolar fractional areas did not demonstrate any significant changes in small neurons (Figures 58 and 59).

SCANNING ELECTRON MICROSCOPE (SEM) OBSERVATIONS:

Control retina

The SEM study of the control retina demonstrates the different layers of the retina (Figure 3) as illustrated in the SEM atlas by Kessel & Kardon (1979). The ganglion cell layer of the control retina shows ganglion cells ensheathed by the end feet of Müller cell processes (Figures 47,50). The processes then flatten to form part of the inner limiting membrane of the retina. The ganglion cells are large and round in shape (Figures 46,47,50).

Experimental retina:

The SEM photographs of the experimental retina in 14 days survival animals may be compared with the control retina (Figures 46-51). This comparative study reveals that the ganglion cell layer of the experimental retina

differs from that of the controls. In the late survival animals the ganglion cell layer contains a few atrophied ganglion cells (Figure 48), a number of normal ganglion cells. There is proliferation of Müller cell processes (Figures 48,49,51) in relation to the atrophied ganglion cell. The injured ganglion cells are deformed and atrophied (Figure 51). The normal form of the end feet of the Müller cell processes is altered (Figures 49,51) so that they occupy the space left vacant by degenerated ganglion cells.

DISCUSSION

The injury apparatus used in the present study is custom designed to deliver a reproducible and measurable amount of elongation to the optic nerve (Gennarelli et al., 1989). It produces axonal damage as documented by Maxwell et al. (1991a) which is morphologically identical to that seen in diffuse injury to the human brain.

In the present study, classical central chromatolysis, comparable to that described in the red nucleus (Review: Barron, 1983) or in extrinsic neurons (Review: Lieberman, 1971), is observed in about one third of the ganglion cells three days after stretch injury to the optic nerve. The chromatolysis becomes widespread throughout the cytoplasm of the affected ganglion cells seven days after injury. The majority of the chromatolytic ganglion cells degenerate and become pyknotic 14 days after injury.

My quantitative analysis of the number of chromatalytic ganglion cells three days after stretch injury suggests that about one third of ganglion cells are injured.

Gennarelli et al. (1989) state that about 17% of axons are injured. However, close examination of their paper reveals the following. In the quantitative morphometrics section of the results in their paper they state that in control optic nerves only 10.2% of nerve fibres are of greater cross-sectional area than 1 μm^2. In the stretch injured optic nerves, in contrast, 27.6% of fibres are larger than 1 μm^2 and 4.3% greater than 2 μm^2. This gives a total of larger fibres of 31.9%. Gennarelli et al.

(1989) state that in fibres of a greater diameter than 1 μm^2 there are many more injured axons. They state that "further analysis shows that 17% of the axons are injured". But no details of the morphological criteria or statistical techniques used to distinguish injured from un-injured axons is given. I therefore suggest that the quoted figure of 31.9% enlarged fibres reflects the one third of damaged neurones undergoing central chromatolysis.

But on the contrary, a few ganglion cells, which I suggest demonstrate morphological changes indicating regeneration, are noted at both seven and 14 days survivals.

GANGLION CELLS WITH CENTRAL CHROMATOLYSIS:

CELL SIZE:

Three days after stretch injury, injured ganglion cells are demonstrated by the morphological features of central chromatolysis. The somal cross-sectional area of these cells increases by 34% when compared to control cells. (Figure 52). This differs from the reported shrinkage of retinal ganglion cells occurring within three days of injury following transection (Grafstein & Ingoglia, 1982) or crush injury (Allcutt et al., 1984; Misantone et al., 1989; Barron et al., 1986) to the optic nerve in mice or rats.

The initial increase in size of the injured ganglion cells reported in the present study may be compared with a similar increase in size of the large rubral neurons (Barron et al., 1977), Betz cells (Egan et al., 1977) or

that reported in regenerating extrinsic neurons (Review: Lieberman, 1971; Review: Barron, 1983; Hall & Borke, 1988) following transection. The increase in cell size, at least in the early stages of the axon reaction is thought to be due to water uptake (Review: Lieberman, 1971).

CYTOPLASM:

Central chromatolysis, that found in the retinal ganglion cells in light microscopy, is consistent with the ultrastructural observations of the present study.

In a few earlier studies in mammals, central chromatolysis was not observed for example in the retinal ganglion cells either following transection (Grafstein & Ingoglia, 1982) or crush injury (Allcutt et al., 1984; Misantone et al., 1984). However, Barron et al (1986) found short term chromatolysis followed by the rapid onset of cell death in retinal ganglion cells after crush injury to the optic nerve in adult rats.

Central chromatolysis also occurs in large rubral neurons and Betz cells of the cat following lateral funiculotomy (Barron et al., 1977; Egan et al., 1977) and in a wide variety of central neurons of different mammalian species (Review: Lieberman, 1971; Review: Barron, 1983). But the central chromatolysis of these central neurons is usually followed by degeneration (Review: Barron, 1983). The central chromatolysis of the retinal ganglion cells in the present study is comparable to that of regenerating extrinsic neurons (Review: Lieberman, 1971; Review:

Barron, 1983; Hall and Borke, 1988).

Central chromatolysis is one of the consistent features of the axon reaction which appears to represent a change to a functional state specially conducive to repair of the axons following axotomy (Grafstein, 1975).

ULTRASTRUCTURAL OBSERVATIONS:

Three days after stretch injury, my ultrastructural study reveals that the rough ER in one third of the ganglion cells becomes disorganized and peripherally marginated (Figures 19,20). These changes are consistent with central chromatolysis seen by light microscopy and confirm the observations of Gennarelli et al. (1989) who reported similar changes in rough ER following identical injury to the optic nerve. The peripheral margination of the persistent rough ER and free polyribosomes of the present study is in accordance with the previous studies of the ultrastructural findings of these organelles in chromatolytic extrinsic neurons (Review: Lieberman, 1971; Review: Barron, 1983).

NUCLEUS:

In the present study, the nuclei of the injured ganglion cells are consistently eccentric in position. This is usually observed after early chromatolytic changes in both motor and sensory extrinsic neurons (Review: Lieberman, 1971). The nuclear shape is almost unchanged except for a few indentations of the nuclear membrane facing the cytoplasm (Figure 19).

The nuclear cross-sectional area of injured ganglion

cells three days after stretch injury increases by 28.78% when compared to that in the control (Figure 53). This increase in nuclear area in the present study during the axon reaction may be compared to the documented, anabolic nature of the response to axotomy in the regenerating extrinsic neurons (Review: Lieberman, 1971). However, nuclear enlargement is not a consistent feature of the axon reaction in all types of regenerating neurons (Review: Barron, 1983).

NUCLEOLUS:

The nucleolar fractional area (%) of the injured ganglion cells three days after injury increases by 55.43% when compared to the control (Figure 55). The increase in nucleolar area at an early stage of the axon reaction described in this study extends the observations of earlier researchers (Review: Lieberman, 1971; Jones and Lavelle, 1986) who reported that an increase in nucleolar volume is one of the earliest events of the axon reaction.

The ultrastructure of the nucleolus at these early survivals does not differ much from that of the control (Figures 36,37).

DEGENERATING GANGLION CELLS:

CELL SIZE:

Most of the injured ganglion cells undergo degeneration by seven days after stretch injury. The somal cross-sectional area (μm^2) of the degenerating ganglion cells decreases progressively and becomes statistically

significant ($P < 0.05$) by day 14 after stretch injury (Figure 52). The decrease in size of the degenerating ganglion cell in the present study is correlated with their atrophy as shown in mice or rats following transection or crush injury to the optic nerve (Grafstein and Ingoglia, 1982; Allcutt et al., 1984; Misantone et al., 1984; Barron et al., 1986). Similarly, atrophy occurs in other degenerating intrinsic neurons (Fry and Cowan, 1972; Kalil and Schneider, 1975; Macchi et al., 1975; Barron et al., 1976, 1977; Egan et al., 1977). Atrophy of degenerating neurons is due to a highly significant degree of cytoplasmic shrinkage and loss of organelles (Review: Barron, 1983).

CYTOPLASM:

The widespread and severe form of chromatolysis that occurred in most of the injured ganglion cells both at seven and 14 days after stretch injury in the present study is comparable to that described in large rubral neurons and Betz cells of the cat (Barron et al., 1977; Egan et al., 1977) in which severe, general loss of chromoidal substances occurred following typical central chromatolysis.

Ultrastructural observations:

Seven days after injury, the amount of rough ER in most of the injured ganglion cells decreases significantly due to degranulation and lysis (Figures 24,25). The loss of rough ER becomes severe 14 days after injury (Figures

30-33). All these changes of RER at 7 and 14 days after injury, are comparable to that seen in retinal ganglion cells following crush injury to the optic nerve in the rat (Barron et al., 1986) and also parallels that of dying intrinsic neurons (Review: Barron, 1983). In parallel, the amount of smooth ER increases in degenerating ganglion cells (Figures 26,33) after stretch injury. This increase is due to detachment of ribosomes from the rough ER (Review: Lieberman, 1971). Fourteen days post-trauma, the degenerating ganglion cells demonstrate a severe form of apoptosis, disappearance of most of the cytoplasmic organelles, leaving a dark cytoplasm indicative of dying cells (Review: Lieberman, 1971).

NUCLEUS:

The eccentric nucleus becomes mis-shapen in degenerating ganglion cells. Severe furrowing of the nuclear surface (Figures 24,30,) and focal aggregation of nuclear hetrochromatin adjacent to the nuclear membrane occurs in degenerating ganglion cells after a stretch injury to their axons. These findings are in agreement with those of Barron et al. (1986) who observed similar changes in the retinal ganglion cells of the rat following crush injury to the optic nerve. Focal aggregation of nuclear chromatin is indicative of necrobiosis of these cells (Review: Barron, 1983).

The nuclear cross-sectional area of the degenerating ganglion cells decreases significantly ($P < 0.05$) 14 days

after stretch injury (Figure 53). Barron et al. (1986) did not observe a significant decrease of nuclear area of retinal ganglion cells following crush injury to the optic nerve in the rat. However, the statistically significant decrease in nuclear area of the degenerating retinal ganglion cells in the present study extends the observations of Barron et al. (1977) who found a measurable nuclear atrophy in feline rubral neurons within one week of cervical rubrospinal tractotomy in the cat.

NUCLEOLUS:

In longer survivals (7-14 days) recognisable nucleoli are not discernible in the degenerating ganglion cells in the present study. These results parallel the findings reported in dying neurons by Barron (1983).

Although the calculated nucleolar fractional area of these cells suggests an increase when compared with the control (Figure 55), this is misleading resulting from the extremely low values for nuclear cross-sectional area obtained in these cells.

REGENERATING GANGLION CELLS:

A small number of different types of reactive ganglion cells is observed both at seven and 14 days after stretch injury. These cells contain a nucleus with an irregular profile, enlarged vacuolated nucleolus and discrete Nissl substances within the cytoplasm (Figures 27,34,38,39). The structure of these ganglion cells is comparable to that reported in regenerating neurons of the facial nucleus in the hamster (Jones & Lavelle, 1986) and of the hypoglossal nucleus in rats (Hall & Borke, 1988) following axotomy by transection.

I suggest that these ganglion cells observed after stretch injury of the optic nerve provide evidence for regenerative activity of some ganglion cells. No evidence for a somal regenerative response of either ganglion cells of the retina or central (intrinsic) mammalian neurons has been published. Misantone et al. (1984) reported that retinal ganglion cells in the rat retain viability for at least several weeks after intracranial crush injury to the optic nerve. These authors comment that the response of the retinal ganglion cells of the rat to crush injury may be compared to documented responses in either goldfish retinal ganglion cells (Whitnall & Grafstein, 1983) or mammalian peripheral neurons. In both examples neuronal regeneration results in the development of new functional axons. The present study, therefore provides the first evidence for a somal regenerative response by intrinsic mammalian neurons which is comparable to that documented

for the extrinsic neurons of mammals or retinal ganglion cells of the goldfish.

CELL SIZE:

The somal cross-sectional area of the regenerating ganglion cells remains at a statistically significant higher level than the control from 7 days onwards in the current study. The somal cross-sectional area of regenerating ganglion cells increases by 54% from control values to 230.50 $\pm$ 16.50 μm^2 fourteen days after stretch injury (Figure 52). The current results are comparable to the reported increase in size of regenerating extrinsic neurons (Review: Lieberman, 1971) and in particular the regenerating neurons of the hypoglossal nucleus (Hall & Borke, 1988) following axotomy by transection. The increase in somal size of the regenerating ganglion cells in the present study is also comparable to that reported for retinal ganglion cells of the goldfish following transection of the optic nerve (Murray & Forman, 1971; Whitnall & Grafstein, 1982, 1983). An increase in somal volume is a consistent feature in regenerating neurons (Review: Lieberman, 1971).

Although the increase in cell volume in the early stages of the axon reaction is thought to be caused by water uptake (Review: Lieberman, 1971) at later stages of the axon reaction it is thought to be due to a numerical increase in cytoplasmic organelles (Review: Lieberman, 1971), in the main free ribosomes and rough ER (Murray & Forman, 1971).

CYTOPLASM:

Ultrastructural observations:

Regenerating ganglion cells contain discrete clumps of rough ER in their cytoplasm seven days after stretch injury (Figure 27) which then begins to form discrete Nissl bodies. At the same time their cytoplasm contains an increased amount of smooth ER (Figure 29). This parallels the findings of Hall & Borke (1988) who observed an increased amount of smooth ER and polyribosomes in regenerating hypoglossal nucleus neurons in the rat seven days after transection of the hypoglossal nerve. The increase of smooth ER in regenerating neurons may be due to either disruptive influences or enhanced metabolism as has been documented in retinal ganglion cells of the goldfish (Whitnall & Grafstein, 1983).

I have found a perinuclear aggregation of rough ER and polyribosomes occurring in regenerating ganglion cells (Figure 28). These results confirm the 'perinuclear cap' observed by light microscopy. A comparable perinuclear concentration of the rough ER and polyribosomes has been described in extrinsic regenerating neurons (Review: Barron, 1983) in particular in regenerating hypoglossal neurons (Hall & Borke, 1988).

The rough ER of the regenerating ganglion cells proliferates and becomes arranged in long parallel stacks (Figures 34,35), fourteen days after stretch injury. These results parallel and extend the observations made in

regenerating ganglion cells in the goldfish retina (Murray & Forman, 1971). The proliferation of rough ER and their arrangement to form parallel stacks of cisternae is comparable to the morphological characteristics of regenerating neurons known to produce a large quantity of extrinsic protein (Murray & Forman, 1971).

I did not find discrete differences in the structure of organelles such as mitochondria, the Golgi-apparatus and lysosome/dense bodies in early chromatalytic cells or regenerating ganglion cells when compared with control cells.

NUCLEUS:

The regenerating ganglion cell contains a prominent nucleus with an irregular nuclear profile. The nuclear cross-sectional area of these ganglion cells does not differ significantly from that of control cells in the present study. My results parallel those of Jones & Lavelle (1986) and Hall & Borke (1988) who also did not find a significant variation in nuclear volume of regenerating neurons in facial and hypoglossal nuclei in the hamster or rat following axotomy by transection. There are also some reports where there is no increase in nuclear size in chromatolyzed extrinsic neurons (Review: Lieberman, 1971). Aldkogius et al. (1980) and Barron (1983) have, in addition, reported smaller nuclei in actively regenerating neurons in both the vagal motor nucleus of the rat and feline cervical motorneurons of the cat after axotomy.

NUCLEOLUS:

The nucleoli of regenerating ganglion cells demonstrate a characteristic, dramatic ultrastructural change seven days after stretch injury (Figures 38,39). These changes are consistent with the known anabolic or reparative nature of the axon reaction (Aldkogius et al., 1980).

The most pronounced nucleolar changes in regenerating ganglion cells in the present study are a loosening of the nucleolonemal strands which contain the active ribosomal RNA genes (Mirre & Stahl, 1978; Goessens, 1984) and an increased amount of nucleolar vacuoles. As a result, the nucleolar fractional area (%) of the regenerating ganglion cells increases by 270% from control values (Figure 54), seven days after injury and remains at a significantly higher level 14 days after injury. This increase in nucleolar area in the regenerating ganglion cells is comparable to morphometric results published by Hall & Borke (1988) who observed an increase in the order of 200% in size of the nucleoli in regenerating hypoglossal neurons seven days following section of the cat hypoglossal nerve. Jones & Lavelle (1986) also reported a similar nucleolar enlargement in regenerating facial nucleus neurons in the hamster two days following transection of the facial nerve.

The ultrastructural changes in the nucleoli of these regenerating ganglion cells in the present study parallel published observations in regenerating neurons of both the facial and hypoglossal nuclei in the hamster or the rat

following axotomy by Jones & Lavelle (1986) and Hall & Borke (1988) respectively. The nucleolar response of the regenerating ganglion cells in the present study is also comparable to the response of the regenerating ganglion cells of the goldfish (Murray and Grafstein, 1969; Whitnall and Grafstein, 1982). Vacuolization has been shown to be a consistent feature of the nucleolar response to injury in extrinsic regenerating neurons (Review: Lieberman, 1971) and has been correlated with increased nuclear activity (Johnsson, 1969).

Crozet et al. (1981) suggested that the increased vacuolar area renders the nucleolus more accessible by increasing the surface area, thereby providing for storage and/or transport mechanisms for the passage of ribosomal precursor granules into the nuclear interior. An acceleration of ribosomal RNA and subsequent protein synthesis has been correlated with nucleolar enlargement and vacuolization in general (Goessens, 1984) and among regenerating neurons (Watson, 1968; Murray and Grafstein, 1969; Whitnall and Grafstein 1982, 1983) in particular.

However, nucleolar enlargement and metabolic activation are not ubiquitous among regenerating neurons. Spinal motorneurons of the cat exhibit neither nucleolar enlargement or heightened nucleolar metabolism following axotomy (Cova & Barron, 1981). The disparity of nucleolar response among these regenerating neuronal populations may reflect, in part, different patterns of axonal regeneration

(Hall & Borke, 1988).

My results show that 'nuclear associated chromatin' is distributed evenly around the nucleolus of regenerating ganglion cells seven days after stretch injury. These distributive changes in the nucleolus associated chromatin parallel those seen in regenerating facial neurons in the hamster two days after axotomy (Jones and Lavelle, 1988). However, there is currently little published information regarding any relationship between nucleolar metabolic changes and ultrastructural changes in nucleolar associated chromatin.

SMALL NEURONS:

The small neurons of the ganglion cell layer of the retina do not undergo any morphological changes throughout the time course of the present study. My results extend and confirm the observations of Gennarelli et al. (1989) who demonstrated that small nerve fibres of the optic nerve were uninjured after stretching to the optic nerve in the guinea pig. However, neither did the small neurons demonstrate any clear response even after crush injury to the optic nerve in the rat (Barron et al., 1986).

Hughes (1981) injected HRP into either the superior colliculus or the optic nerve to label the cells of the ganglion layer of the retina. He reported that a portion of the small neurons were not labelled by retrograde HRP and concluded that small neurons of the ganglion cell layer includes a population of displaced amacrine cells which do

not contribute axons to the optic nerve. The small neurons observed in the present study do not respond following stretch injury to the optic nerve. I suggest, these are either small neurons sending small nerve fibres to the optic nerve which are not injured after stretch (Gennarelli et al., 1989), or are displaced amacrine cells of the retina.

RETINAL GLIAL CELLS:

MICROGLIA:

Microglial cells occur in increased number and size 14 days after injury. Paired microglia are also observed in the longer survival animals of the present study (Figure 8) indicating the possible proliferation of these cells.

In the control retina, the microglial cells contribute to the regularly arranged mosaic of cell bodies and processes in the internal plexiform layer and ganglion cell layer (Schnitzer, 1989). The possible proliferation of the microglia in longer survival animals of the present study confirm and extend the observation of Schnitzer & Scherer (1990) who demonstrated mitotic figures in microglial cells on Nissl stained whole mounts of the retina after transection of the rabbit optic nerve.

Enlarged microglia containing cellular debris and lipid inclusions occur 14 days after injury in the present study (Figures 43,45). This may be correlated with the presence of dying ganglion cells in these animals. Miller & Oberdorfer (1981) demonstrated microglial cells actively

engulfing debris, and their cytoplasm was packed with lipid droplets and lysosome-like bodies in the lesioned retina of neonatal rats. Thanos (1991) employed a new technique for labelling phagocytosing microglia in the axotomized retina of adult rats. He concluded that one major function of microglia within the ganglion cell layer and inner plexiform layers of the lesioned retina is to remove the debris produced after degradation of neurons.

ASTROCYTE:

The cell body of the astrocyte does not occur in the ganglion cell layer (Karschin et al., 1986). In this study, proliferation of astrocytic processes is observed seven days after injury (Figures 42,44) and is marked 14 days after injury. A similar astrocytic response has been reported by Barron et al. (1986) in the retina of the rat following crush injury to the optic nerve. The proliferation of astrocytic cell processes is suggested to fill any space that is vacated by atrophy or destruction of neural cells of the retina after injury.

MÜLLER CELL:

The end feet of the Müller cells become hypertrophied 14 days after stretch injury to the optic nerve (Figures 44,49,51). This finding may parallel the observations of Barron et al. (1986) who observed a hypertrophy of Müller cell processes 7 days after crush injury to the optic nerve in rats. Miller and Oberdorfer (1981) reported that the the Müller cell cytoplasm also actively phagocytosed

degenerating ganglion cells following a lesion in the retina of neonatal rats. In the present study, phagocytic inclusions in the cytoplasm of Müller cells were not observed.

COMPARISON OF RESPONSE OF RETINAL GANGLION CELL TO STRETCH, CRUSH OR SECTIONING TO THE OPTIC NERVE IN MAMMALS:

In the present study, the ganglion cell response to axonal injury is analysed following stretch injury to the optic nerve in the adult guinea pig. Central chromatolysis is established by the third day after stretch injury. A few ganglion cells demonstrate central chromatolysis still occurring seven days after injury. Central chromatolysis in ganglion cells was not observed in mice or rats following sectioning or crush injury to the optic nerve (Grafstein & Ingoglia, 1982; Allcutt et al., 1984; Misantone et al., 1984). But was observed by Barron et al. (1984) who observed central chromatolysis on the third day after injury in rats following crush injury to the optic nerve.

In the present study, the majority of injured ganglion cells undergo degeneration at seven days after stretch injury. No dead cells, however, are found at this time. The noble and exciting finding in this study is that a few ganglion cells demonstrate morphological changes which are suggestive of a regenerative response seven days after stretch injury. Only one publication, Misantone et al. (1984) has not reported degeneration of ganglion cells in

rats following crush injury to the optic nerve. This differs from the majority of studies where cellular death of at least 20% of ganglion cells in mice or rats within seven days after sectioning or crush injury to the optic nerve occurs (Grafstein & Ingoglia, 1982; Allcutt et al., 1984; Barron et al., 1986). In the present study degenerating or dying ganglion cells are only seen 14 days after stretch injury.

Cheng & Povlishock (1988) observed reactive axonal changes until 14 days following fluid-percussion brain injury in the highly organized afferent pathways of the cat visual system, in particular in the terminal part of the optic tract as it enters the lateral geniculate body. They claimed that the reactive axonal change took place in an otherwise unaltered brain parenchyma. The findings reported by Cheng & Povlishock (1988) "that axons reacted to the traumatic injury despite the fact that their cells of origin were undamaged" has no foundation in their data, since they did not examine ganglion cell bodies in the retina after fluid percussion injury. Therefore, the only conclusion that can be drawn from their data is that they obtained no evidence for trans-neuronal degeneration. The present study provides good morphological evidence that axonal injury evokes a clear, somal response and therefore contradicts the hypothesis provided by Cheng & Povlishock (1988).

In the backdrop of the above discussion, I suggest

In the backdrop of the above discussion, I suggest that the time course of chromatolysis is longer in stretch injury than in either crush or transection of the optic nerve.

CONCLUSION

1. Central chromatolysis occurs in about one third of larger ganglion cells 3 days after stretch injury.
2. The time course of chromatolysis is longer in the stretch injury than in either crush or transection of the optic nerve.
3. The small ganglion cells do not undergo central chromatolysis.
4. Confirmed glial responses are seen 14 days after injury.
5. I suggest that regenerative morphological changes occur in the soma of a small number of larger ganglion cells.

BIBLIOGRAPHY

ADAMS, J.H., GENNARELLI, T.A., GRAHAM, D.I. (1982a): Brain damage in non-missile head injury: observations in man and subhuman primates. In: Recent Advances in Neuropathology (Edited by SMITH, W.T. & CAVANAGH, J.B.). pp.165-190. Edinburgh: Churchill Livingstone.

ADAMS, J.H., GRAHAM, D.I., MURRY, L.S. & SCOTT, G. (1982b): Diffuse axonal injury due to non-missile head injury in humans: an analysis of 45 cases. Annal. Neurol. **12**, 557-563.

ALDKOGIUS, H., BARRON, K.D. & REGAL, R. (1980): Axon reaction in dorsal motor vagal and hypoglossal neurons of the adult rat. Light microscopy and RNA-cytochemistry. J. Neurol. **193**, 165-178.

ALLCUTT, D., BERRY, M. & SIEVERS, J. (1984): A quantitative comparison of the reactions of retinal ganglion cells to optic nerve crush in neonatal and adult mice. Dev. Brain Res. **16**, 219-230.

BAKER, P.J. & PERRY, V.H. (1985): The effect of ganglion cell depletion on the development of astrocytes and the blood vessel distribution in the retina. Neurosci. Lett. [Suppl.] **21**, 68 (Abstr.).

BARR, M.L. & KIERNAN, J.A. (1988): The Human Nervous System. An Anatomical Viewpoint. 5th Edition. pp.296-311. London: J.B. Lippincott Company.

BARRON, K.D. (1982): Axon reaction and its relevance to CNS trauma. In: Head Injuries: Basic and Clinical Aspects (edited by GROSSMAN, R.G. & GILDENBERG, P.L.) pp.45-55. New York: Raven Press.

BARRON, K.D. (1983):Comparative observations on the cytologic reactions of central and peripheral nerve cells to axotomy. In: Spinal Cord Reconstruction (edited by KAO, C.C., BUNGE, R.P. & PEIER, P.J.) pp.7-40. New York: Raven Press.

BARRON, K.D., DENTIGER, M.P., KROHEL, G., EASTON, S.K. & MANKES, R. (1986): Qualitative and quantitative ultrastructural observations on retinal ganglion cell layer of rat after intraorbital optic nerve crush. J. Neurocytol. **15**, 345-362.

BARRON, K.D., DENTIGER, M.P., NELSON, L.R. & SCHEIBLY, M.E. (1976): Incorporation of tritiated leucine by axotomized rubral neurons. Brain Res. **116**, 251-266.

BARRON, K.D., DOOLIN, P.F. & OLDERSHAW, J.B. (1967): Ultrastructural observations on retrograde atrophy of lateral geniculate body. I. Neuronal alterations. J. Neuropath. Exp. Neurol. **26**, 300-326.

BARRON, K.D., MEANS, E.D. & LARSEN, E. (1973): Ultrastructure of retrograde degeneration in thalamus of rat. I. Neuronal somata and dendrites. J. Neuropath. Exp. Neurol. **25**, 443-478.

BARRON, K.D., SCHREIBER, S.S., COVA, J.L. & SCHREILBY, M.E. (1977): Quantitative cytochemistry of RNA in axotomized feline rubral neurons. Brain Res. **130**, 469-481.

BARRON, K.D. & TUNCBAY (1962): Histochemistry of acid phosphatase during axon reaction. Amer. J. Pathol. **40**, 637-652.

BOYA, J., CALVO, J. & CARBONELL, A.L. (1987): Appearance of microglial cells in the postnatal rat retina. Arch. Histol. Jpn. **50(2)**, 223-231.

BOYCOTT, B.B. & DOWLING, J.E. (1969): Organization of primate retina: Light microscopy. Proc. Roy. Soc., Lond. (Biol.) **255**, 109-120.

BOYCOTT, B.B. & WASSLE, H. (1974): The morphological types of ganglion cells of the domestic cat's retina. J. Physiol. (London) **240**, 397-419.

BUNT, A.H., LUND, R.D. & LUND, J.S. (1974): Retrograde axonal transport of horseradish peroxidase by ganglion cells of the Albino rat. Brain Res. **73**, 215-228.

CATSICAS, S.M., CATSICAS & CLARKE, P.G.H. (1987): Long distance retinal connections in birds. Nature **326**, 186-187.

CAUSEY, G. & HOFFMAN, H. (1955): Cytoplasmic synthesis in nerve cells. Brit. J. Cancer **9**, 666-673.

CHENG, C.L.Y. & POVLISHOCK, J.T. (1988): The effect of traumatic brain injury on the visual system: a morphologic characterization of reactive axonal change. J. Neurotrauma **5(1)**, 47-60.

CHOUDHURY, B.P. (1978): Retinotopic organization of the guinea pig visual cortex. Brain Res. **144**, 19-29.

COVA, J.L. & BARRON, K.D. (1981): An autoradiographic study of uptake of tritiated leucine by axotomized cervical motoneurons of kittens. Exp. Mol. Pathol. **34**, 159-169.

COWEY, A. & PERRY, V.H. (1979): The projection of the temporal retina in rats, studied by retrograde transport of horseradish peroxidase. Exp. Brain Res. **35**, 457-464.

CROZET, N., MOTLIC, J. & SZOLLUSI, D. (1981):Nucleolar fine structure and RNA synthesis in porcine oocytes during the early stages of antrum formation. Biol. Cell **41**, 35-42.

DACEY, D.M. (1989): Axon bearing amacrine cells of macaque retina. J. Comp. Neurol. **284**, 275-293.

DREHER, Z.M., WEGNER, & STONE, J. (1988): Müller cell end feet at the inner surface of the retina: Light microscopy. Vis. Neurosci **1**, 169-180.

EGAN, D.A., FLUMERFELT, B.A. & GWYN, D.G. (1977): A light and electron microscopic study of axon reaction in the red nucleus of the rat following cervical and thoracic lesions. Neuropathol. Appl. Neurobiol. **3**, 423-439.

ERB, D.E. & POVLISHOCK, J.T. (1988): Axonal damage in severe traumatic brain injury: an experimental study in the cat. Acta. Neuropathol. **76**, 347-358.

FRY, F.J. & COWAN, W.M. (1972): A study of retrograde cell degeneration in the lateral mammillary nucleus of the cat, with special reference to the role of axonal branching in the preservation of the cell. J. Comp. Neurol. **144**, 1-23.

GENNARELLI, T.A., THIBAULT, L.E., ADAMS, J.H., GRAHAM, D.I., THOMPSON, C.J. & MARCINCIN, R.P. (1982): Diffuse axonal injury and traumatic coma in the primate. Annal. Neurol. **12**, 564-574.

GENNARELLI, T.A., THIBAULT, L.E., TIPPERMAN, R., TOMEI, G., SERGOT, R., BROWN, M., MAXWELL, W.L., GRAHAM, D.I., ADAMS, J.H., IRVINE, A., GENNARELLI, L.M., DUHAIME, A.C., BOUCK, R. & GREENBERG, J. (1989): Axonal injury in the optic nerve: a model simulating diffuse axonal injury in the brain. J. Neurosurg. **71**, 244-253.

GLAUERT, A.M. (1965): The fixation and embedding of biological specimens. In: Technique for Electron Microscopy (edited by KAY, D.H.). pp.166-212. Oxford: Blackwell Scientific Publications.

GOESSENS, G. (1984): Nucleolar structure. Int. Rev. Cytol. **87**, 107-158.

GRAFSTEIN, B. (1975): The nerve cell body response to axotomy. Exp. Neurol. **48** (Part 2), 32-51.

GRAFSTEIN, B. & INGOGLIA, N.A. (1982): Intracranial transection of the optic nerve in adult mice: Preliminary observations. Exp. Neurol. **76**, 318-330.

HALL, L.L. & BORKE, R.C. (1988): A morphometric analysis of the somata and organelles of regenerating hypoglossal motoneurons from the rat. J. Neurocytol. **17**, 835-849.

HARTMANN, J.F. (1954): Electromicroscopy of motor nerve cells following sections of axons. Anat. Rec. **118**, 19-29.

HOGAN, M.J., ALVARADO, A.B. & WEDDELL, J.E. (1971): Histology of the human eye. (1st Edition). pp.393-522. London: W.B. Saunders Company.

HUGHES, A. (1975): A quantitative analysis of the cat retinal ganglion cell topography. J. Comp. Neurol. **163**, 107-128.

HUGHES, A. (1981): Population magnitudes and distribution of the major modal classes of cat retinal ganglion cell as estimated from HRP filling and systematic survey of the same diameter spectra for classical neurons. J. Comp. Neurol. **197**, 303-339.

HUGHES, A. (1985): New perspectives in retinal organization. In: Progress in Retinal Research (edited by OSBORNE, N. & CHADER, G.) pp.243-313. Oxford: Pergamon Press.

HUGHES, A. & VANEY, D.I. (1980): Coronate cells: Displaced Amactins of the rabbit retina. J. Comp. Neurol. **189**, 169-189.

JOHNSSON, J.M. (1969): A study of nucleolar vacuoles in cultured tobaccoa cells using radioautography, actinomycin D, and electron microscopy. J. Cell Biol. **43**, 197-206.

JONES, K.J. & LAVELLE, A. (1986): Differential effects of axotomy on immature and mature facial neurons: a time course study of initial nucleolar and nuclear changes. J. Neurocytol. **15**, 197-206.

KALIL, K. & SCHNEIDER, G.E. (1975): Retrograde cortical and axonal changes following lesions of the pyramidal tract. Brain Res. **89**, 15-27.

KARSCHIN, A., WASSLE, H. & SCHNITZER (1986): Shape and distribution of astrocytes in the cat retina. Invest. Ophthalmol. Vis. Sci. **27**(5), 828-831.

KESSEL, R.G. & KARDON, R.H. (1979): Tissues and organs: a text-atlas of scanning electron microscopy. pp.84-105. San Francisco: W.H. Freeman & Company.

KOHNO, T., INOMATA, H. & TANIGUCHI, Y. (1982): Identification of microglia cell of the rat retina by light and electron microscopy. Jpn. J. Ophthalmol. **26**(1), 53-68.

LIEBERMAN, A.R. (1971): The axon reaction: A review of the principal features of perikaryal responses to axon injury. Int. Rev. Neurobiol. **14**, 49-124.

LOEWY, A.D. & SCHADER, R.E. (1977): A quantitative study of retrograde neuronal changes in Clarke's column. J. Comp. Neurol. **171**, 65-81.

MACCHI, G., QUATTRINI, A., CHINZARI, P., MARCHESI, G. & CAPOCCHI, G. (1975): Quantitative data on cell loss and cellular atrophy of intralaminar nuclei following cortical and subcortical lesions. Brain Res. **89**, 43-59.

MAXWELL, W.L., IRVINE, A., GRAHAM, D., ADAMS, J.H., GENNARELLI, T.A., TIPPERMAN, R. & STUART, S.M. (1991a): Focal axonal injury: The early axonal response to stretch. J. Neurocytol. **20**, 157-164.

MAXWELL, W.L., IRVINE, A., WATT, C., GRAHAM, D.I., ADAMS, J.H. & GENNARELLI, T.A. (1991b): The microvascular response to stretch injury in the adult guinea pig visual system. J. Neurotrauma **8**, 271-279.

MEYER, A. (1901): On parenchymatous systemic degenerations mainly in the central nervous system. Brain **24**, 47-115.

MILLER, N.M. & OBERDORFER, M. (1981): Neuronal and neuroglial responses following retinal lesions in the neonatal rats. J. Comp. Neurol. **202**, 493-504.

MIRRE, C. & STAHL, A. (1978): Peripheral RNA synthesis of fibrillar centre in nucleoli of Japanese quail oocytes and somatic cells. J. Ult. Res. **64**, 377-387.

MISANTONE, L.J., GERSHENBAUM, M. & MURRAY, M. (1984): Viability of retinal ganglion cells after optic nerve crush in adult rats. J. Neurocytol. **13**, 449-465.

MURRAY, M. & FORMAN, D.S. (1971): Fine structural changes in goldfish retinal ganglion cells during axonal regeneration. Brain Res. **32**, 287-298.

MURRAY, M. & GRAFSTEIN, B. (1969): Changes in morphology and amino acid incorporation of regenerating goldfish optic neurons. Exp. Neurol. **23**, 544-560.

NEWMAN, E.A. (1986): The Müller cell. In: Development, Morphology and Regional Specialization of Astrocytes. Vol. 1 (edited by FEDOROFF, S. & VERNA DAKIS, A.) pp.149-171. New York: Academic Press.

PERRY, V.H. (1981): Evidence for an Amacrine cell system in the ganglion cell layer of the rat retina. Neurosci. **6**, 931-944.

POVLISHOCK, J.T. (1986): Traumatically induced reactive axonal change without concomitant change in focally related neuronal somata and dendrites. Acta Neuropathol. **70**, 53-59.

POVLISHOCK, J.T., BECKER, D.P., CHENG, C.L.Y. & VAUGHAN, G.W. (1983): Axonal damage in minor head injury. J. Neuropathol, Exp. Neurol. **42**, 225-242.

POVLISHOCK, J.T. & BECKER, D.P. (1985): Fate of reactive axonal swellings induced by head injury. Lab. Invest. **52**, 540-552.

PROVIS, J.M. (1979): The distribution and size of ganglion cells in the retina of the pigmented rabbit: A qualitative analysis. J. Comp. Neurol. **185**, 121-138.

RAISMAN, G. (1973): An ultrastructural study of the effects of hypo-physectomy on the supraoptic nucleus of the rat. J. Comp. Neurol. **147**, 181-207.

RICHARDSON, P.M., ISSA, V.M.K. & SHEMIE, S. (1982): Regeneration and retrograde degeneration of axons in the rat optic nerve. J. Neurocytol. **11**, 949-966.

RIPPS, H. & WITKOVSKY, P. (1985): Neuron glia interaction in the brain and retina. Prog. Ret. Res. **4**, 171-219.

ROBINSON, S.R. & DREHER, Z. (1990): Müller cells in adult rabbit retinae: Morphology, distribution and implications for function and development. J. Comp. Neurol. **292**, 178-192.

SCHEER, U., KLEINSCHMIDT, J.A. & FRANKE, W.W. (1982): In: The Nucleolus (edited by JORDON, E.G. & CURTIC, C.A.) pp.25-42. London: Cambridge University Press.

SCHNITZER, J. (1988): Astrocytes in the guinea pig, horse and monkey retina: Their occurrence coincides with the presence of blood vessels. Glia **1**, 74-89.

SCHNITZER, J. (1989): Enzyme-histochemical demonstration of microglial cells in the adult and postnatal rabbit retina. J. Comp. Neurol. **282**(2), 249-263.

SCHNITZER, J. & KARSCHIN, A. (1986): The shape and distribution of astrocytes in the retina of the adult rabbit. Cell Tissue Res. **246**(1), 91-102.

SCHNITZER, J. & SCHERER, J. (1990): Microglial cell responses in the rabbit retina following transection of the optic nerve. J. Comp. Neurol. **302**, 779-791.

STONE, J. & DREHER, Z. (1987): Relationship between astrocytes, ganglion cells and vasculature of the retina. J. Comp. Neurol. **255**, 35-49.

STONE, J. & FUKUDA, Y. (1974a): Properties of cat retinal ganglion cells: A comparison of W-cells with x- and y-cells. J. Neurophysiol. **37**, 722-749.

THANOS, S. (1991): Specific transcellular carbocyamine-labelling of rat retinal microglia during injury induced neuronal degeneration. Neurosci. Lett. **127(1)**, 108-112.

VANEY, D.I., PEICHL, L. & BOYCOTT, B.B. (1981): Matching populations of amacrine cells in the inner nucleus and ganglion cell layers of the rabbit retina. J. Comp. Neurol, **199**, 373-391.

WASSLE, H., LEVICK, W.R. & CLELAND, B.G. (1975): The distribution of the alpha type of ganglion cells in the cat's retina. J. Comp. Neurol. **159**, 419-438.

WATSON, W.E. (1965): An autoradiographic study of the incorporation of nucleic acid precursors by neurons and glia during nerve regeneration. J. Physiol. (Lond.), **180**, 741-753.

WATSON, W.L. (1968): Observations on the nucleolar and total cell body nucleic acid of injured nerve cells. J. Physiol. **196**, 655-676.

WATSON, W.E. (1970): Some metabolic responses of axotomized neurons to contact between their axons and denervated muscle. J. Physiol. (Lond.) **210**, 321-343.

WHITNALL, M.H. & GRAFSTEIN, B. (1982): Perikaryal routing of newly synthesized proteins in regenerating neurons: Quantitative electron microscopic autoradiography. Brain Res. **239**, 41-56.

WHITNALL, M.H. & GRAFTSTEIN, B. (1983): Changes in perikaryal organelles during axonal regeneration in goldfish retinal ganglion cells: An analysis of protein synthesis and routing. Brain Res. **272**, 49-56.

WONG, R.O.L. & HUGHES, A. (1987): The morphology, number and distribution of a large population of confirmed displaced amacrine cells in the adult cat retina. J. Comp. Neurol. **255**, 159-177.

FIGURES

FIGURE 1

A schematic drawing of stretch injury apparatus.

CH channels A & B on the oscilloscope; DT - displacement transducer; FT - force transducer; PS - power supply; SOL - solenoid piston.

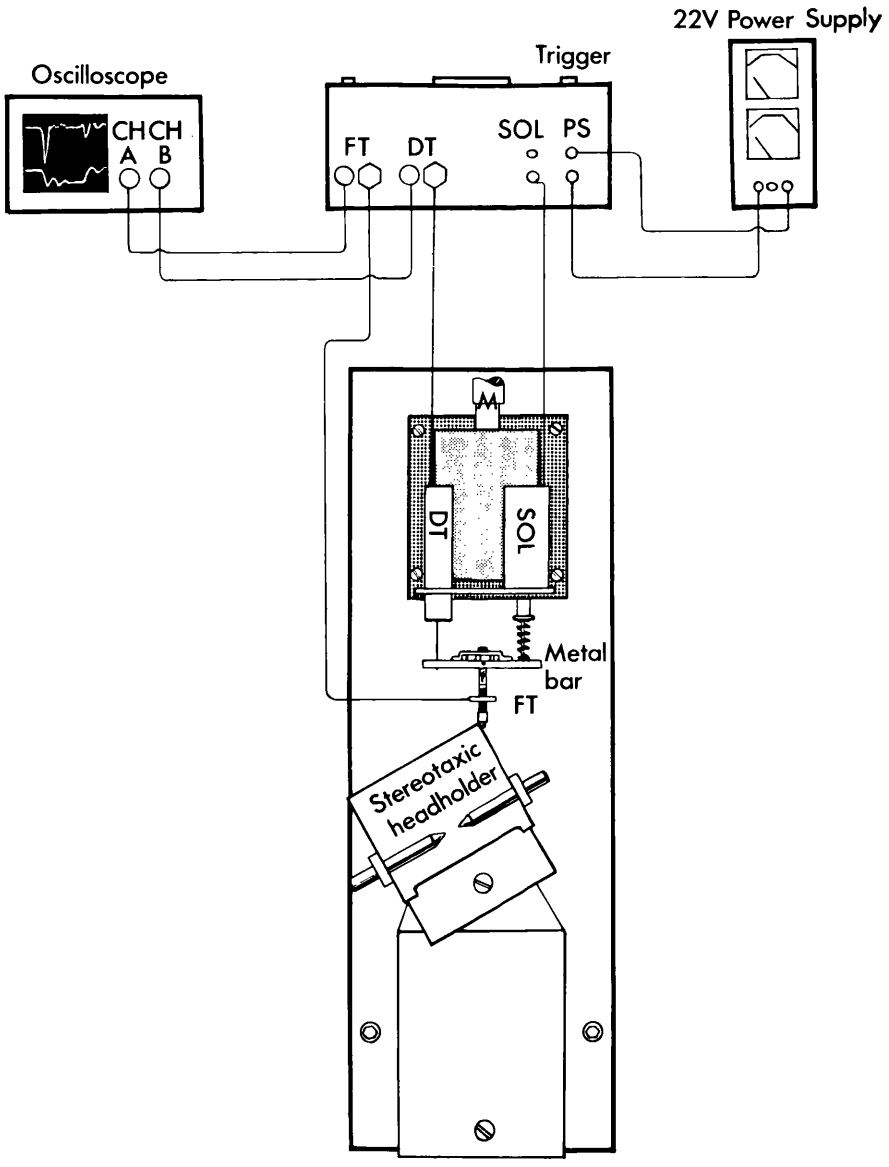
22V Power Supply
Trigger
Oscilloscope
CH A
CH B
FT
DT
SOL
PS
DT
SOL
Metal bar
FT
Stereotaxic headholder

FIGURE 2

Control retina

A semithin section, cut along the radial axis of the retina, showing its different layers. Ganglion cell layer (GCL) is of one cell thickness and it contains only a few ganglion cells in the section.

(Mags. x 450)

Retinal layers:

PL - Pigmented layer
RC - Rods and cones layer
OLM - Outer limiting membrane
ONL - Outer nuclear layer
OPL - Outer plexiform layer
INL - Inner nuclear layer
IPL - Inner plexiform layer
GCL - Ganglion cell layer
NFL - Nerve fibre layer
ILM - Inner limiting membrane.

FIGURE 3

Control retina

An SEM photograph showing the different layers of the control retina labelled as Figure 2.

(Mags. x 750)

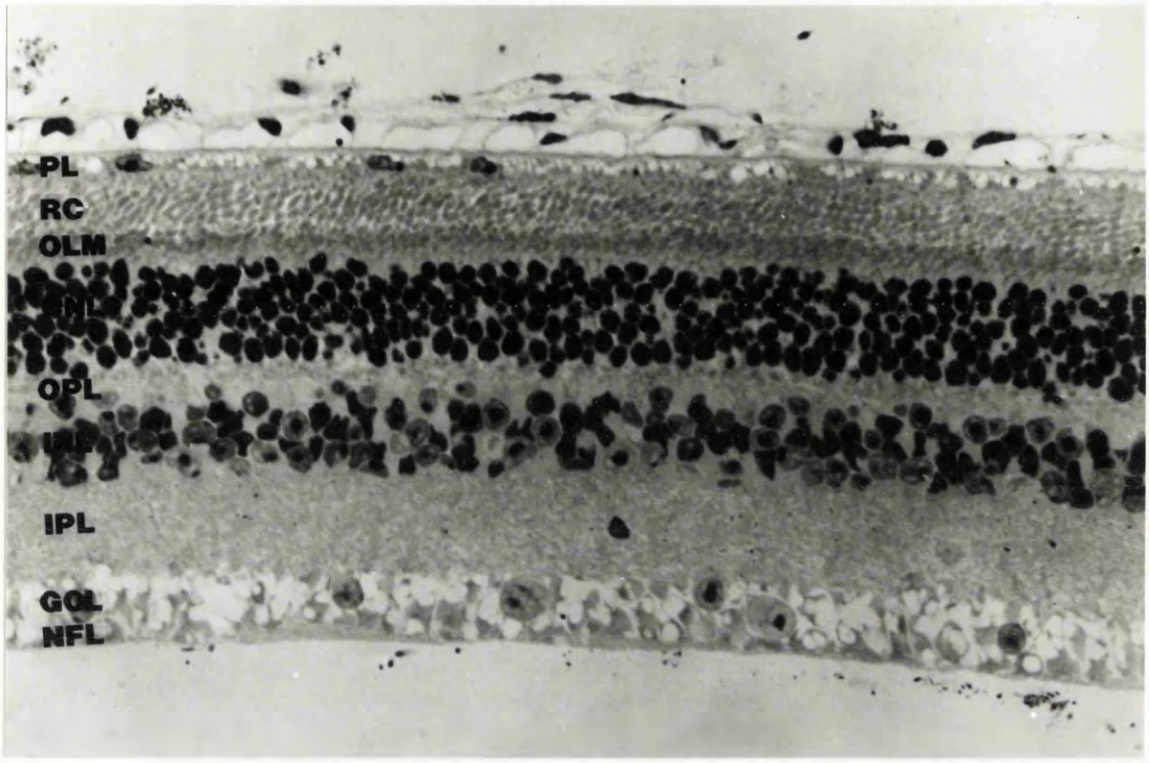
PL
RC
OLM
ONL
OPL
INL
IPL
GCL
NFL

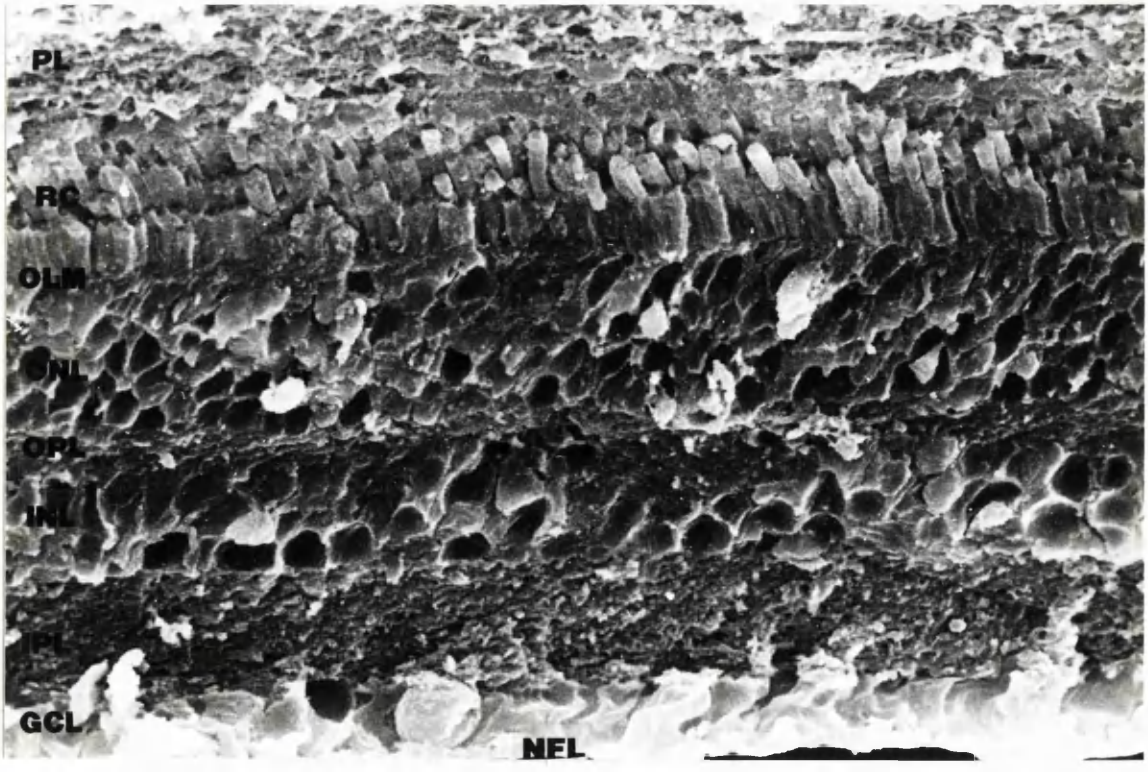
PL
RC
OLM
ONL
OPL
INL
IPL
GCL
NFL

FIGURE 4

Control retina

A semithin section, cut tangentially through the ganglion cell layer, showing cells of the ganglionic layer of the retina. Ganglion cells (large arrows) are larger and contain an eccentric nucleus with one/two prominent nucleoli. Small neurons (small arrows) are smaller and contain a large nucleus surrounded by a small amount of cytoplasm. One glial cell is marked with arrow heads.

(Mags. x 530)

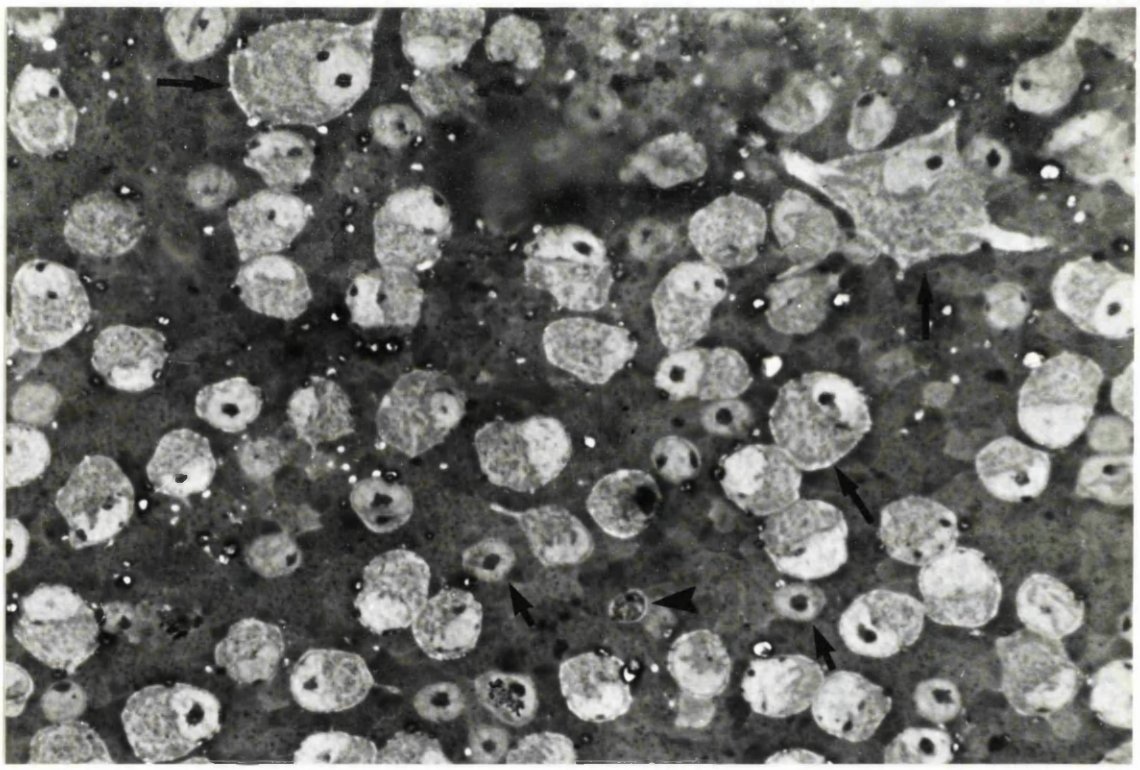

FIGURE 5

Three days post-trauma

A semithin section of the retina, cut tangentially through the ganglion cell layer, showing central chromatolysis (arrows) in the ganglion cells.

(Mags. x 625)

FIGURE 6

Seven days post-trauma

A tangentially cut semithin section of the ganglion cell layer of the retina showing the widespread chromatolysis in the cytoplasm of the ganglion cells (arrows).

(Mags. x 625)

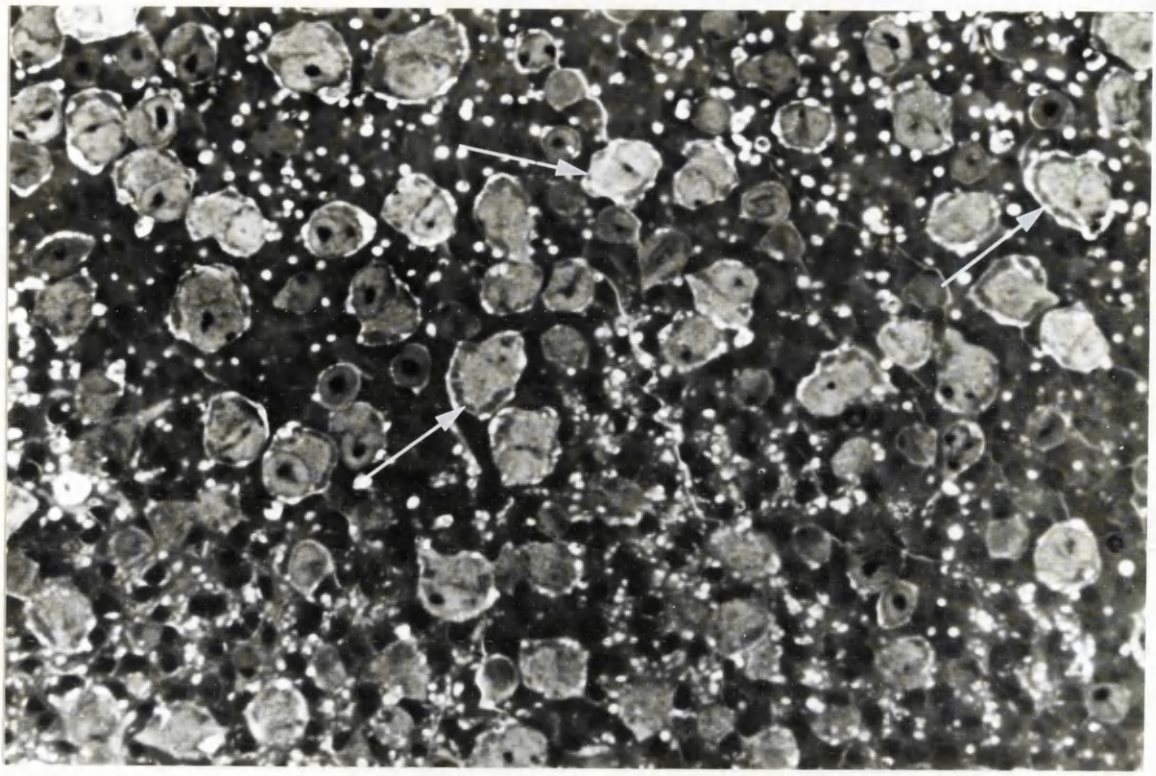

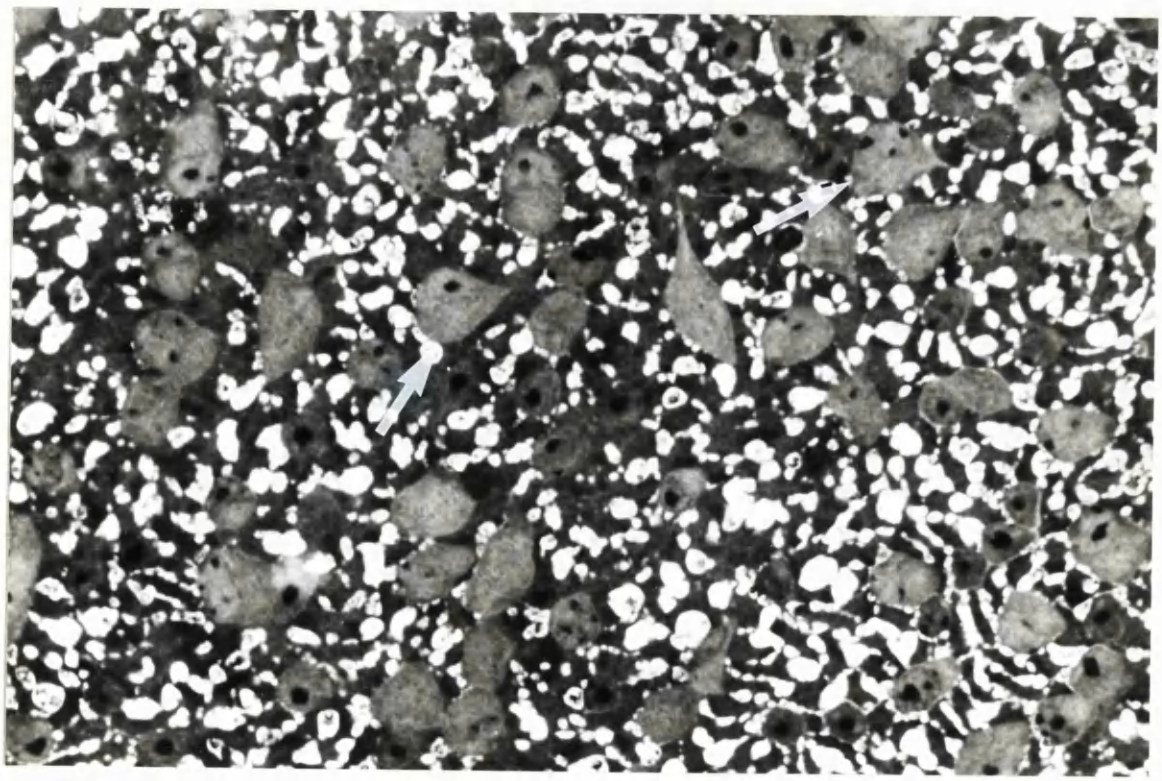

FIGURE 7

Fourteen days post-trauma

A tangentially cut semithin section of the ganglion cell layer of the retina, showing the chromatolytic ganglion cells (long arrows), pyknotic cells (short arrows) and small neurons (arrow heads). The cell population is reduced in comparison to control or short survival animals.

(Mags. x 625)

FIGURE 8

Fourteen days post-trauma

A semithin section of the ganglion cell layer cut tangentially, showing the paired microglia (arrows) reflecting the proliferation of these cells, and chromatolytic ganglion cells.

(Mags. x 1,000)

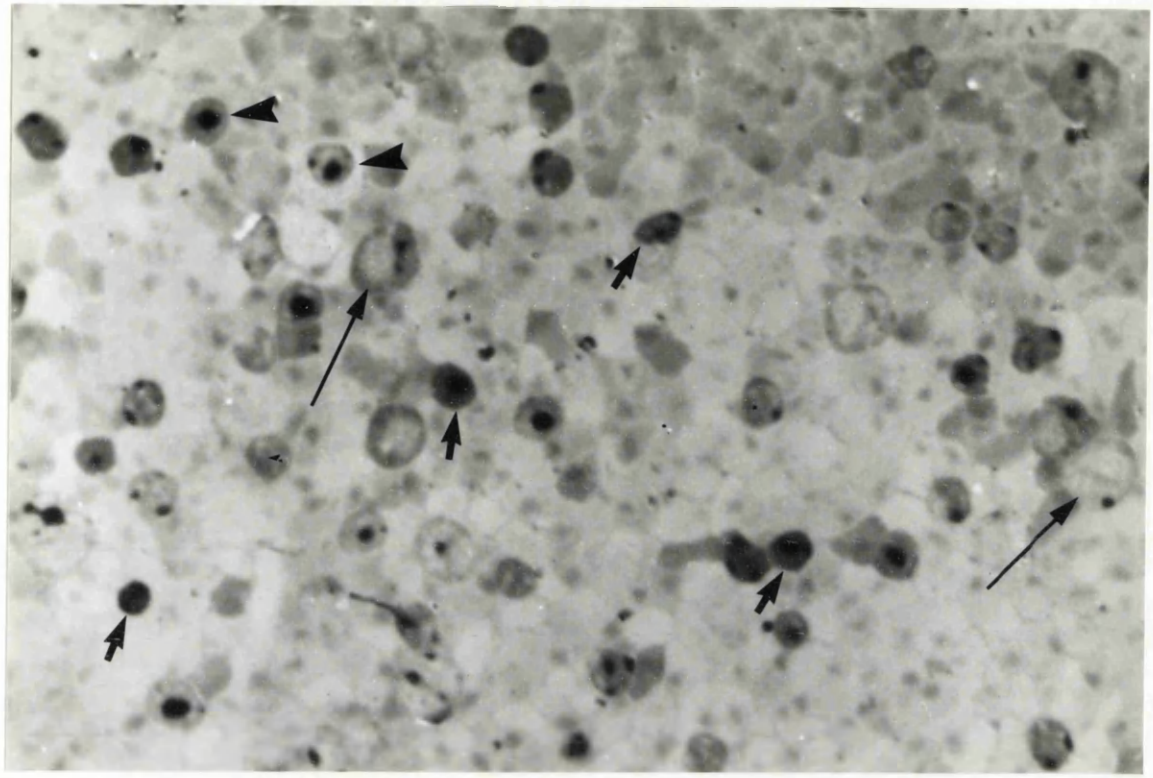

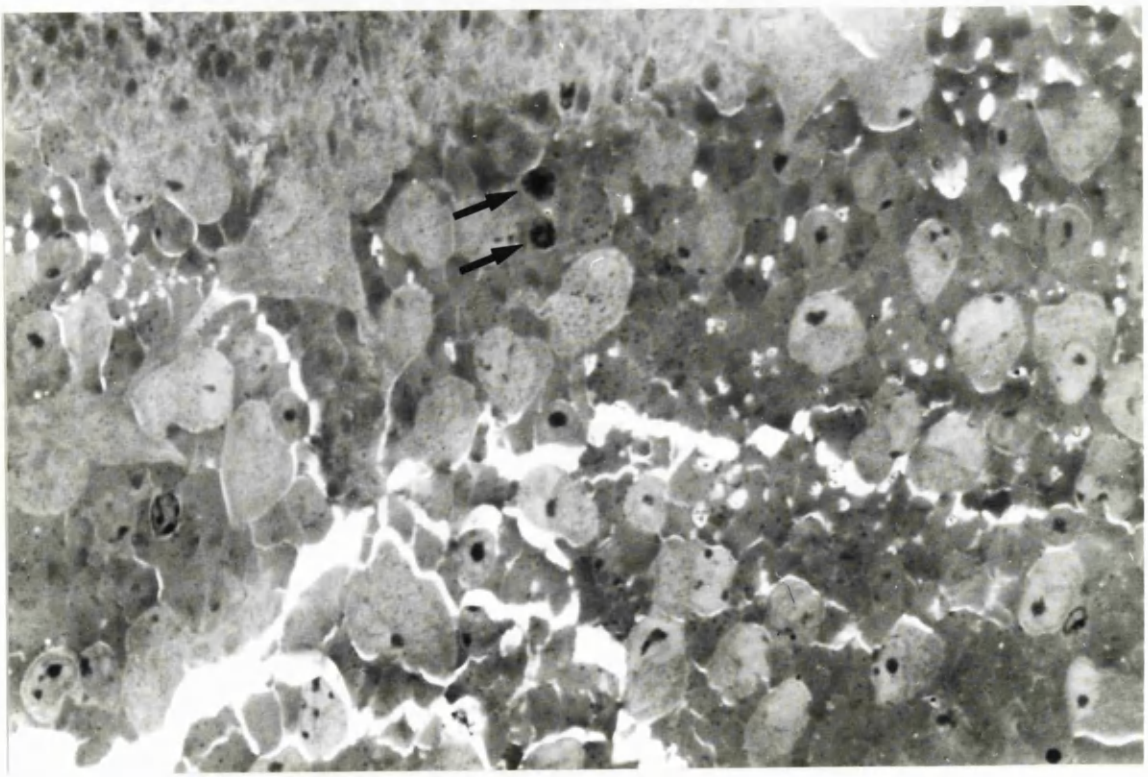

FIGURE 9

Control retina

A TEM micrograph showing ganglion cell (GC) part of small neuron (SN) and surrounding Müller cell process (M). The ganglion cell contains an eccentric nucleus (N) with a prominent nucleolus and the cytoplasm contains prominent Nissl bodies (NB), Golgi-apparatus (G) and other organelles.

(Mags. x 7,000)

FIGURE 10

Control retina

A TEM micrograph showing a normal ganglion cell with two nucleoli within the nucleus.

(Mags. x 7,000)

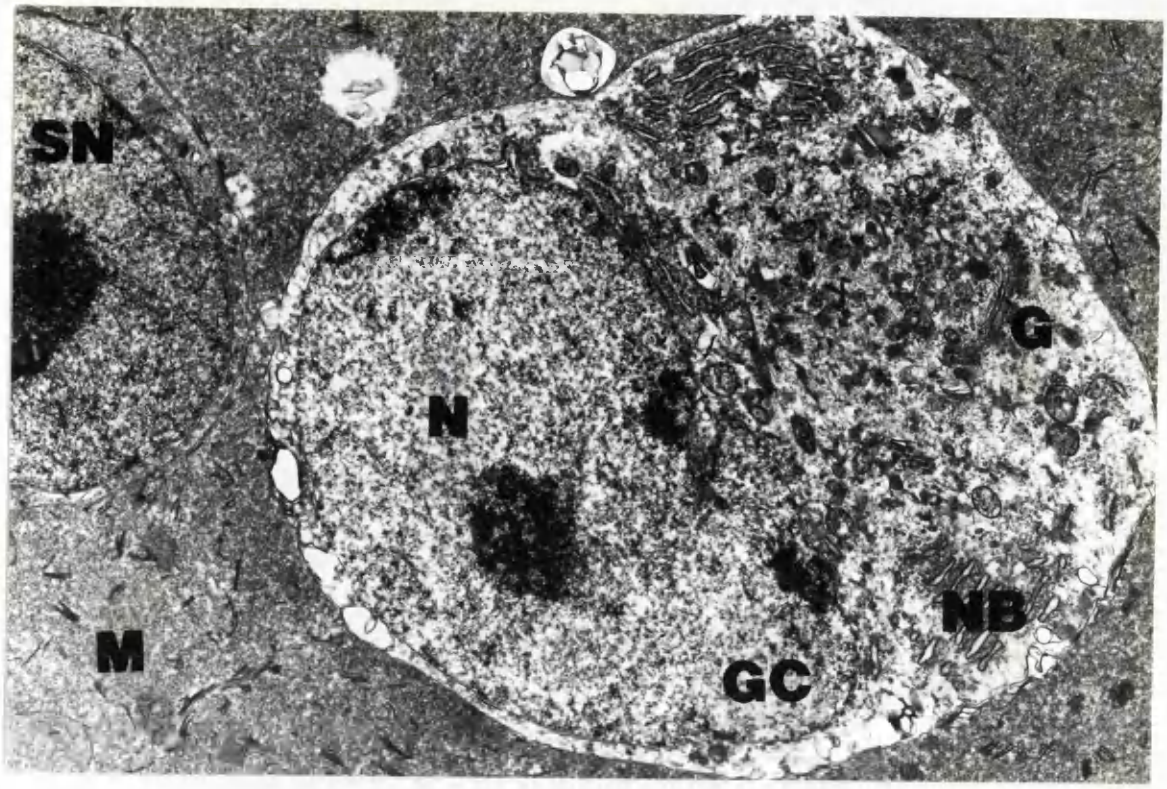
SN
N
G
NB
M
GC

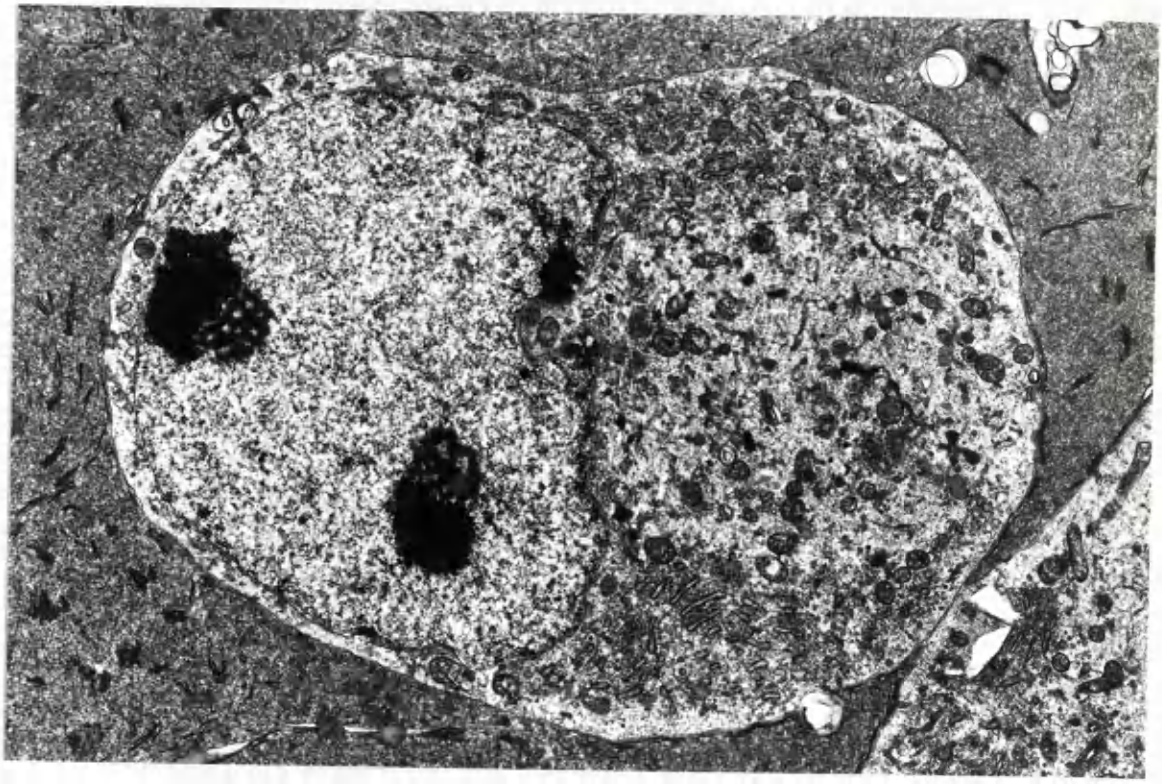

FIGURE 11

Control retina

A TEM micrograph of a ganglion cell showing a deep indentation (arrow) of the nuclear membrane facing the cytoplasm.

(Mags. x 5,600)

FIGURE 12

Control retina

A TEM micrograph of ganglion cell cytoplasm showing the normal distribution of Nissl bodies (NB), Golgi-apparatus (G), mitochondria (m), polyribosomes and dense bodies, N - nucleus.

(Mags. x 14,000)

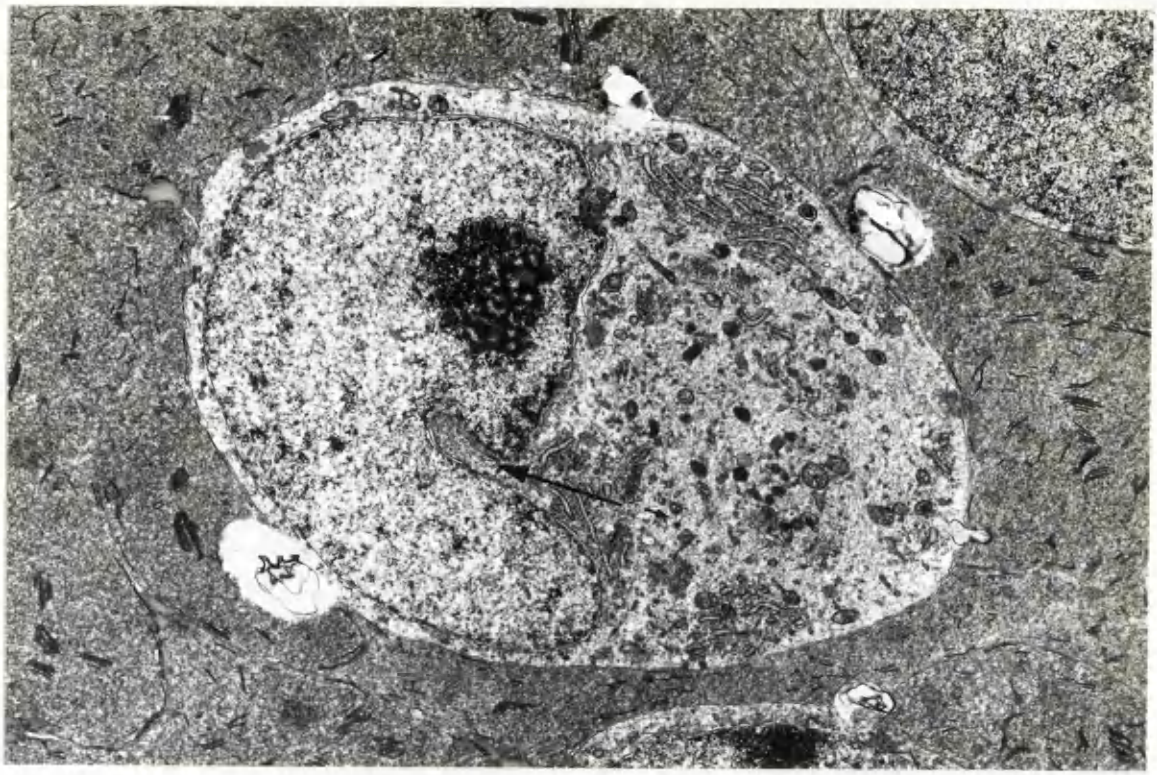

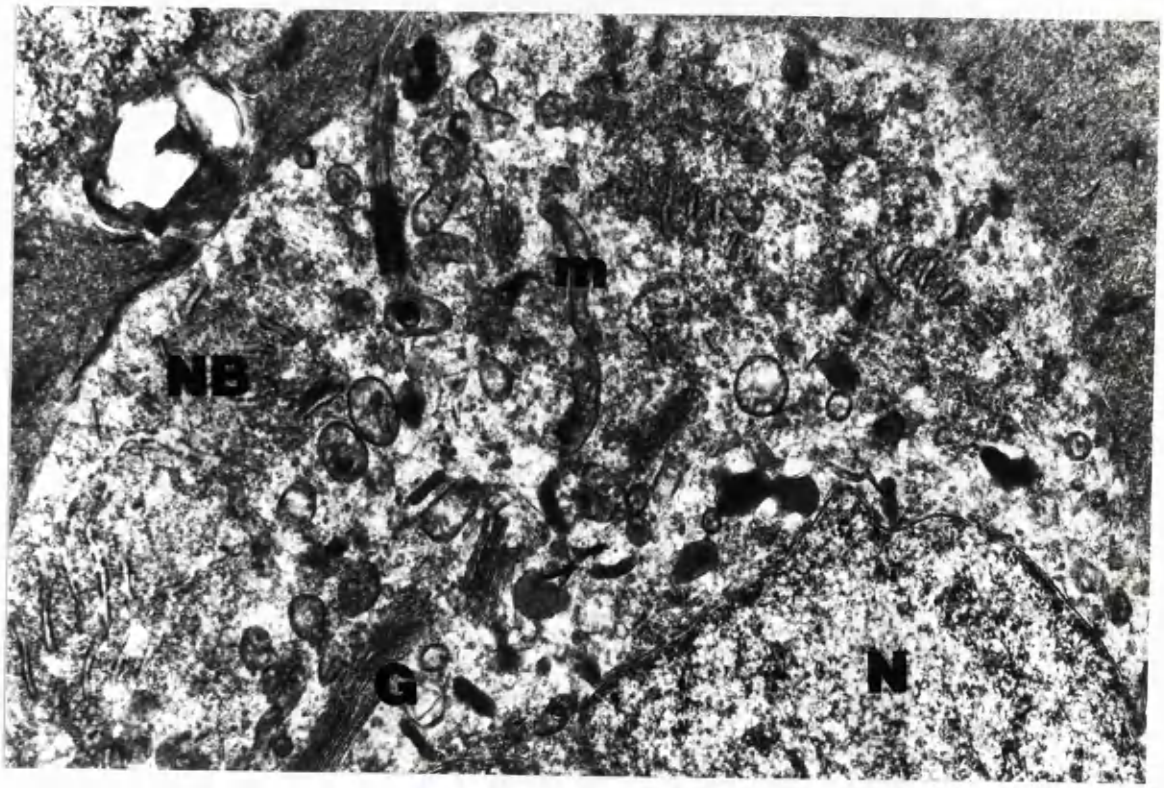
NB
M
G
N

FIGURE 13

Control retina

A TEM micrograph of a ganglion cell showing the Golgi-apparatus (G) lying peripherally, parallel arrays of rough ER forming the Nissl bodies (NB) and other organelles of the cytoplasm, together with part of the nucleus (N).

(Mags. x 6,000)

FIGURE 14

Control retina

A TEM micrograph showing the Golgi apparatus (G) which consists of a series of parallel stacks of agranular cisternae, N - nucleus.

(Mags. x 52,000)

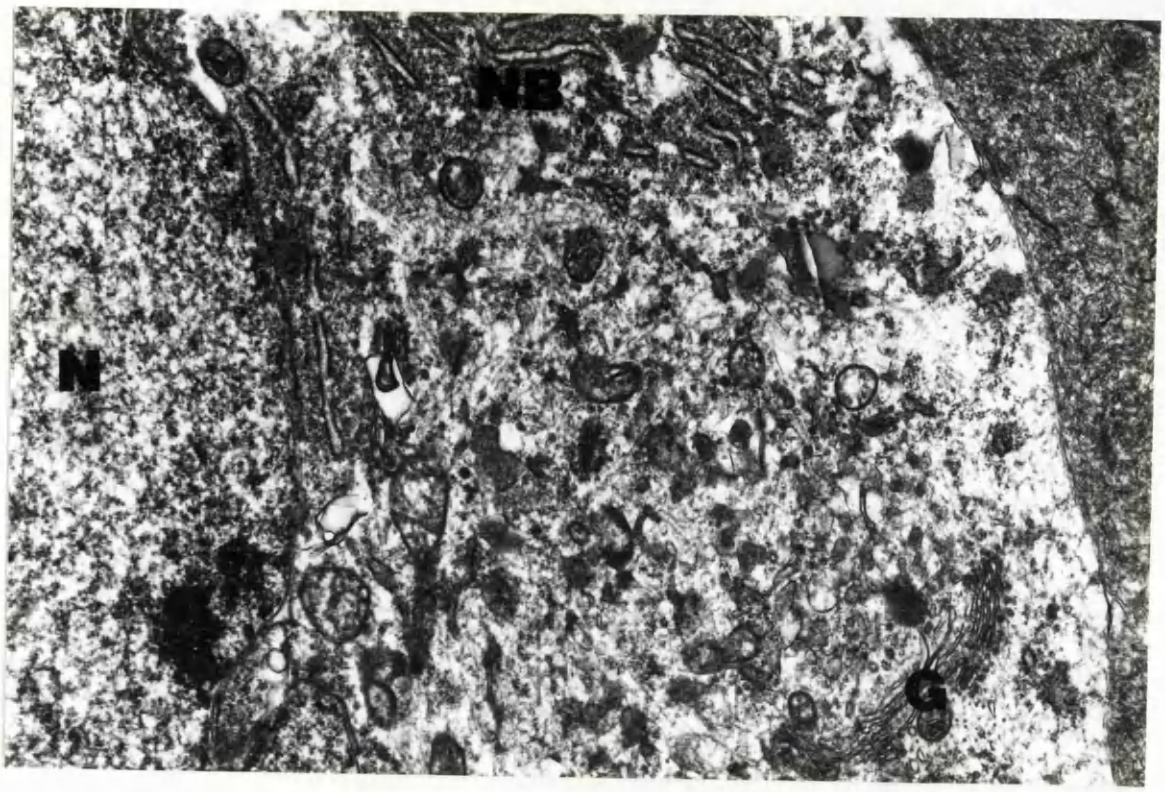
NB
N
G

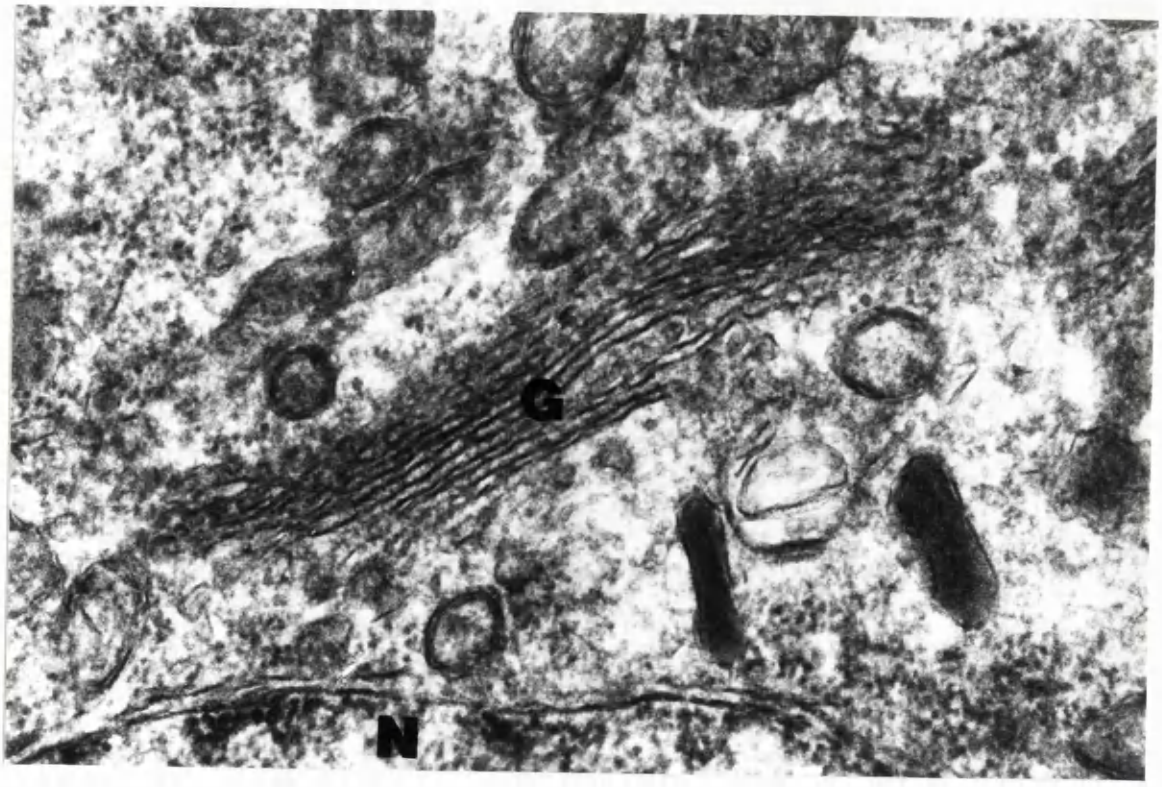
G
N

FIGURE 15

Control retina

A TEM micrograph showing a Nissl body consisting of parallel cisternae of rough ER and intercisternal free polyribosomes.

(Mags. x 37,800)

FIGURE 16

Control retina

A TEM micrograph showing a Nissl body consisting of a whorl-like arrangement of the cisternae of the rough ER and free polyribosomes.

(Mags. x 49,000)

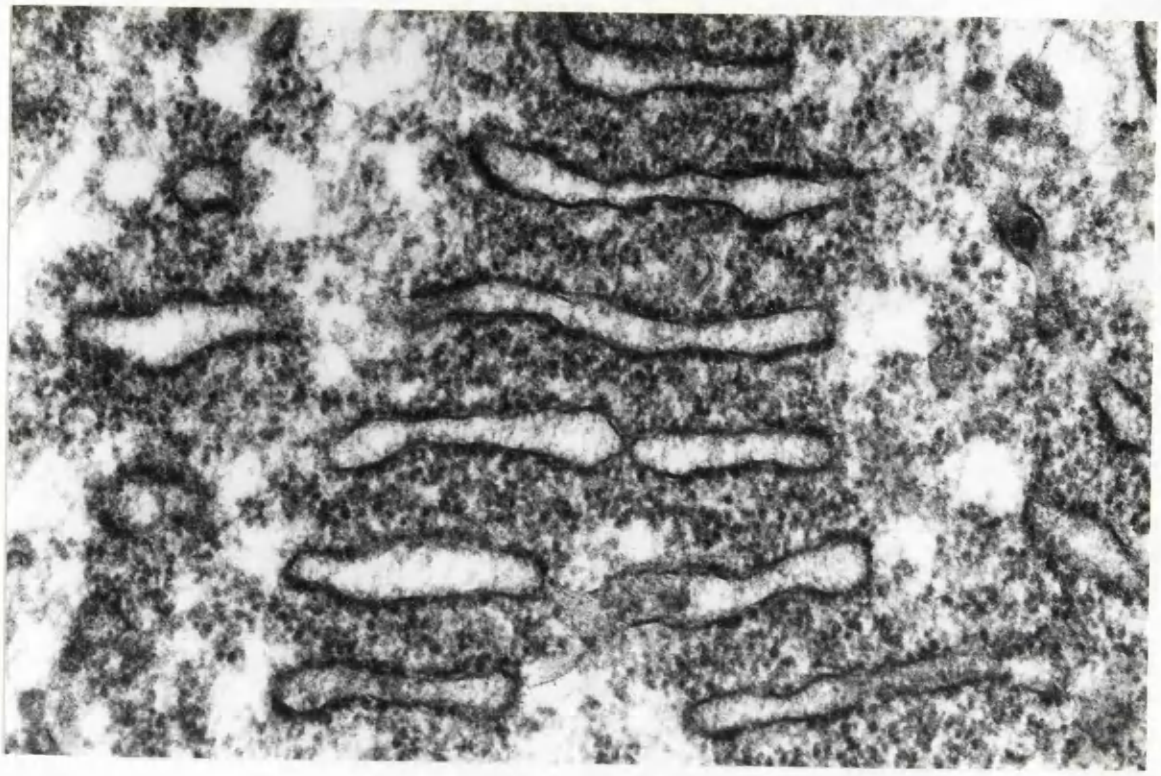

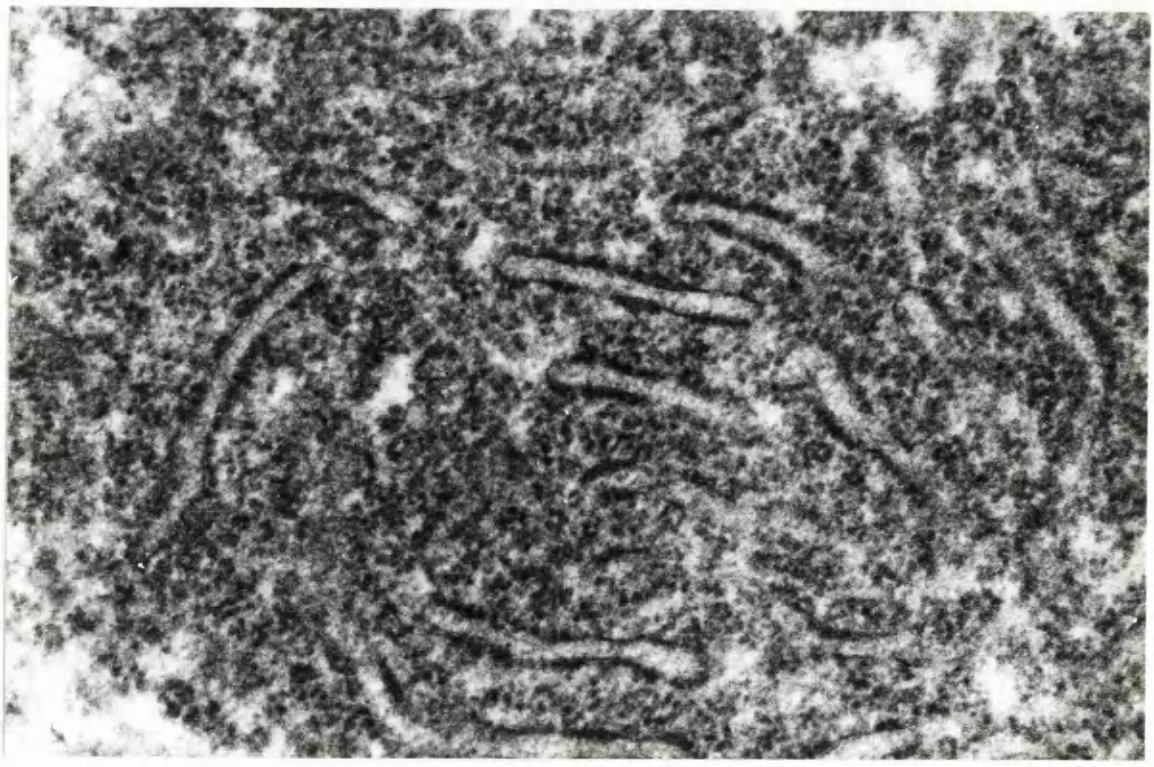

FIGURE 17

Control retina

A TEM micrograph showing a small neuron of the ganglion cell layer. It has a comparatively large nucleus with nucleolus. The thin rim of cytoplasm surrounds the nucleus.

(Mags. x 4,500)

FIGURE 18

Control retina

A TEM micrograph showing the cytoplasm of a small neuron. The cytoplasm contains only a few scattered organelles.

(Mags. x 11,000)

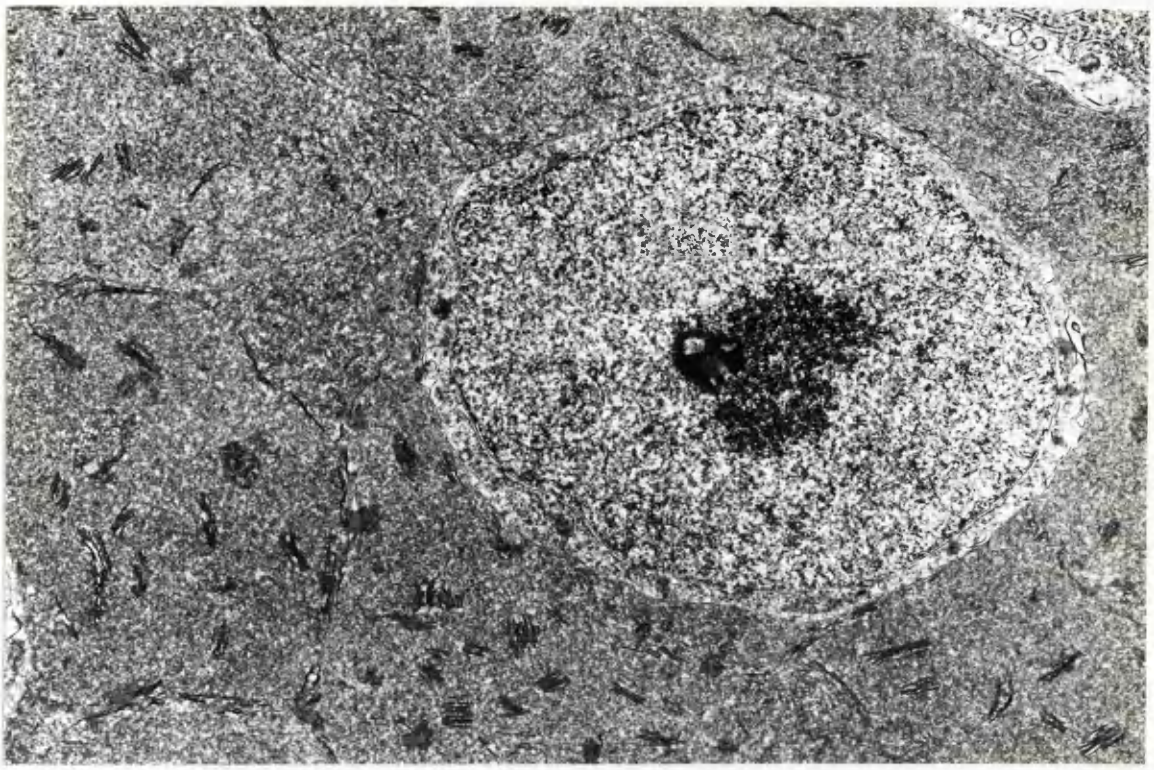

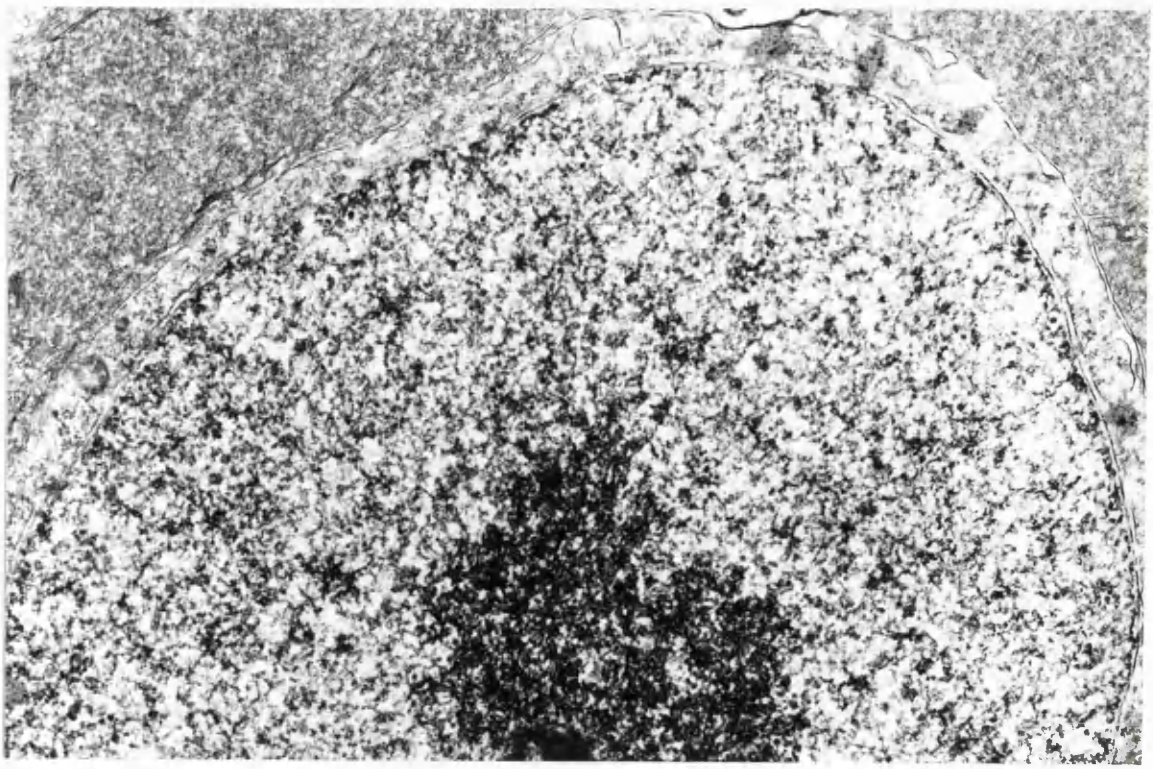

FIGURE 19

Three days post-trauma

A TEM micrograph showing two ganglion cells with the features of central chromatolysis:- i.e. peripheral margination of rough ER (RER), and polyribosomes, an eccentric nucleus (N), and an irregular nuclear profile facing the cytoplasm.

(Mags. x 6,300)

FIGURE 20

Three days post-trauma

A TEM micrograph showing the cytoplasm of a ganglion cell with central chromatolysis. The central chromatolytic zone contains mitochondria, dense bodies and a few polyribosomes. There is a clear line of demarcation (curved arrows) between the central chromatolytic and peripheral non-chromatolytic zones. A part of the nucleus (N) is seen.

(Mags. x 15,300)

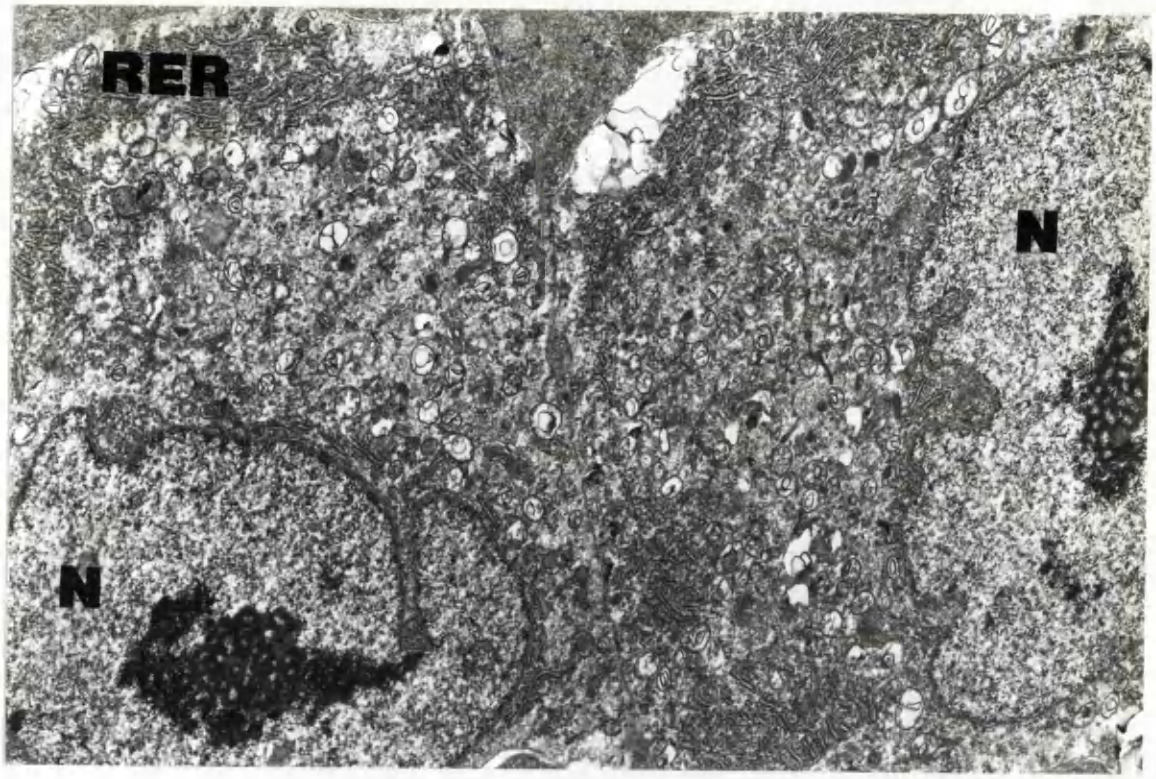
RER
N
N

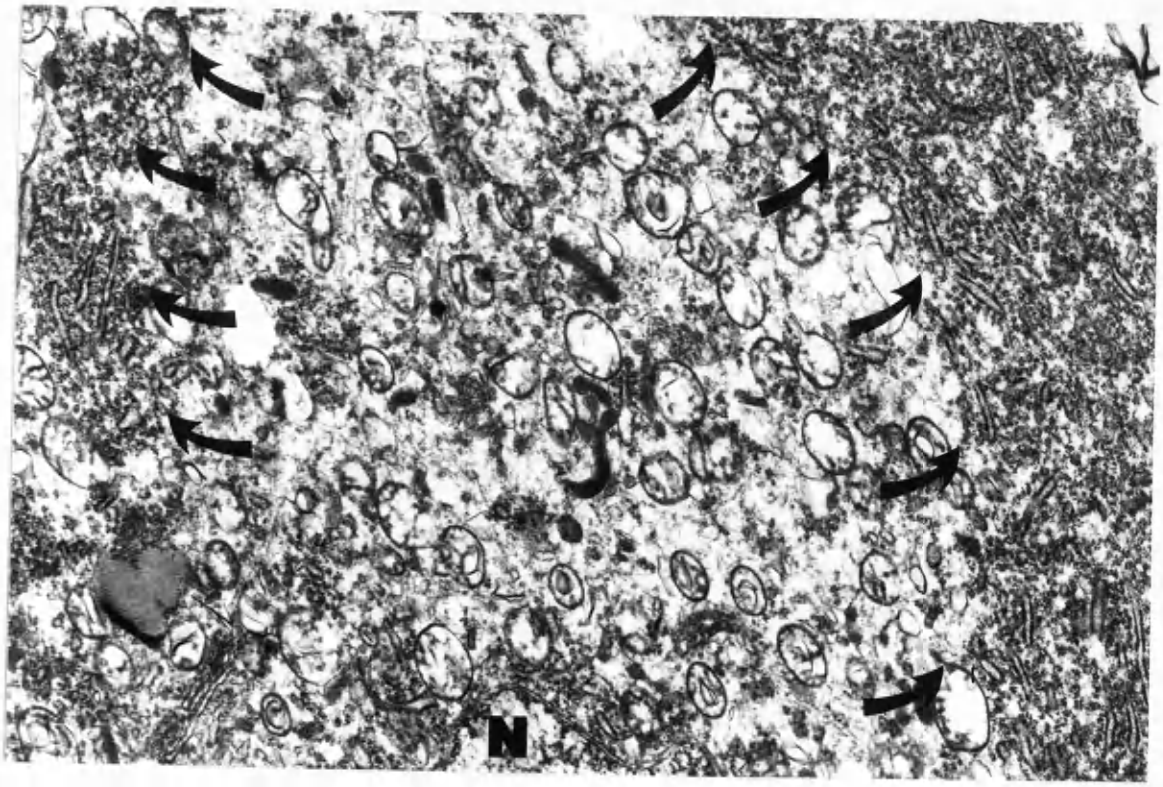
N

FIGURE 21

Seven days post-trauma

A degenerating ganglion cell:

A TEM micrograph showing a ganglion cell with wide spread chromatolysis in the cytoplasm. The eccentric, irregular nucleus (N) contains a nucleolus. The Golgi-apparatus (G) lies peripherally.

(Mags. x 6,300)

FIGURE 22

Seven days post-trauma

A degenerating ganglion cell

A TEM micrograph of the chromatolytic region of the cytoplasm of a ganglion cell (Figure 21) showing Golgi-apparatus (G) mitochondria, dense bodies and neurofilaments. No rough ER is visible in this field.

(Mags. x 14,000)

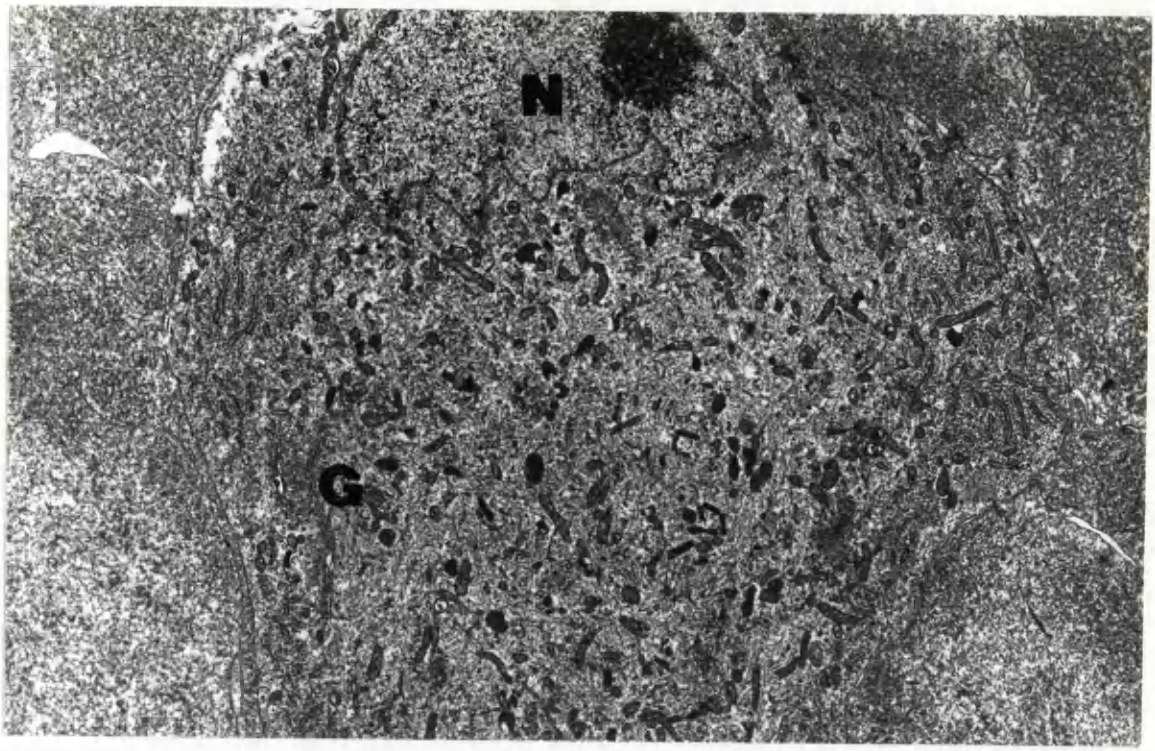
N
G

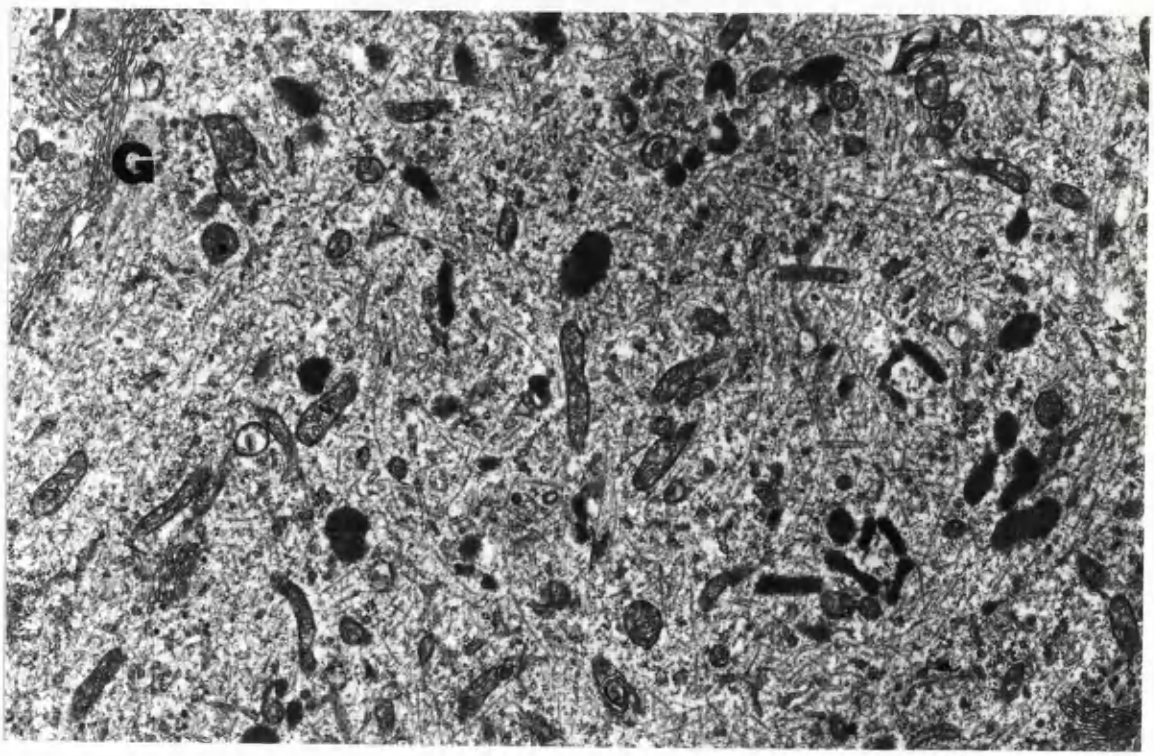
G

FIGURE 23

Seven days post-trauma

A TEM micrograph. In this survival group, a few injured ganglion cells exhibit central chromatolysis comparable to that of the three days survival. There is a clear line (curved arrows) between the central chromatolytic zone and peripheral non-chromatolytic zone. Part of the nucleus (N) is seen.

(Mags. x 16,500)

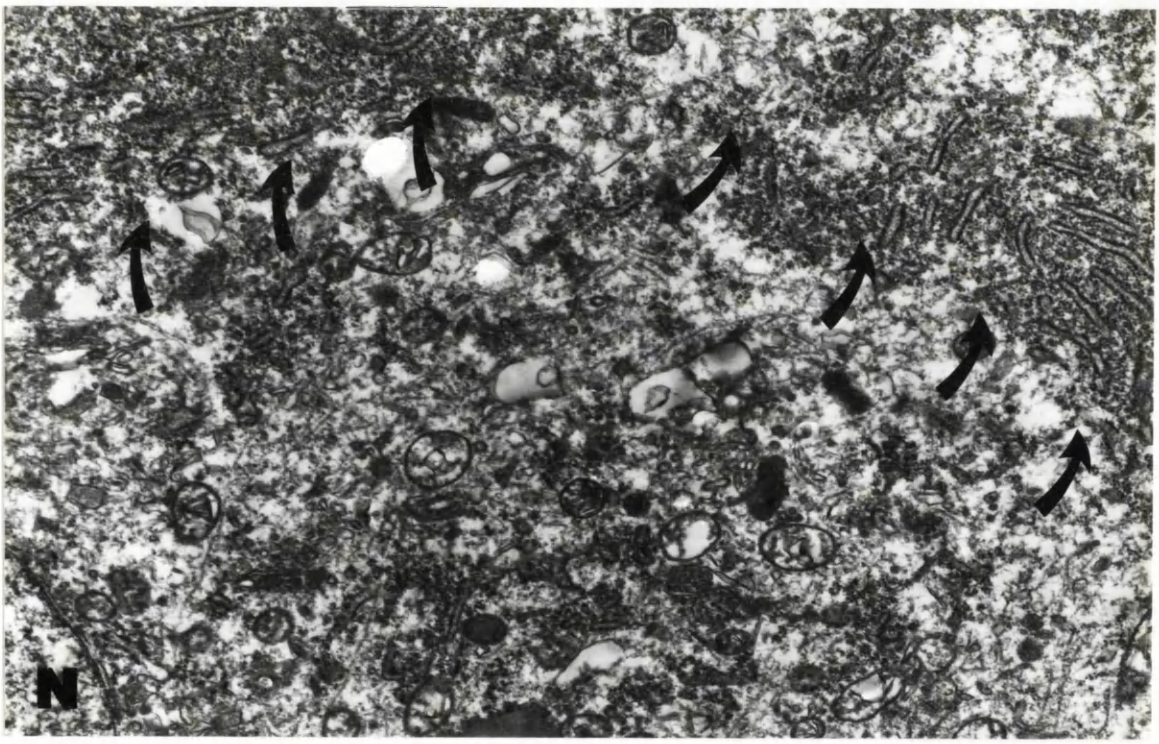
N

FIGURE 24

Seven days post-trauma

Degenerating ganglion cells:

A TEM micrograph showing two degenerating ganglion cells. The nuclei (N) are eccentric and mis-shapen. Focal aggregations of chromatin are present along the nuclear envelope. Nissl substances have disappeared from the cytoplasm leaving only a few dense bodies and Golgi-apparatus (G).

(Mags. x 6,200)

FIGURE 25

Seven days post-trauma

A degenerating ganglion cell:

A TEM micrograph. The cytoplasm of the degenerating ganglion cell (Figure 24) shows the absence of rough ER and polyribosomes, but the presence of the Golgi-apparatus (G) and an increased number of dense bodies.

(Mags. x 14,000)

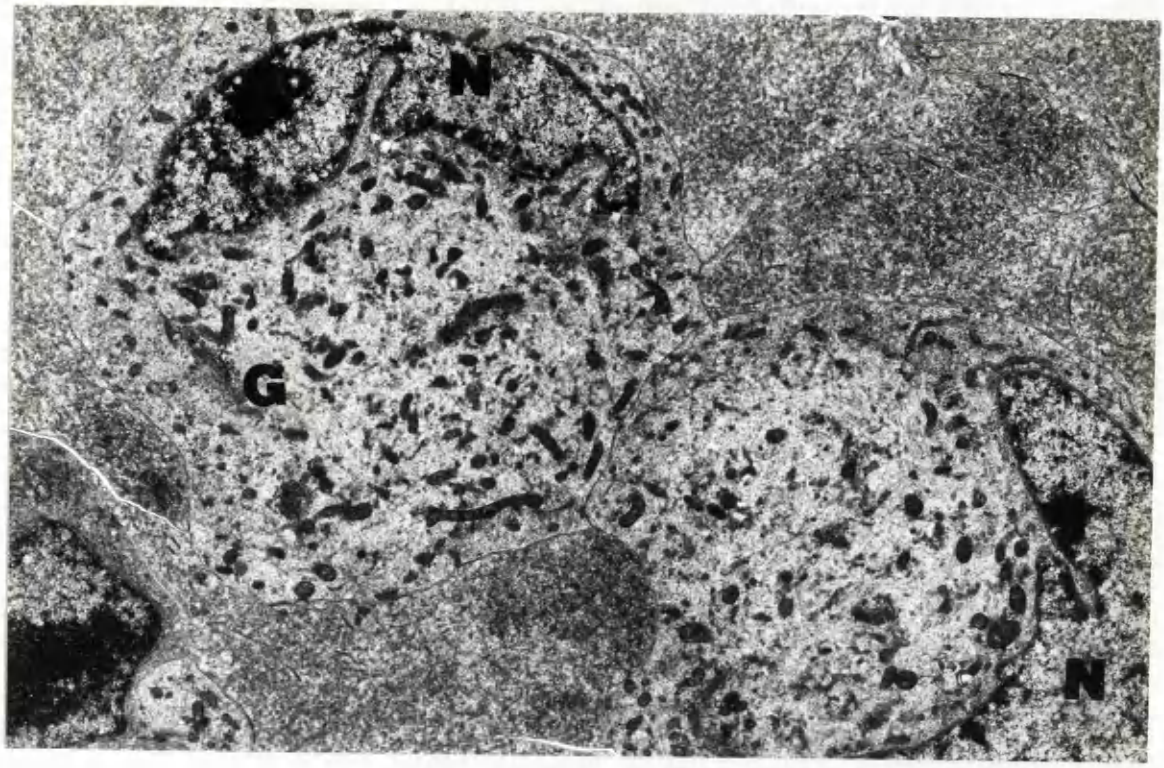
N
G
N

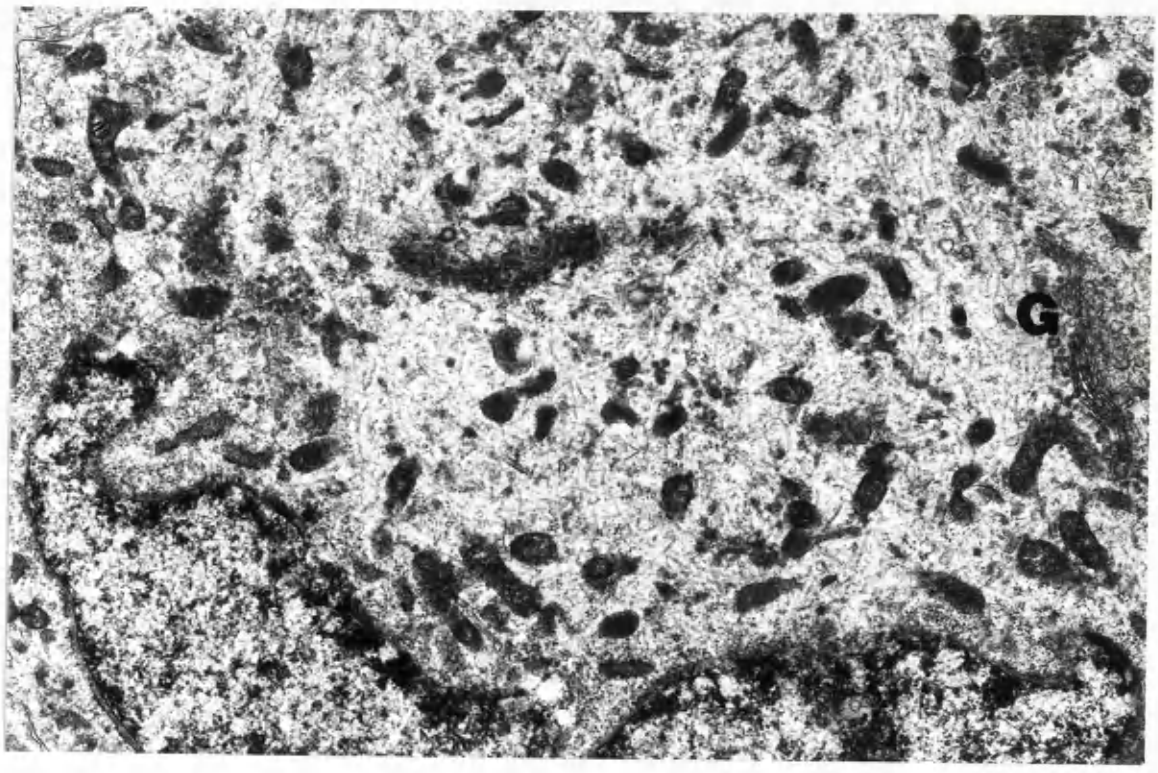
G

FIGURE 26

Seven days post-trauma

A degenerating ganglion cell:

A TEM micrograph at high magnification showing the increased amount of smooth ER (arrows) in the cytoplasm due to degranulation of rough ER.

(Mags. x 51,000)

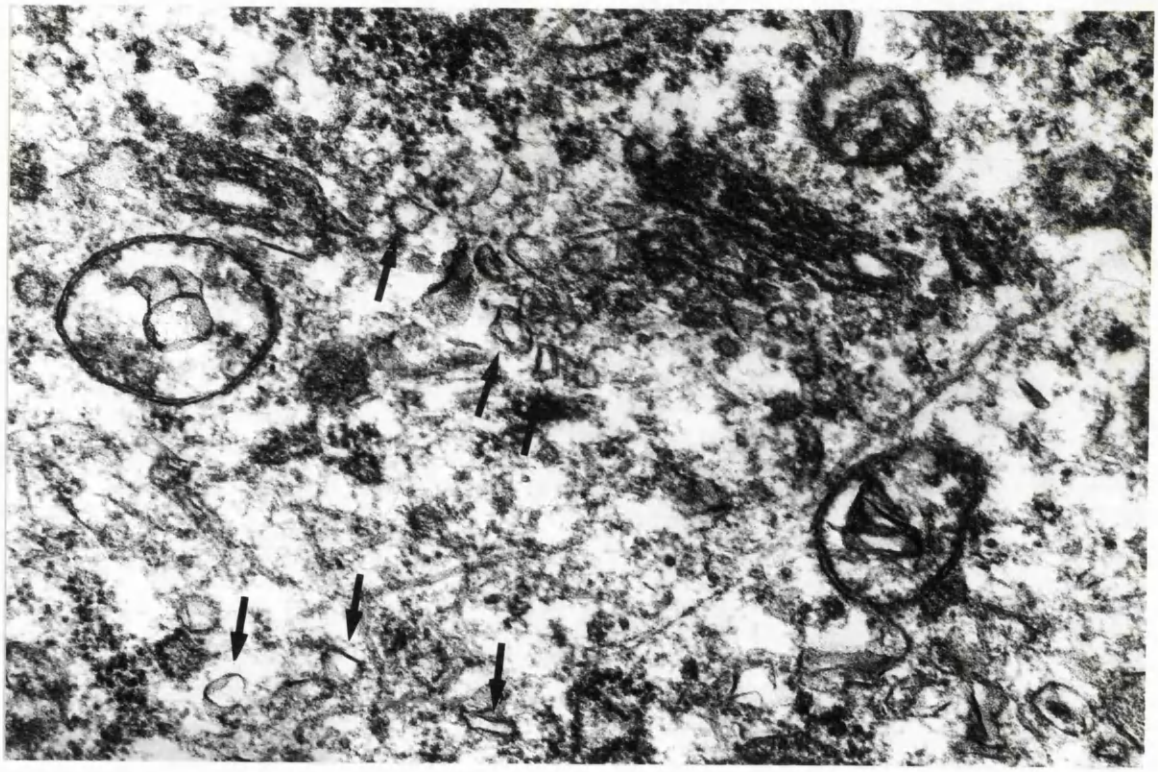

FIGURE 27

Seven days post-trauma

A regenerating ganglion cell:

A TEM micrograph showing a regenerating ganglion cell. The nucleus (N) has an irregular nuclear profile and contains an enlarged, vacuolated nucleolus (n). The cytoplasm contains discrete Nissl bodies (stars), a good number of Golgi-apparati (G) and other organelles.

(Mags. x 7,000)

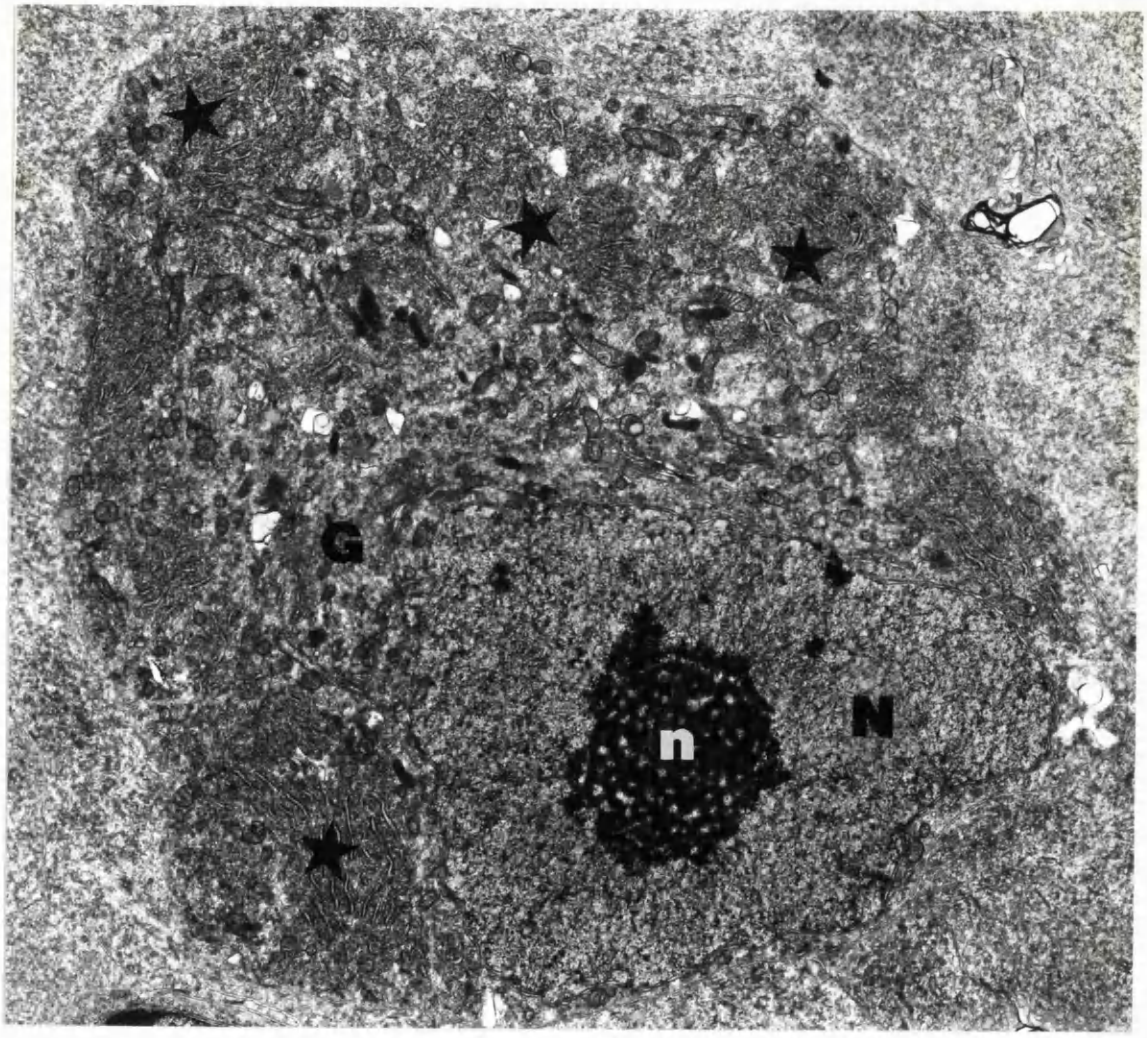
G
n
N

FIGURE 28

Seven days post-trauma

A regenerating ganglion cell:

A TEM micrograph of the cytoplasm of a regenerating ganglion cell showing the rough ER and polyribosomes abutted to the nuclear membrane and indentation (arrow).

(Mags. x 14,000)

FIGURE 29

Seven days post-trauma

A regenerating ganglion cell:

A TEM micrograph of the cytoplasm (Figure 27) at high magnification, showing the increased amount of smooth ER (arrows) formed perhaps due to enhanced metabolism (Whitnall & Grafstein, 1983).

(Mags. x 52,500)

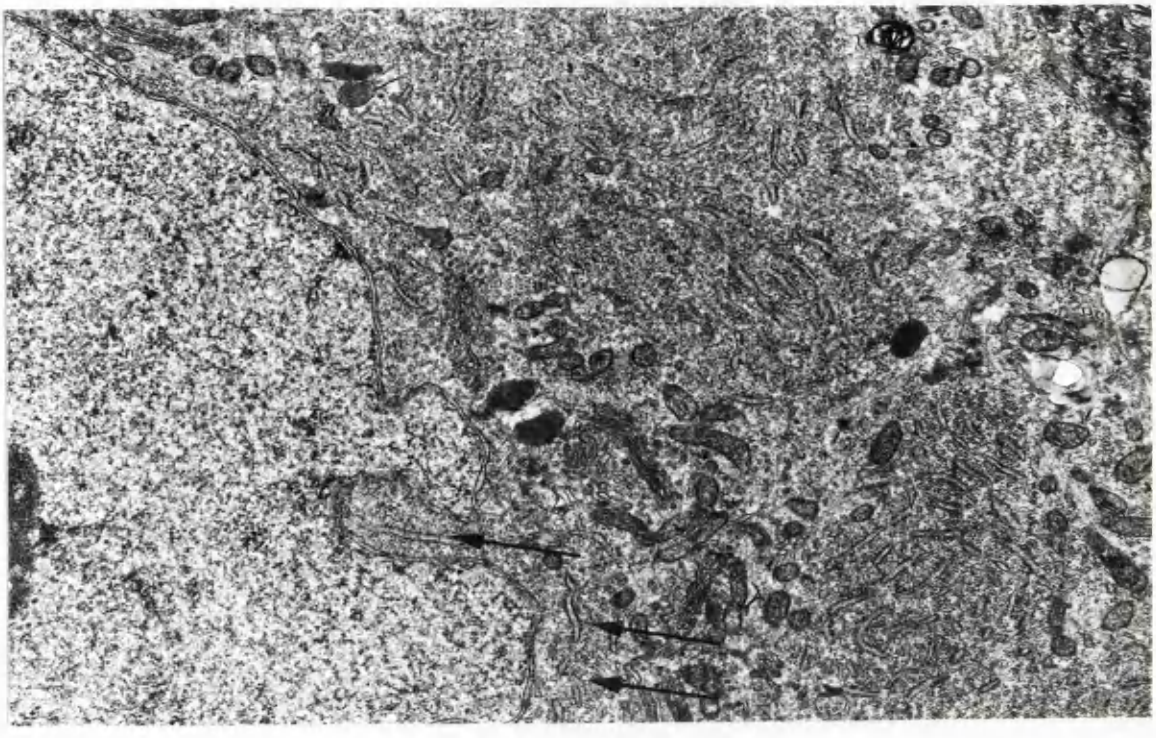

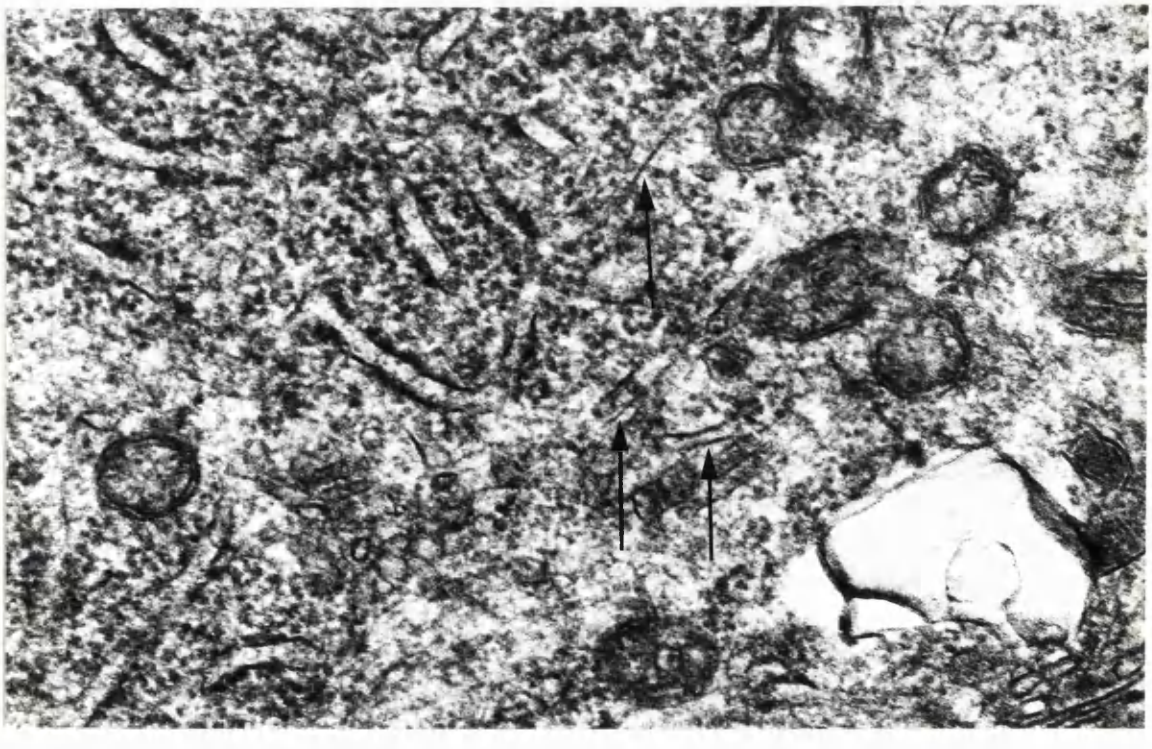

FIGURE 30

Fourteen days post-trauma

A degenerating ganglion cell:

A TEM micrograph showing a degenerating ganglion cell (GC), small neuron (SN) and transverse sections of Müller cell processes (MP). The degenerating ganglion cell has atrophied to the size of the small neurons (SN). The nucleus (N) is deeply furrowed. Focal aggregations of chromatin are present mainly along the nuclear envelope. Most of the cytoplasmic organelles have disappeared and the cytoplasm become electron lucent.

(Mags. x 6,200)

FIGURE 31

Fourteen days post-trauma

A degenerating ganglion cell:

A TEM micrograph at high magnification of the ganglion cell (Figure 30). The cytoplasm contains Golgi-apparatus (G), few dense bodies and mitochondria, N - nucleus.

(Mags. x 15,500)

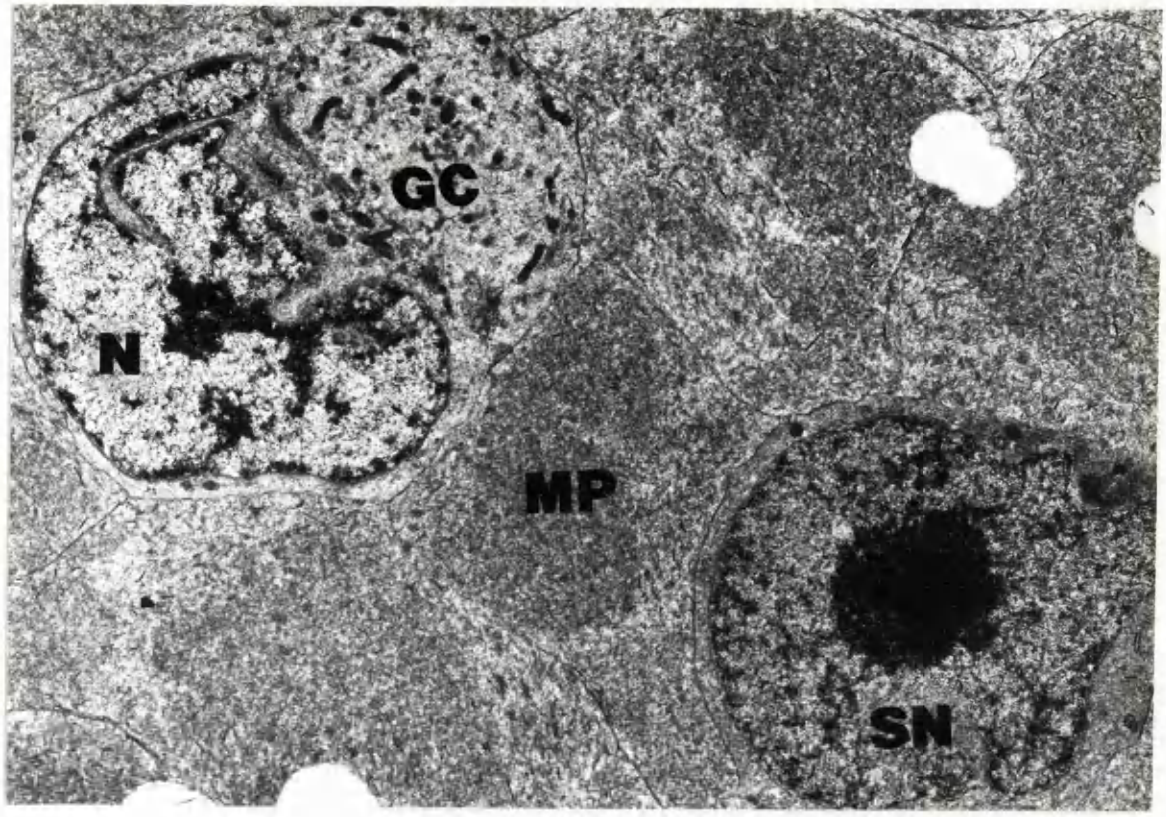
GC
N
MP
SN

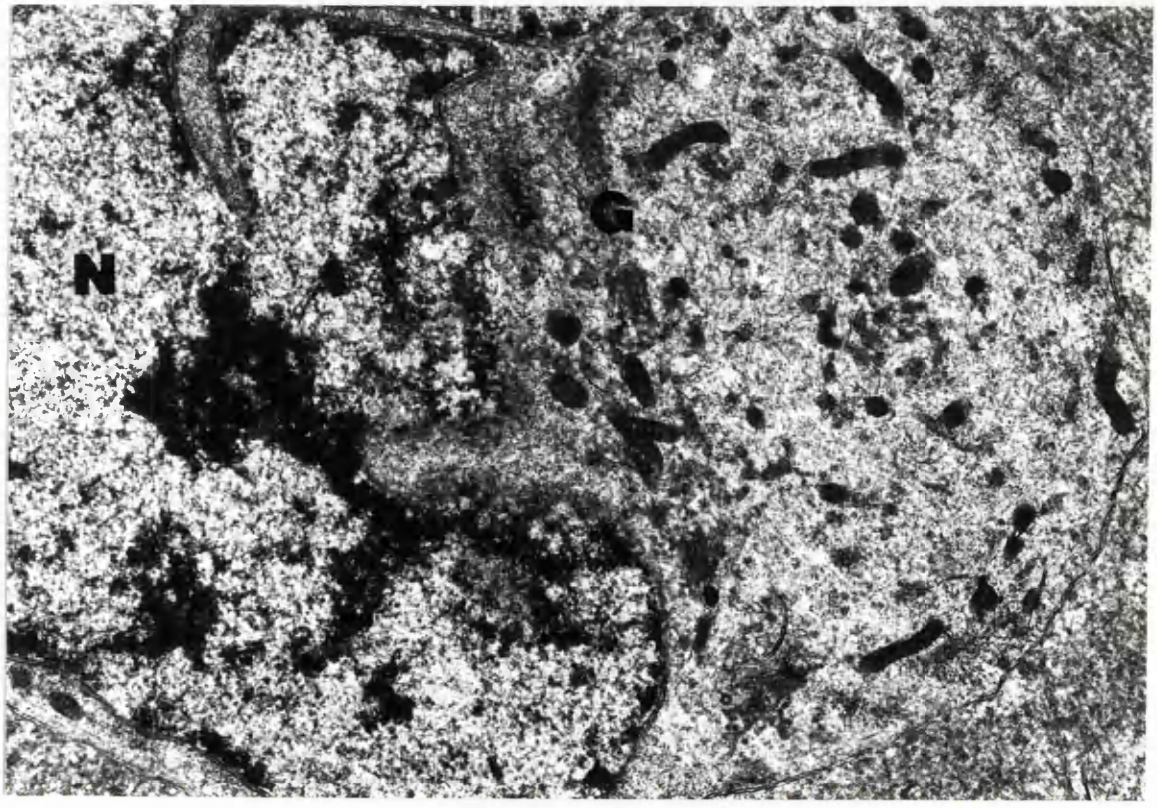
N
G

FIGURE 32

Fourteen days post-trauma

Degenerating ganglion cell:

A TEM micrograph showing a degenerating ganglion cell surrounded by a proliferation of astrocytic (AP) and Müller cell processes (MP). The mis-shapen nucleus (N) contains focal aggregations of chromatin. The cytoplasm lacks organelles and is electron dense.

(Mags. x 8,400)

FIGURE 33

Fourteen days post-trauma

Degenerating ganglion cell:

A TEM micrograph of the cytoplasm at high magnification showing the increased amount of smooth ER (long arrows) and electron dense mitochondria (short arrows).

(Mags. x 52,500)

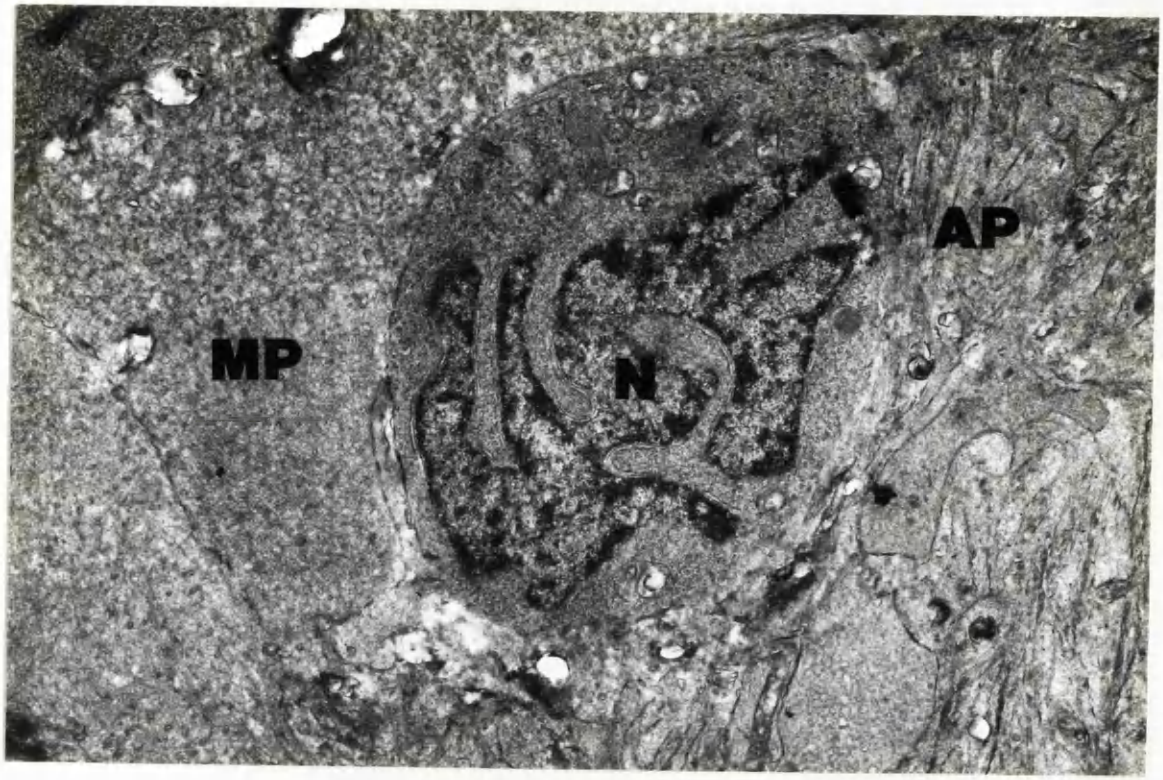
AP
MP
N

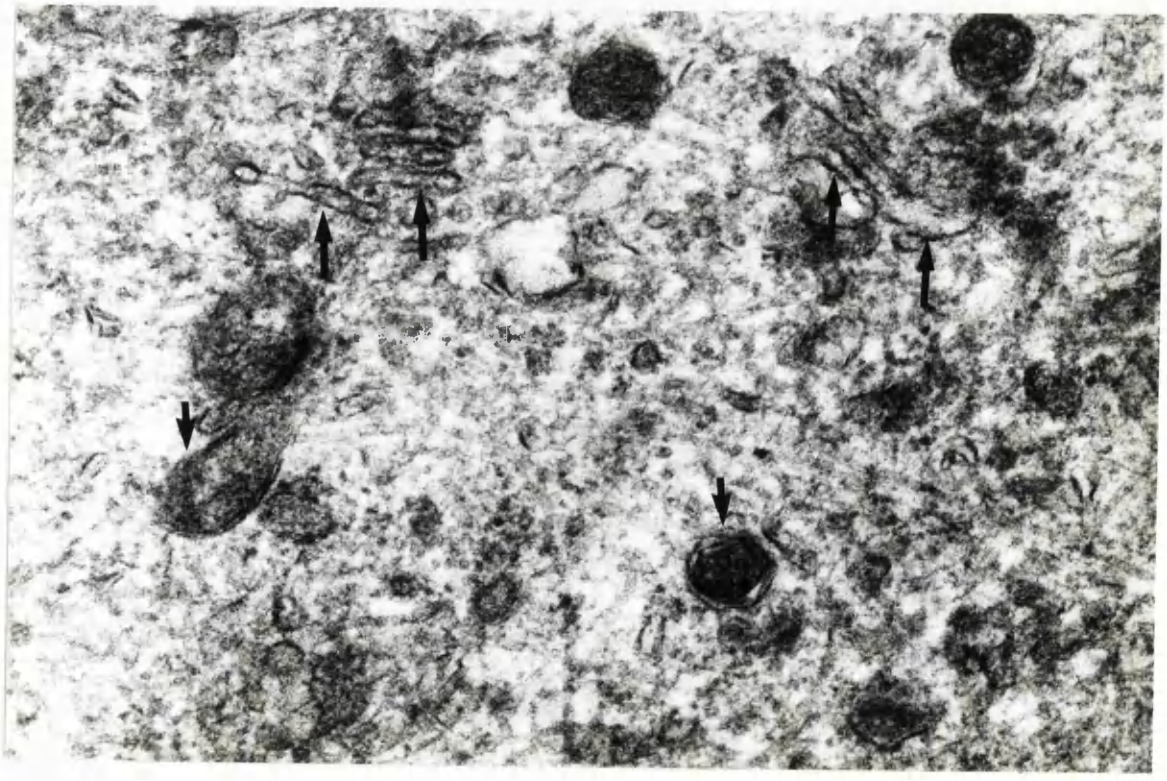

FIGURE 34

Fourteen days post-trauma

A regenerating ganglion cell:

A TEM micrograph of a regenerating ganglion cell showing the irregular profile of the nuclear outline, the enlarged vacuolated nucleolus (N) and long parallel stacks of rough ER (RER) in the cytoplasm. N - nucleus.

(Mags. x 5,600)

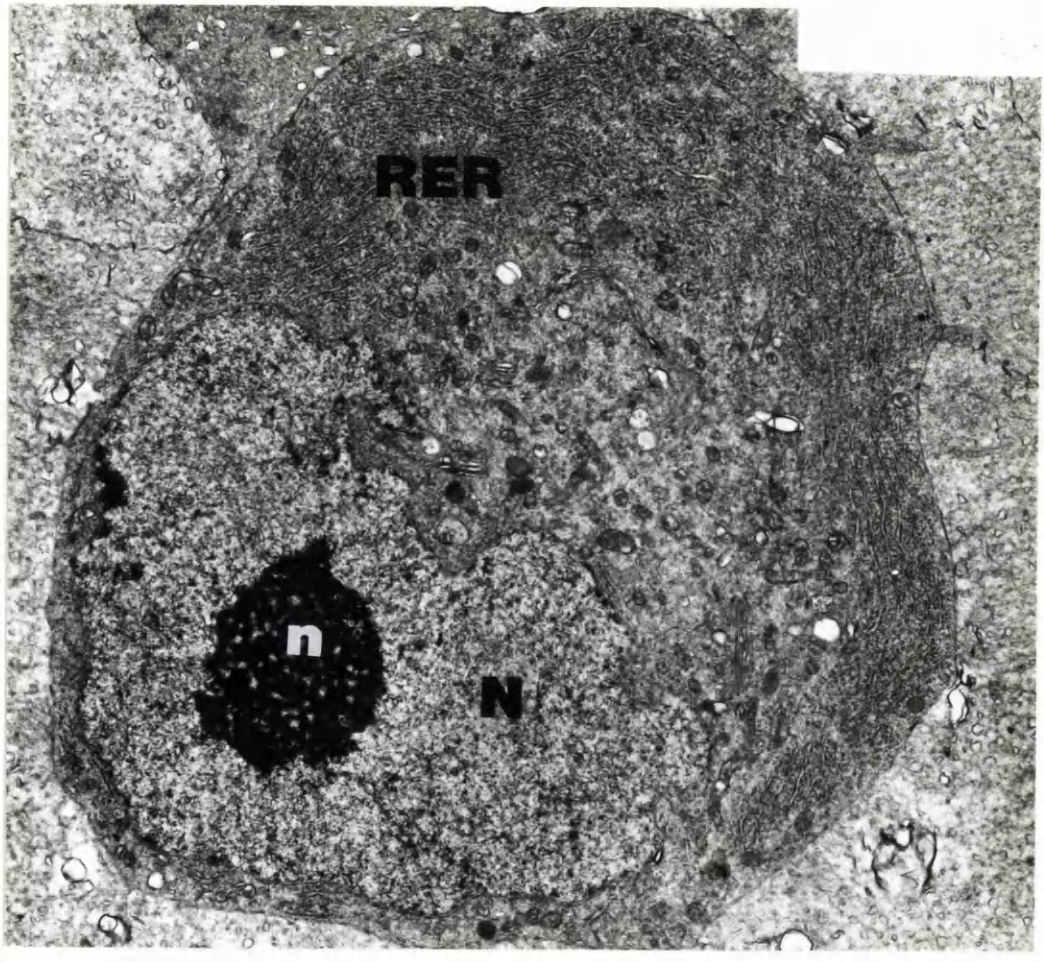
RER
n
N

FIGURE 35

Fourteen days post-trauma

A regenerating ganglion cell:

A TEM micrograph of the cytoplasm of a regenerating ganglion cell (Figure 34) showing parallel arranged stacks of rough ER (RER) reflecting the increased synthesis of extrinsic proteins (Murray & Forman, 1971).

(Mags. x 16,800)

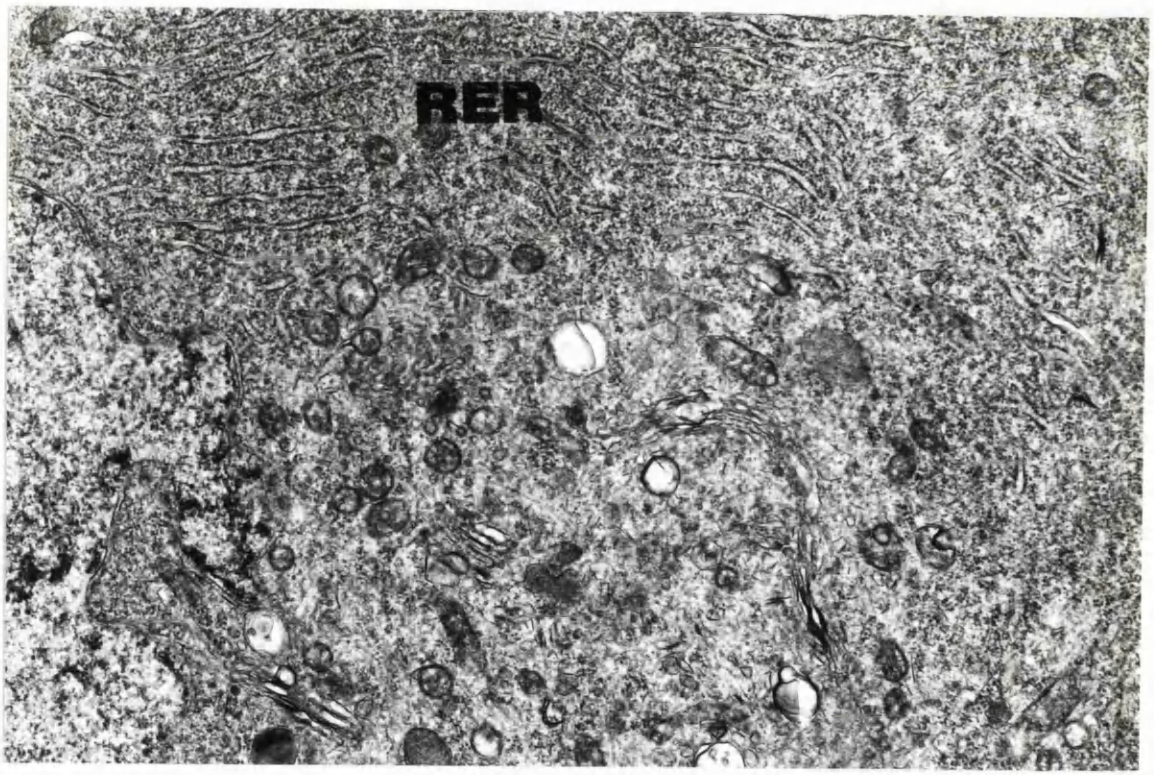
RER

FIGURE 36

Control retina

Nucleolus of a ganglion cell:

A TEM micrograph of a control nucleolus. The nucleolus consists of nucleolonemal strands (NS), (a reticular arrangement of fibrillar protein), fibrillar centres (FC) (spherical-shaped fibrillar protein), nucleolar vacuoles (V) and nucleolar associated chromatin (NAC) adjacent to the nucleolus proper.

(Mags. x 30,800)

FIGURE 37

Three days post-trauma

Nucleolus of a central chromatolytic ganglion cell:

A TEM micrograph of a nucleolus of a ganglion cell with central chromatolysis. There is no significant ultrastructural difference of the nucleolus in comparison to the control (Fig. 36).

(Mags. x 30,800)

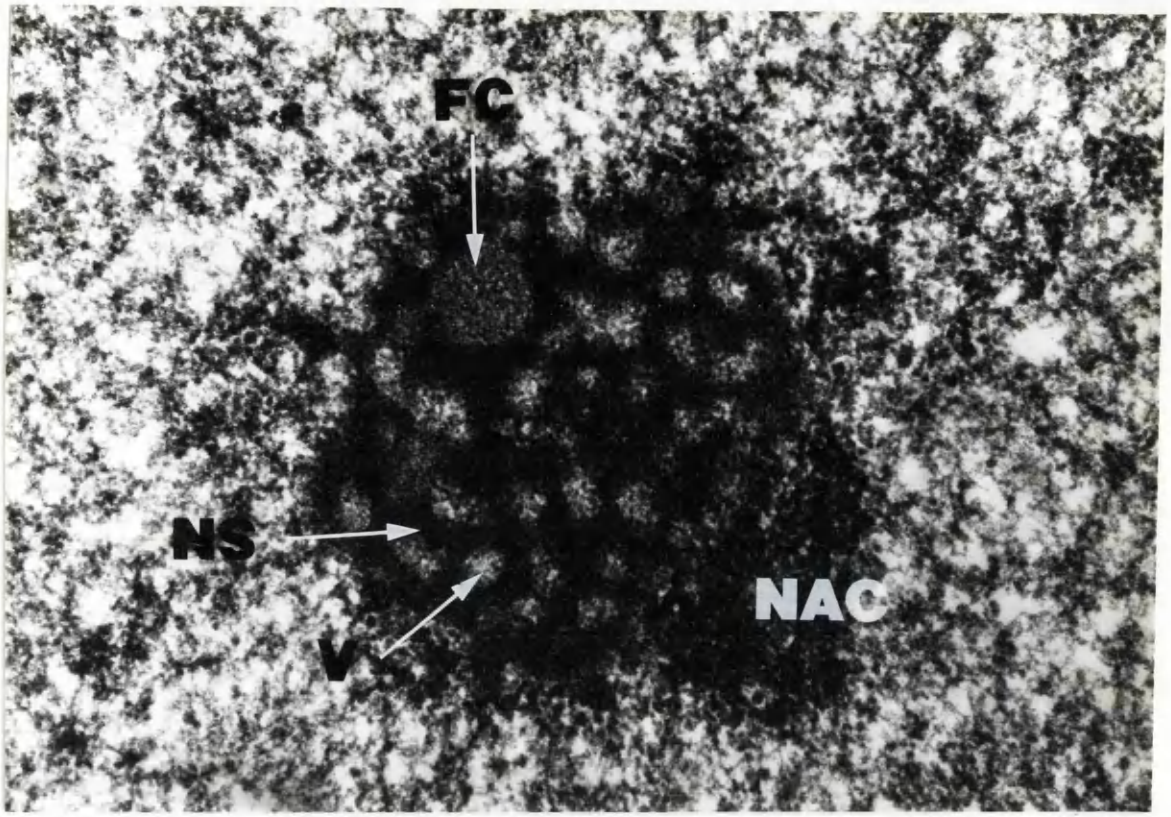
FC
NS
V
NAC

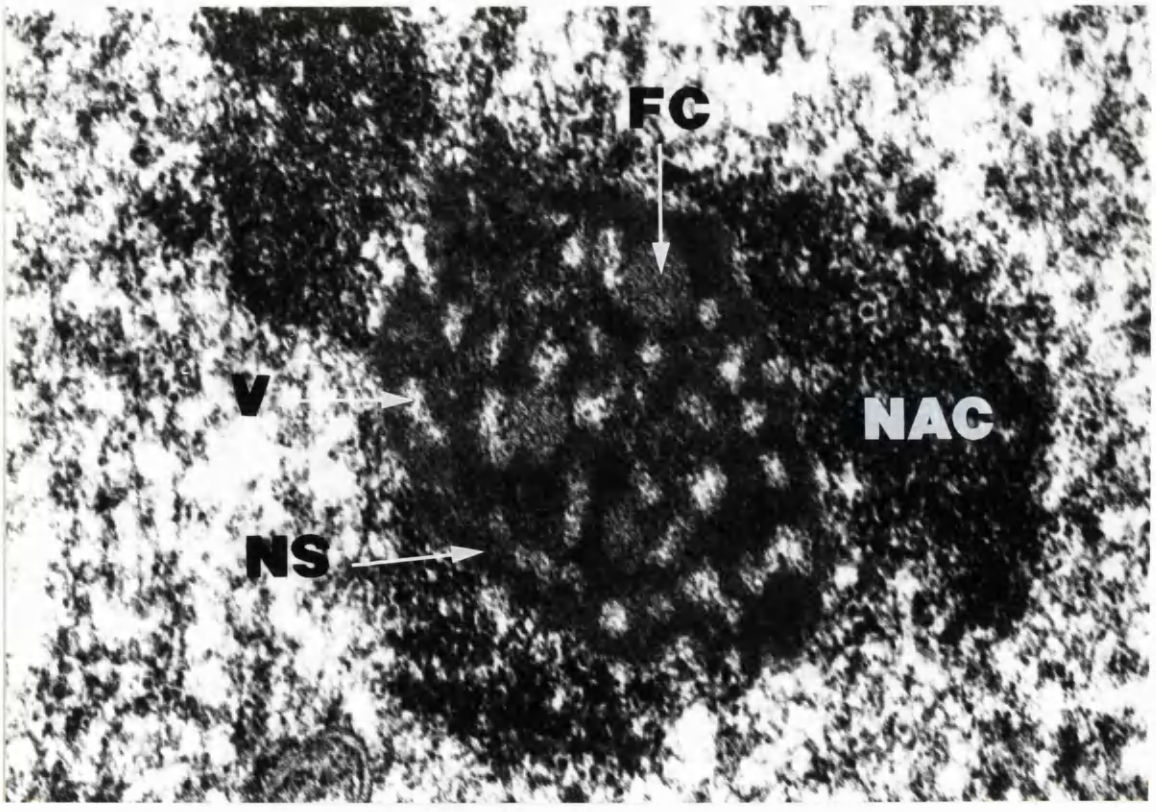
FC
V
NAC
NS

FIGURE 38

Seven days post-trauma

The nucleolus of a regenerating ganglion cell:

A TEM micrograph showing the loosening of nucleolonemal strands (NS), increased amount of nucleolar vacuoles (V) and the granular appearance of the nucleus in comparison to the control (Figure 36). Spherical shaped fibrillar centres (FC) are present. Nucleolar associated chromatin (NAC) is distributed around the nucleolus.

(Mags. x 30,800)

FIGURE 39

Fourteen days post-trauma

The nucleolus of a regenerating ganglion cell:

A TEM micrograph showing the nucleolus of a regenerating ganglion cell. The ultrastructure of the nucleolus does not differ much in comparison to (Figure 38) except for the presence of nucleolar associated chromatin (NAC) which reforms clumps. Nucleolonemal strands (NS); fibrillar centre (FC).

(Mags, x 30,800)

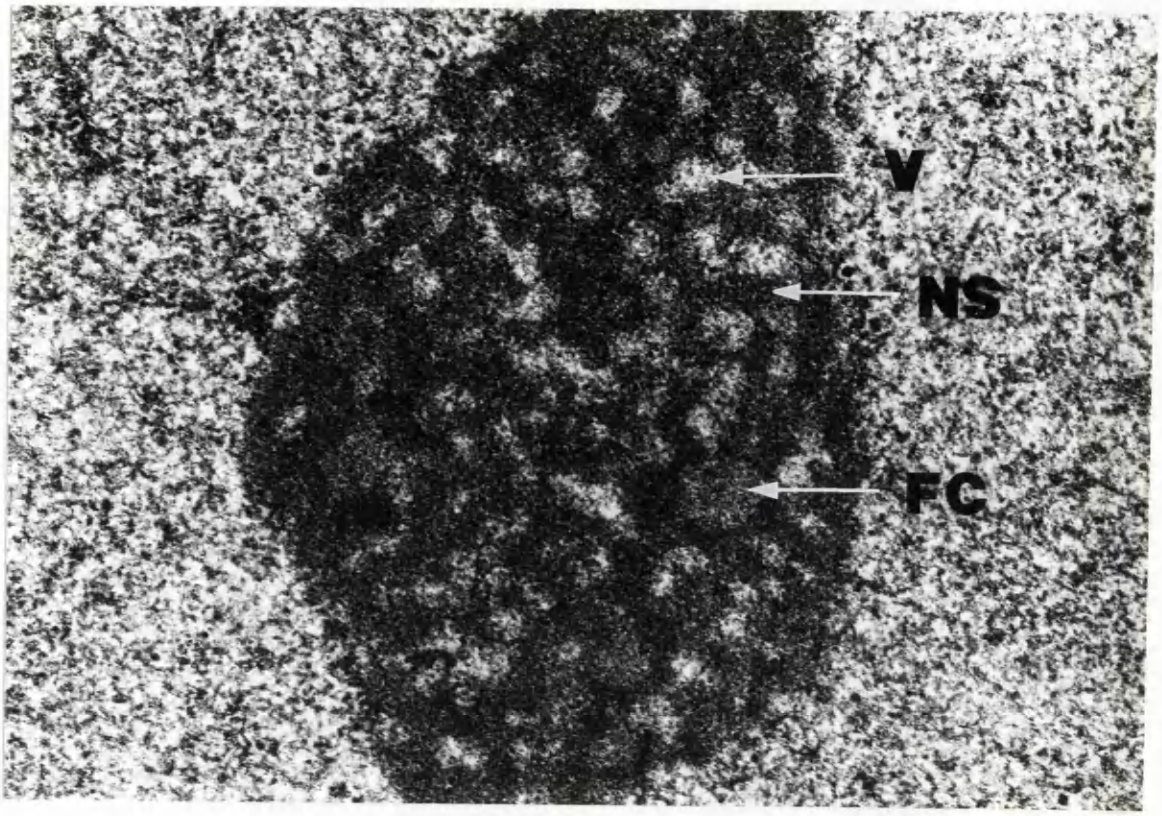
V
NS
FC

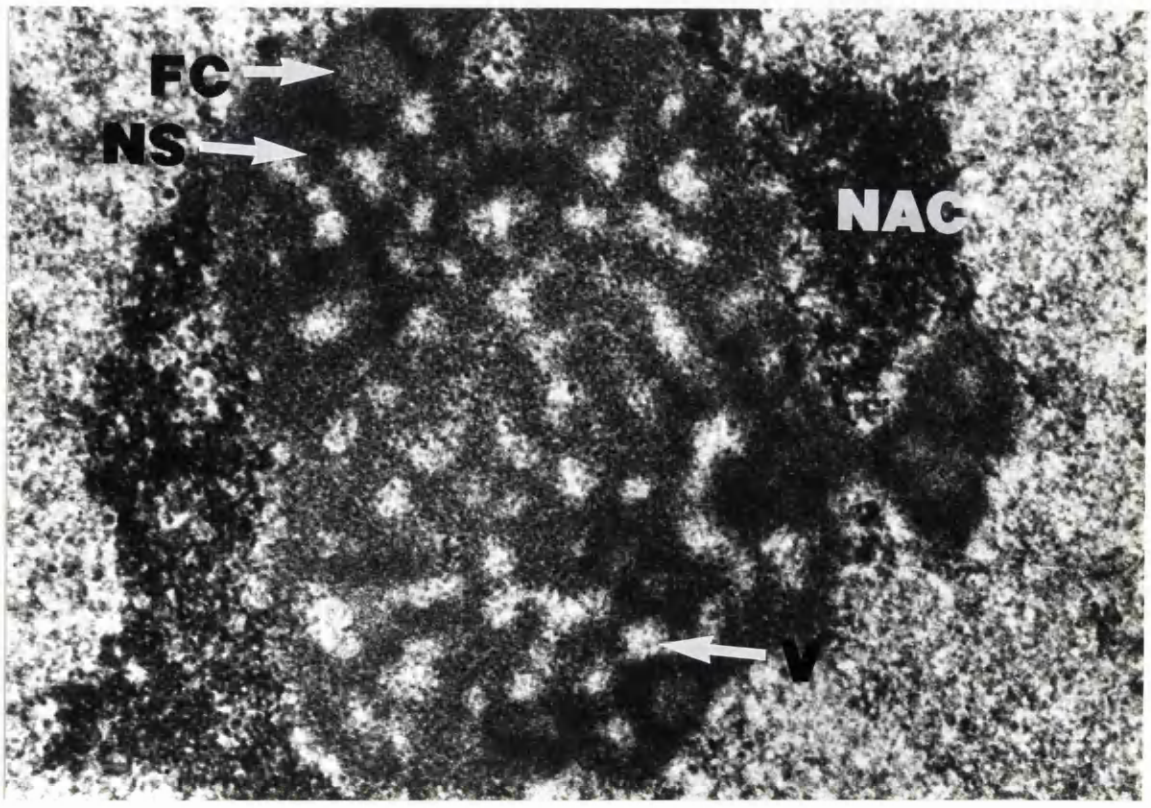
FC
NS
NAC
V

FIGURE 40

Control retina

The retinal glial cells:

A TEM micrograph of the ganglion cell layer cut tangentially showing a portion of the microglia (MG), astrocytic process (AP), Müller cell process (MP). Astrocytic processes are cut longitudinally. Astrocytic processes contain intermediate glial fibrils and ensheath the nerve fibres (NF) and cells of the ganglionic layer. Müller cell processes (MP) are cut transversely and appear round and darker.

(Mags. x 14,000).

FIGURE 41

Control retina

A microglia cell:

A TEM micrograph showing a microglial cell (MG), Müller cell process (MP) and astrocytic process (AP). The microglial cell (MG) is characterized by the presence of clumps of hetro-chromatin in the nucleus, and a thin rim of cytoplasm around the nucleus.

(Mags. x 14,000)

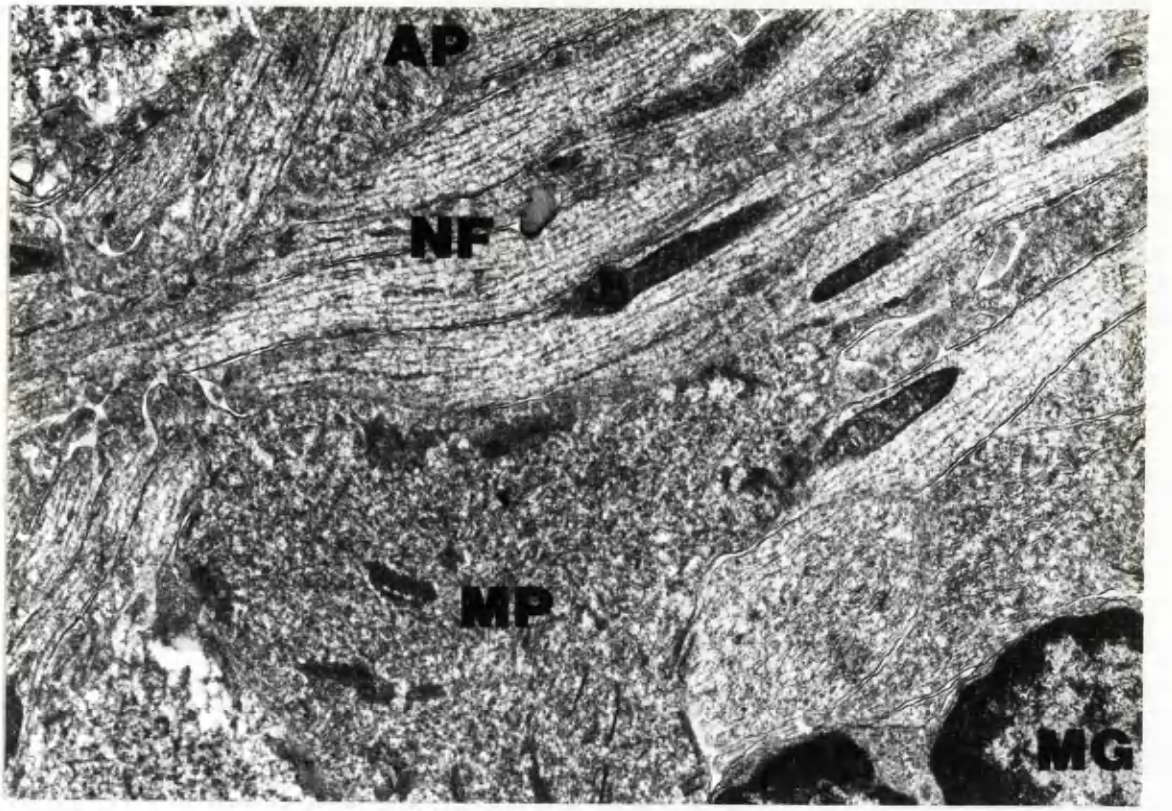
AP
NF
MP
MG

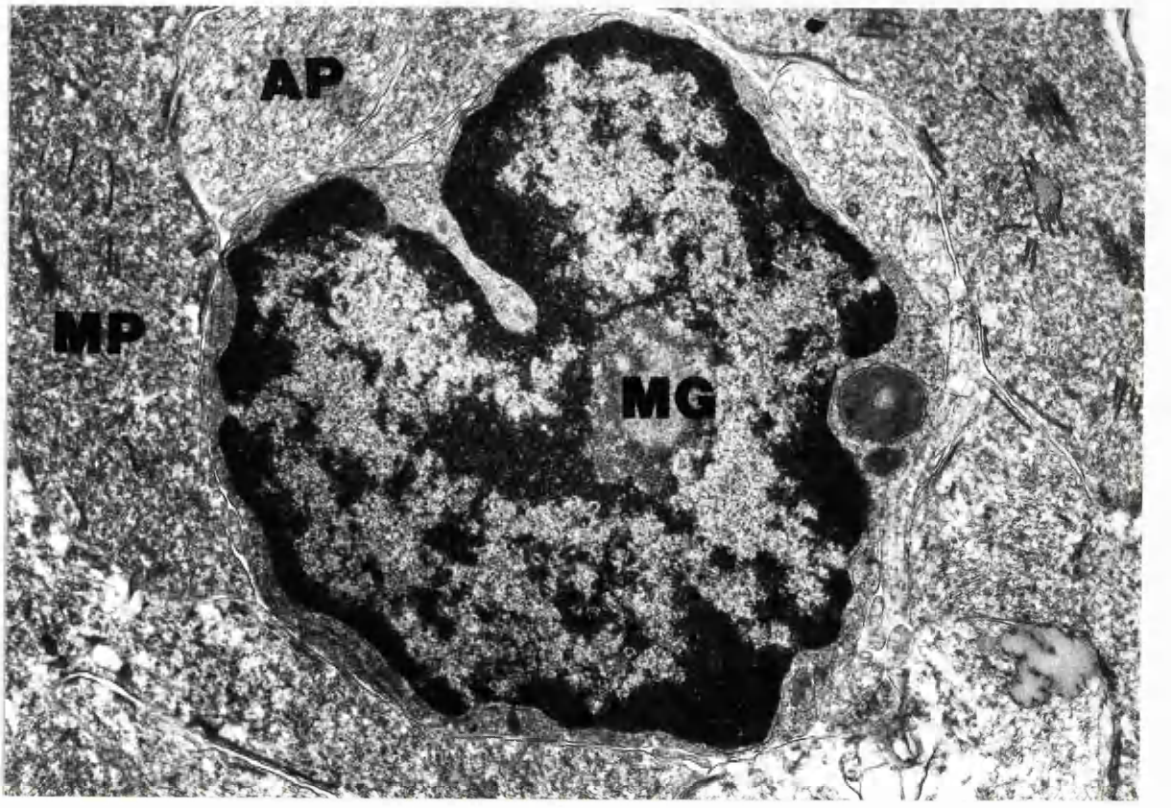
AP
MP
MG

FIGURE 42

Seven days post-trauma

The retinal glial cell:

A TEM micrograph of the ganglion cell layer cut tangentially showing a microglial cell (MG), neural processes and electron dense, round Müller cell processes (MP). The nucleus of the microglia contains peripheral clumps of hetrochromatin and a central electron-lucent area, AP - astrocytic process.

(Mags. x 19,500)

FIGURE 43

Seven days post trauma

A migroglia cell:

A TEM micrograph showing a reactive, enlarged microglia cell. The cytoplasm contains foreign material (arrows).

(Mags. x 16,800)

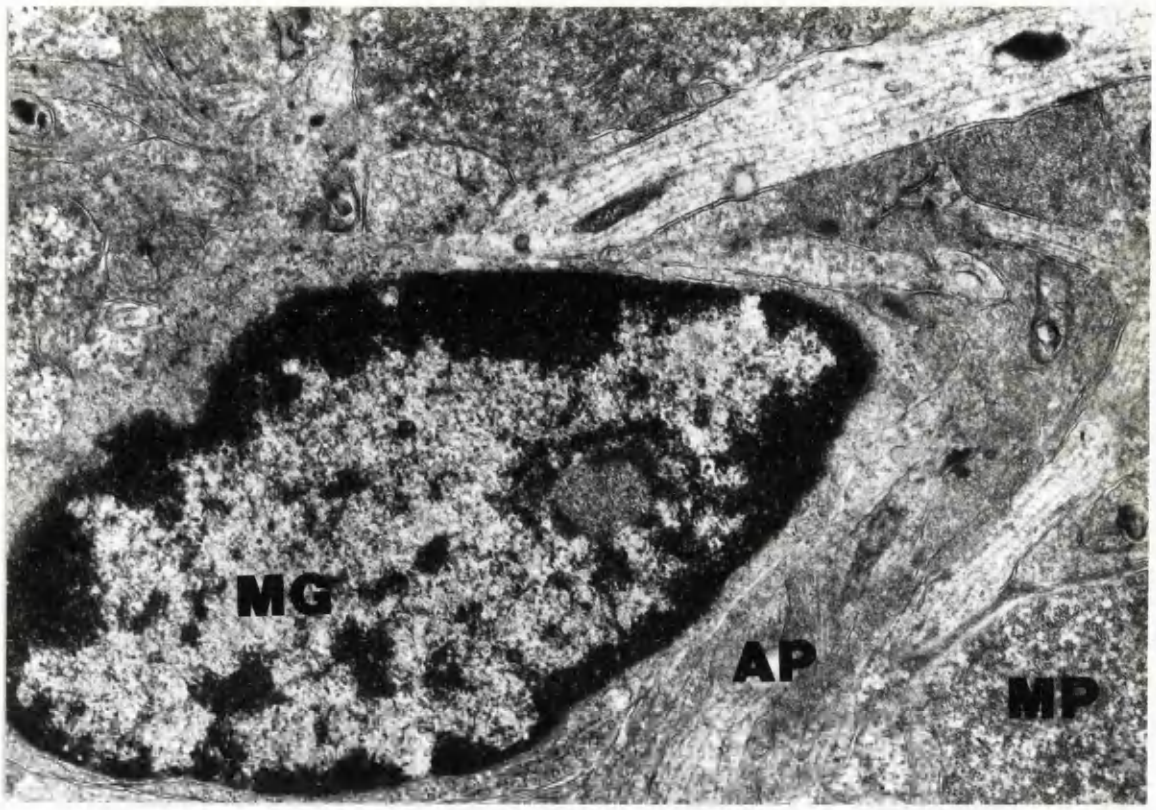
MG
AP
MP

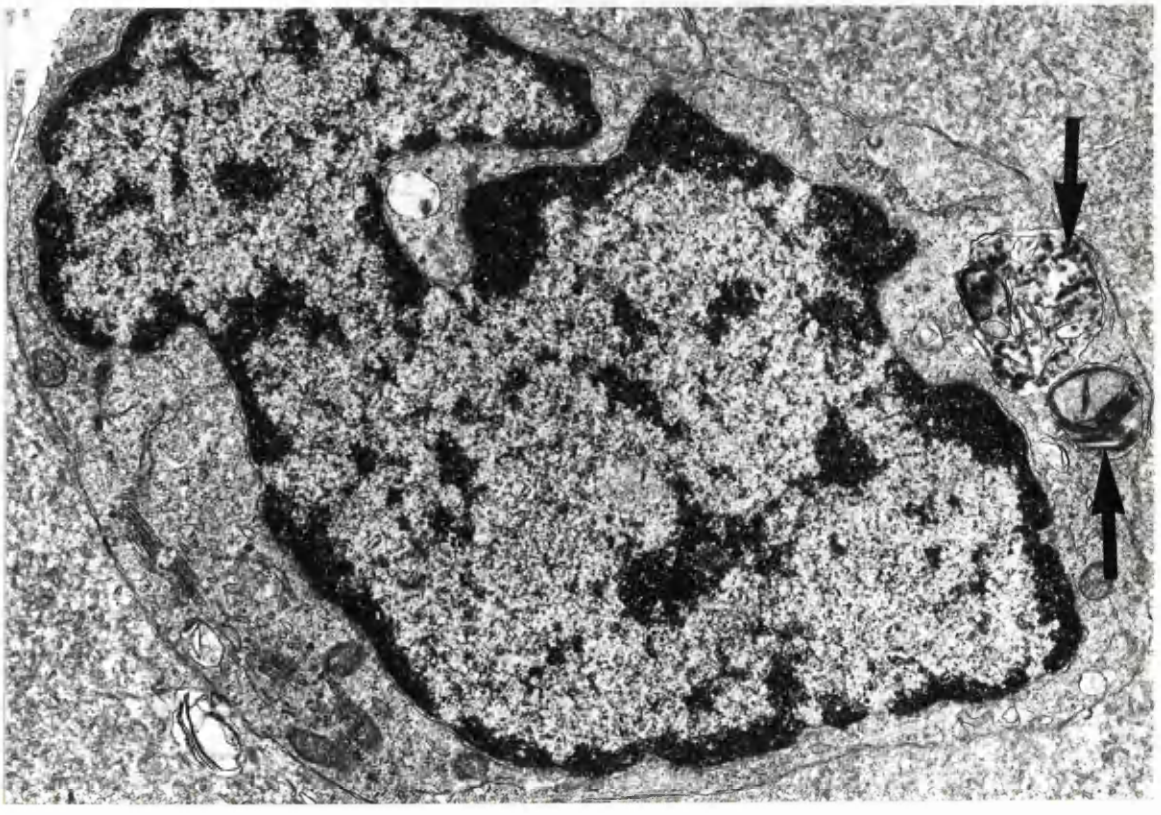

FIGURE 44

Fourteen days post-trauma

The retinal glial cell:

A TEM micrograph showing an enlarged reactive microglial cell (MG) with surrounding proliferated astrocytic cell processes (AP) and Müller cell processes (MP).

(Mags. x 15,300)

FIGURE 45

Fourteen days post-trauma

A microglia cell:

A TEM micrograph showing an enlarged reactive microglial cell. The cytoplasm is loaded with engulfed substance (arrow) and lipid inclusions (arrowheads). It also contains large mitochondria (m) and lysosome (Ly).

(Mags. x 14,000)

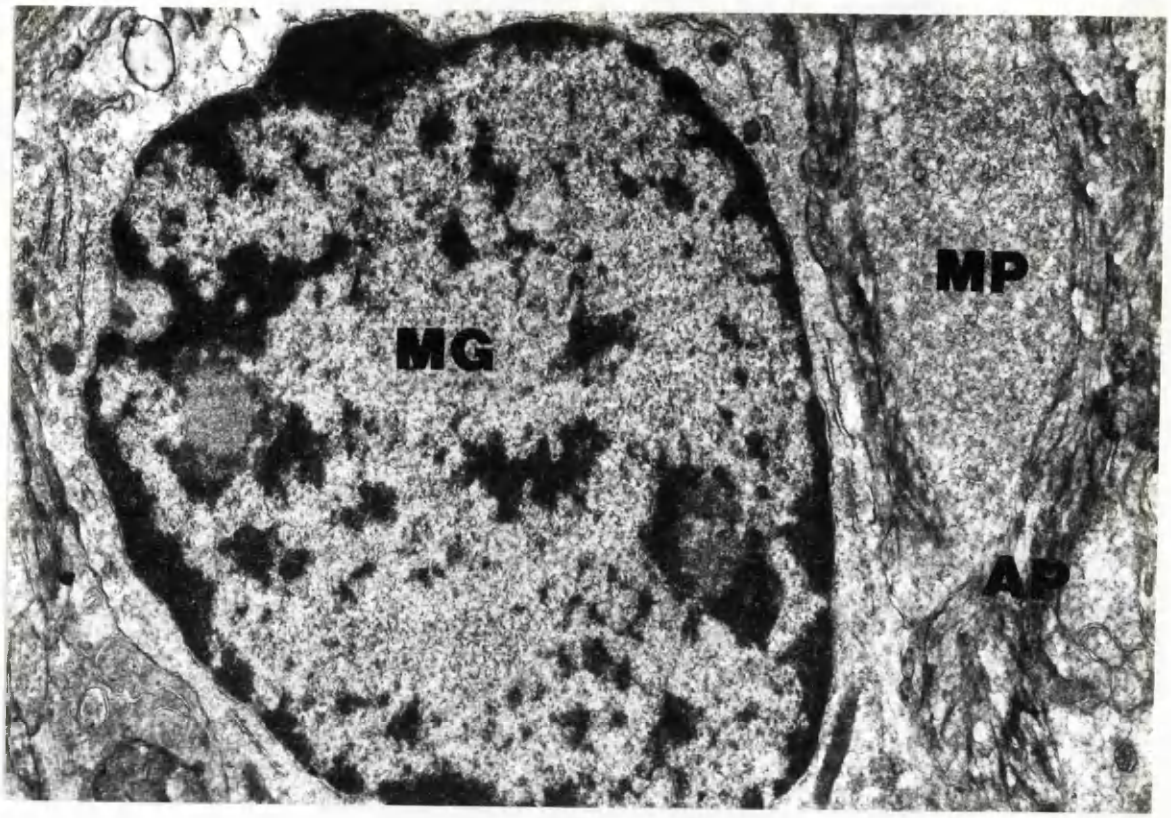
MG
MP
AP

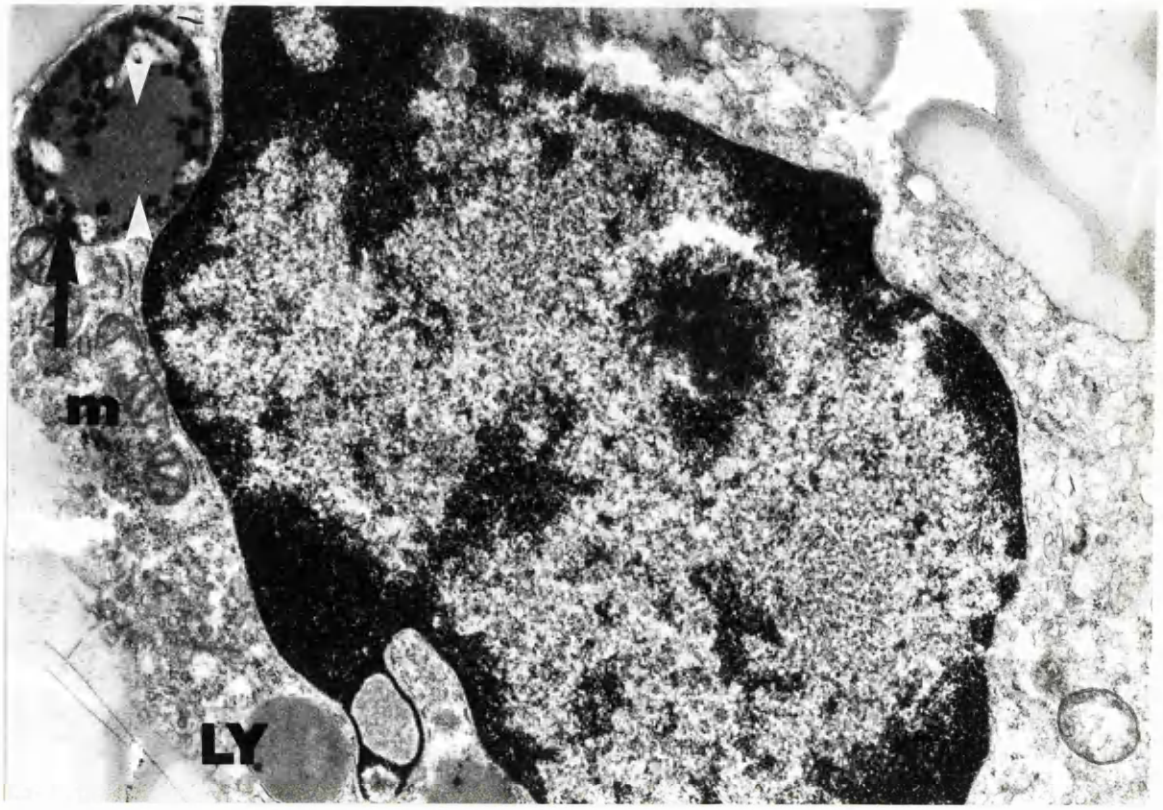
m
LY

FIGURE 46

Control retina

An SEM photograph showing the normal cyto-architecture of the retina. The ganglion cell layer (GCL) contains ganglion cells ensheathed by Müller cell processes.

(Mags. x 650)

FIGURE 47

Control retina

An SEM photograph of the outlined area marked of Figure 46 at higher magnification showing a ganglion cell (GC), gaps for ganglion cells (*) Müller cell processes (MP), and the inner plexiform layer (IPL). The end feet of the Müller cell processes ensheath the ganglion cell (GC) and then broaden to form part of the inner limiting membrane.

(Mags. x 2,700)

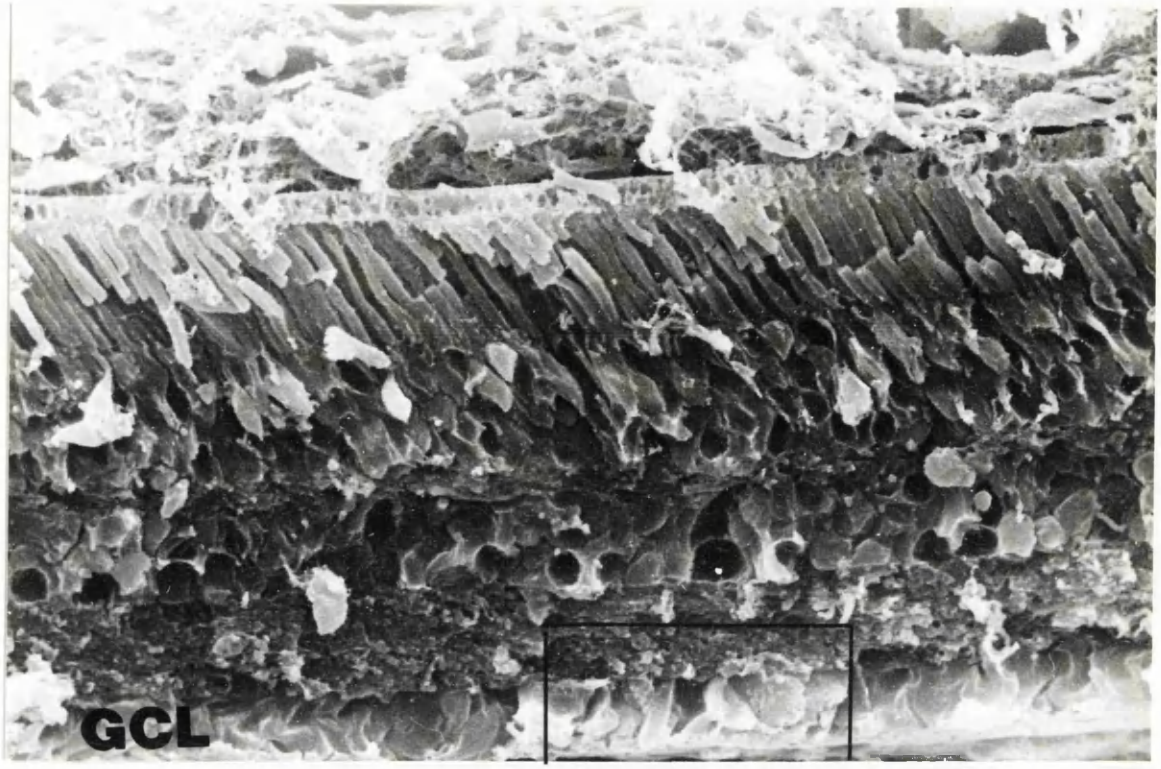
GCL

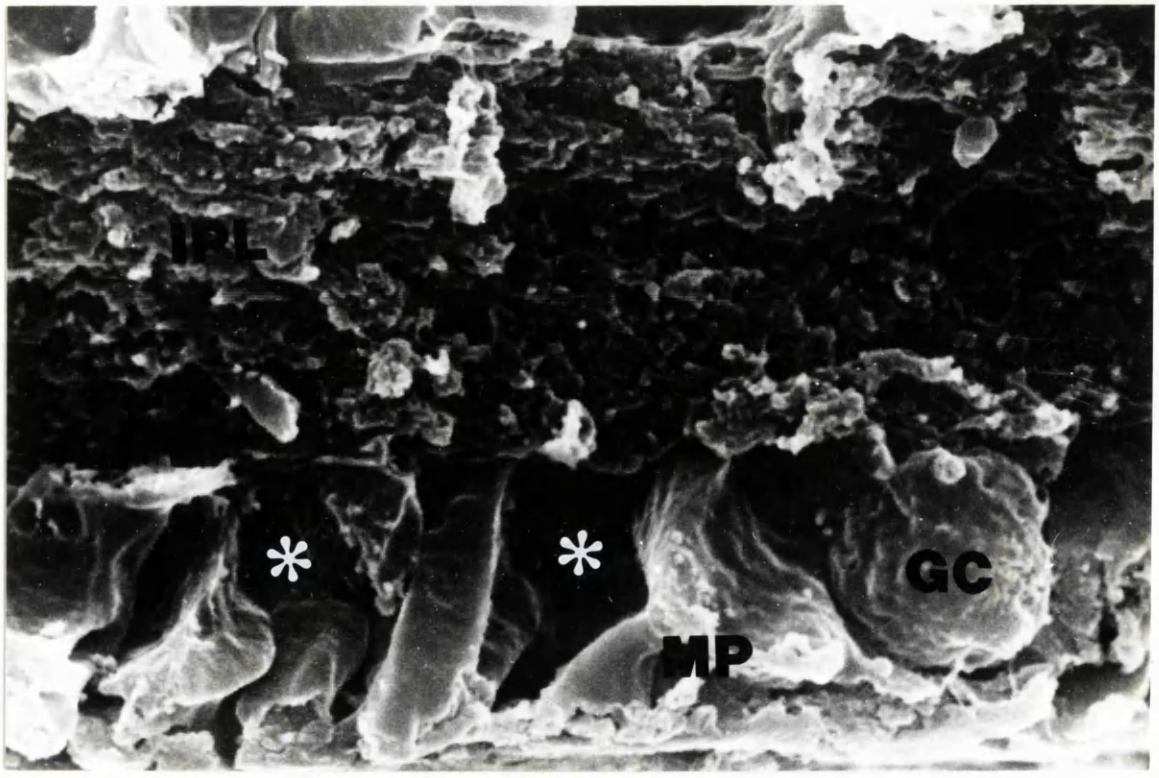
IPL
*
*
GC
MP

FIGURE 48

Experimental retina

Fourteen days after injury:

An SEM photograph of retina showing the altered form of the ganglion cell layer (GCL) which contains a few atrophied ganglion cells or gaps where ganglion cells have been removed during vibrotome sectioning. There is a proliferation of Müller cell processes.

(Mags. x 650)

FIGURE 49

Fourteen days after injury

Experimental retina:

An SEM photograph of the outlined area of Figure 48 at higher magnification, showing the atrophied ganglion cells (GC), proliferated Müller cell processes (MP), nerve fibre layer (NFL) and inner plexiform layer (IPL), * - gaps for ganglion cells; ILM - inner limiting membrane.

(Mags. x 2,750)

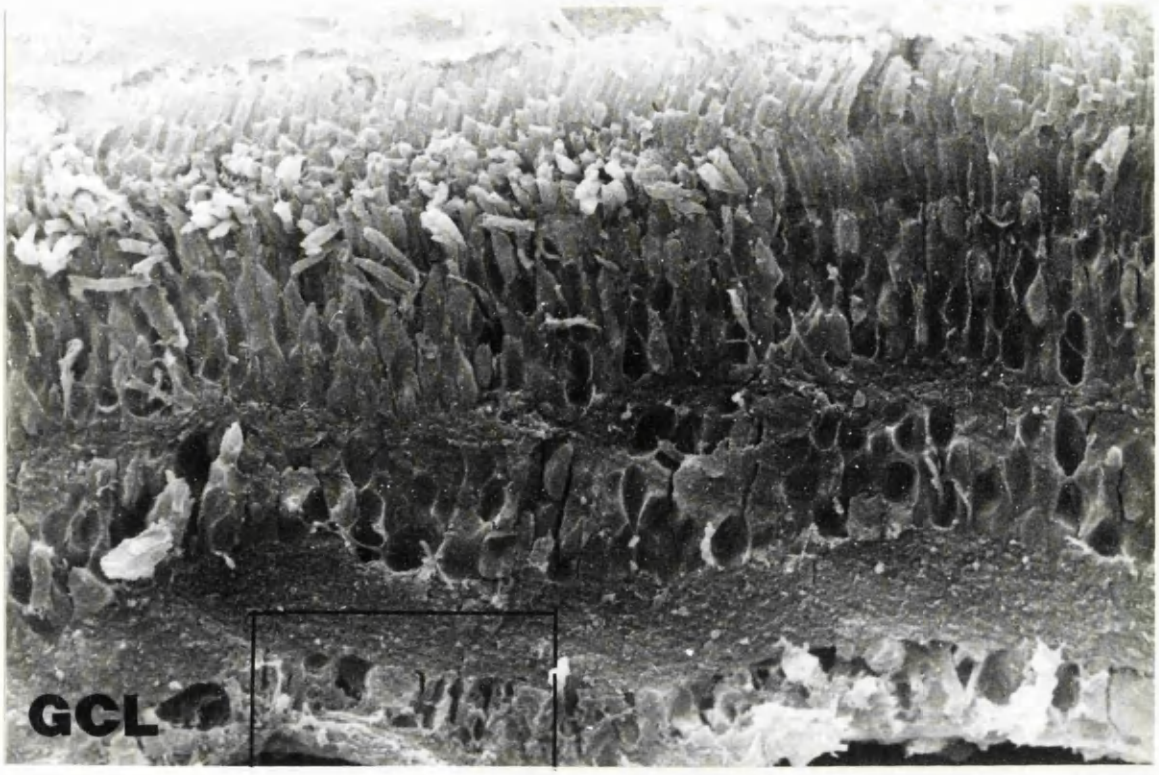
GCL

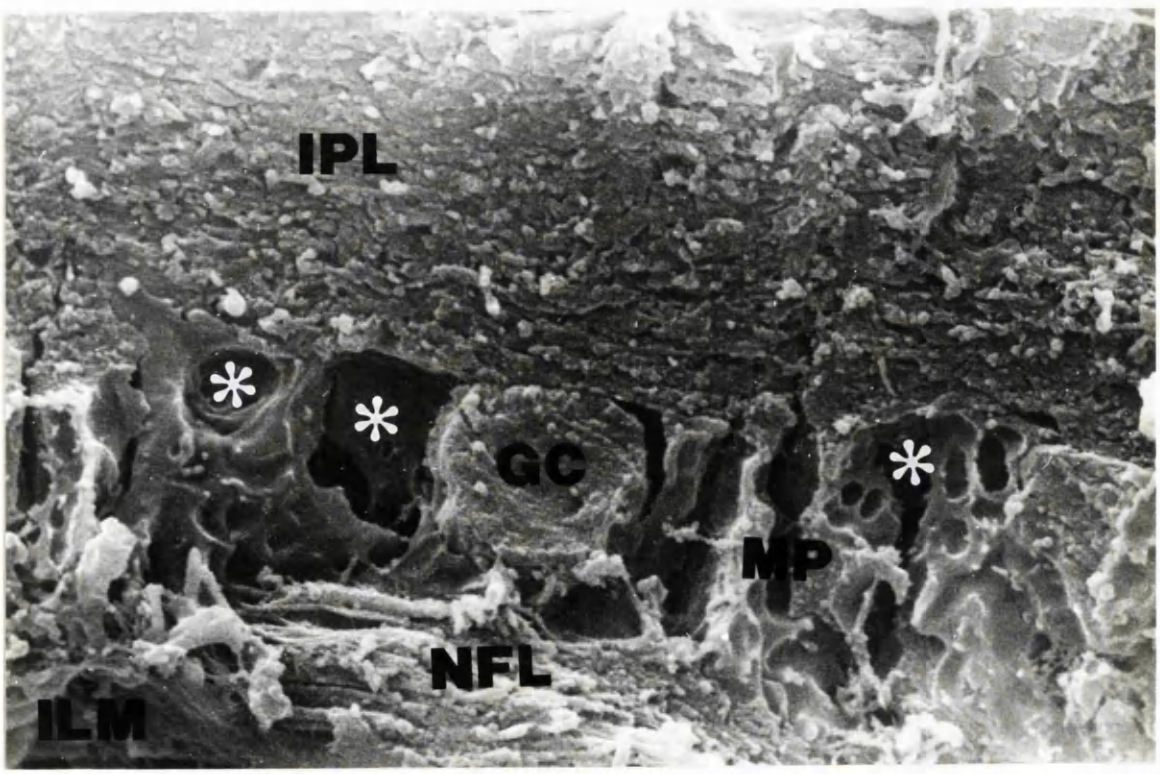
IPL
GC
MP
NFL
ILM

FIGURE 50

Control retina

A high magnification SEM photograph showing a ganglion cell (GC), ensheathed by normal Müller cell processes (MP) which broaden to form the inner limiting membrane. In the upper part of the photograph the inner plexiform layer (IPL) may be seen (MP).

(Mags. x 2,700)

FIGURE 51

Fourteen days after injury

Experimental retina

An SEM photograph showing atrophied ganglion cells (GC) and proliferated Müller cell processes (MP) in the ganglion cell layer. The inner plexiform layer (IPL) of the retina is also seen.

(Mags. x 2,800)

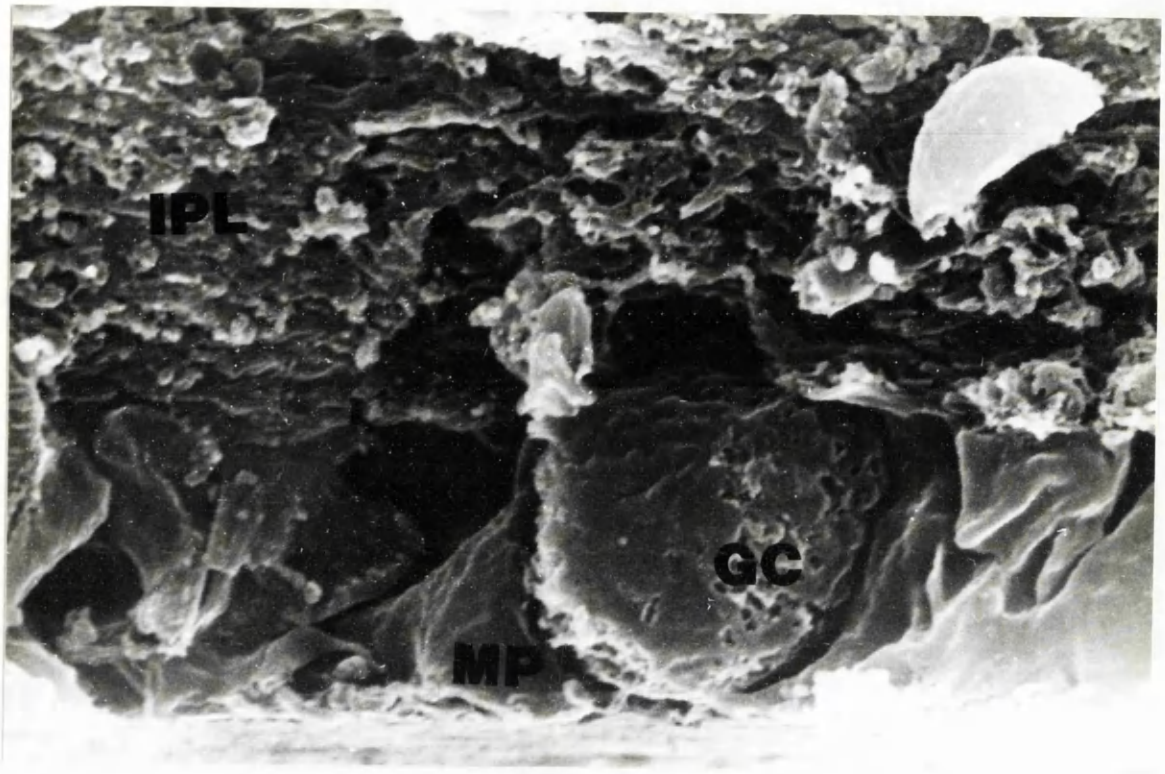
IPL
GC
MP

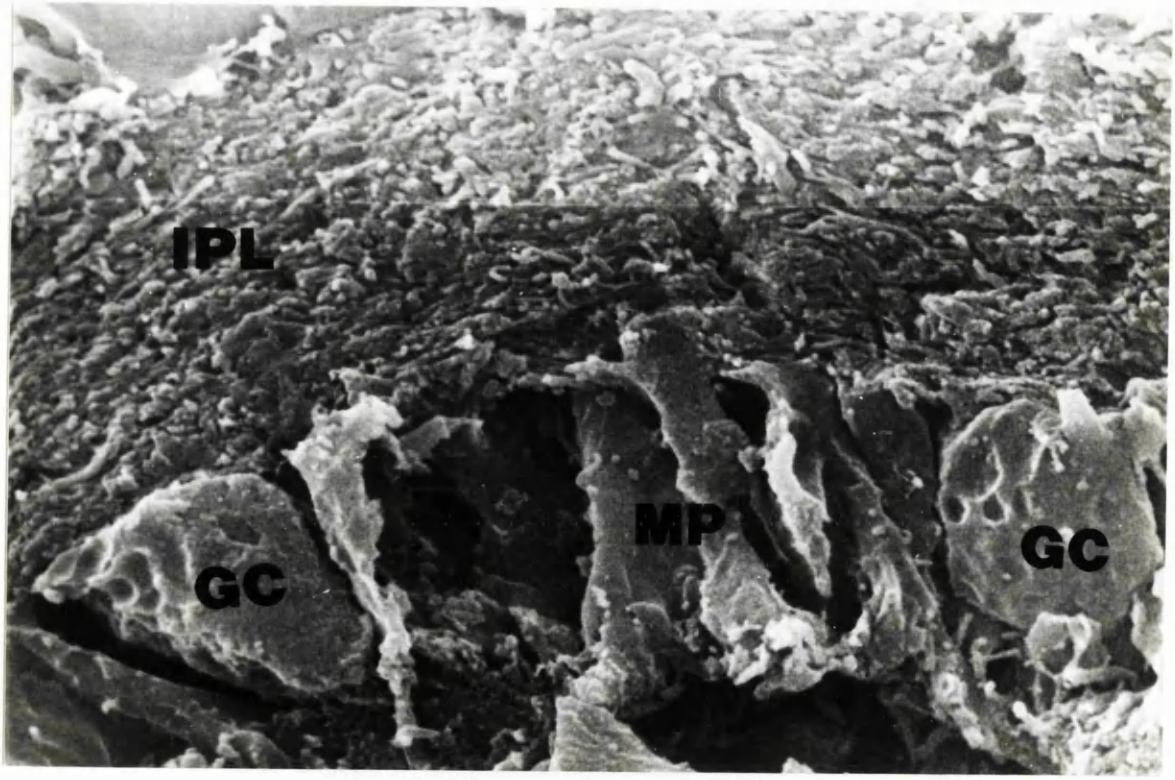
IPL
GC
MP
GC

FIGURE 52

A graph showing comparison of the somal cross-sectional areas in square micrometers (gangsoma) for control (con), fourteen day degenerating (deg) and regenerating (reg), seven day degenerating (deg) and regenerating (reg), and chromatolytic (three) ganglion cells; three, seven and fourteen days after stretch injury to the optic nerve. All figures show means plus/minus 95% confidence limits.

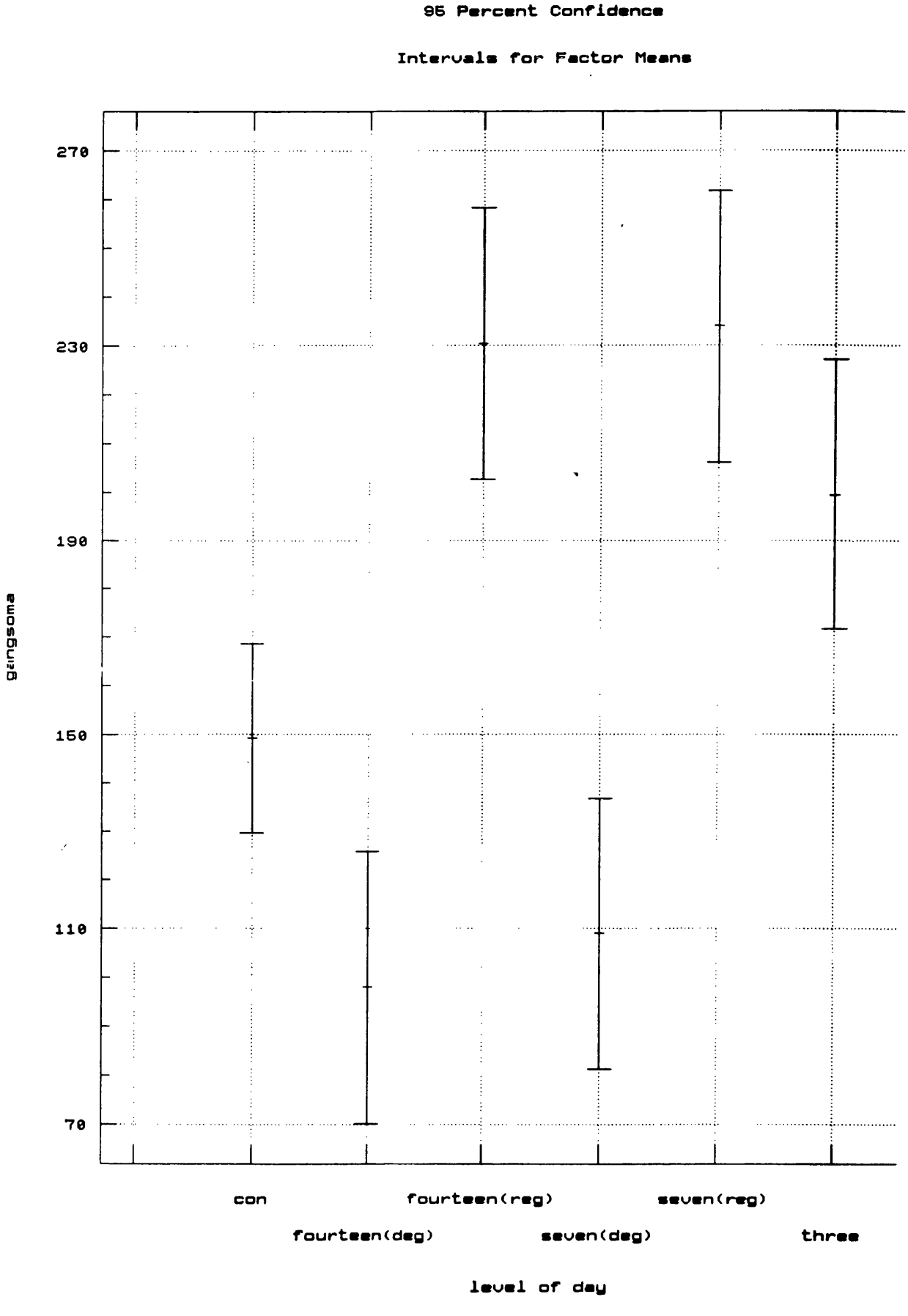
95 Percent Confidence
Intervals for Factor Means
270
230
190
150
110
70
gingsoma
con
fourteen(deg)
fourteen(reg)
seven(deg)
seven(reg)
three
level of day

FIGURE 53

A graph showing comparison of the nuclear cross-sectional area in square micrometers (gangna) for control (con), fourteen day degenerating (deg) and regenerating (reg), seven day degenerating (deg) and regenerating (reg), and chromatolytic (three) ganglion cells: three, seven and fourteen days after stretch injury to the optic nerve. All figures show means plus/minus 95% confidence limits.

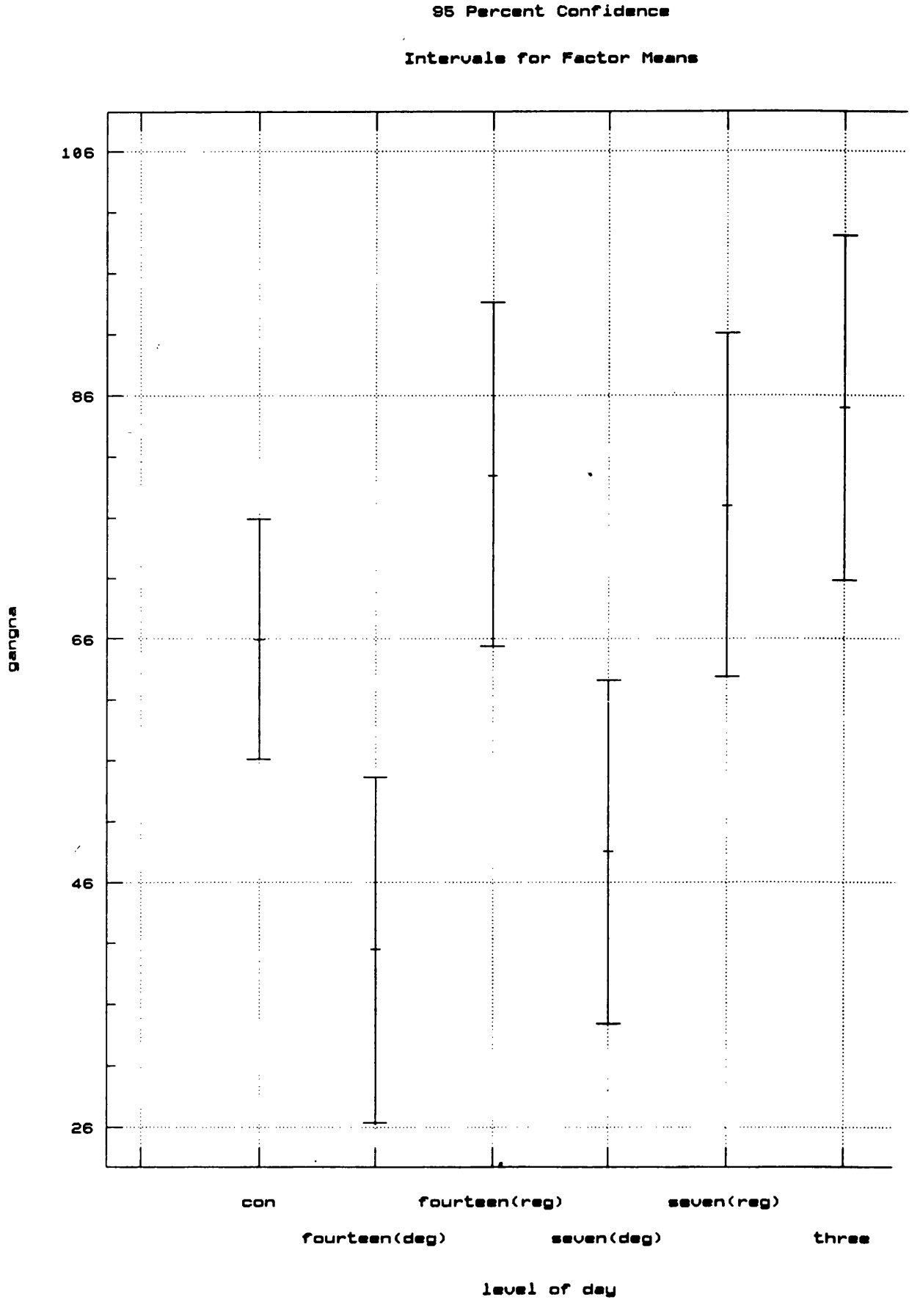
95 Percent Confidence
Intervals for Factor Means
106
86
66
46
26
ganga
con
fourteen(deg)
fourteen(reg)
seven(deg)
seven(reg)
three
level of day

FIGURE 54

A graph showing comparison of the nucleolar cross-sectional area in square micrometers (gangnu) for control (con), fourteen day degenerating (deg) and regenerating (reg), seven day degenerating (deg) and regenerating (reg) and chromatolytic (three) ganglion cells; three, seven and fourteen days after stretch injury to the optic nerve. All figures show means plus/minus 95% confidence limits.

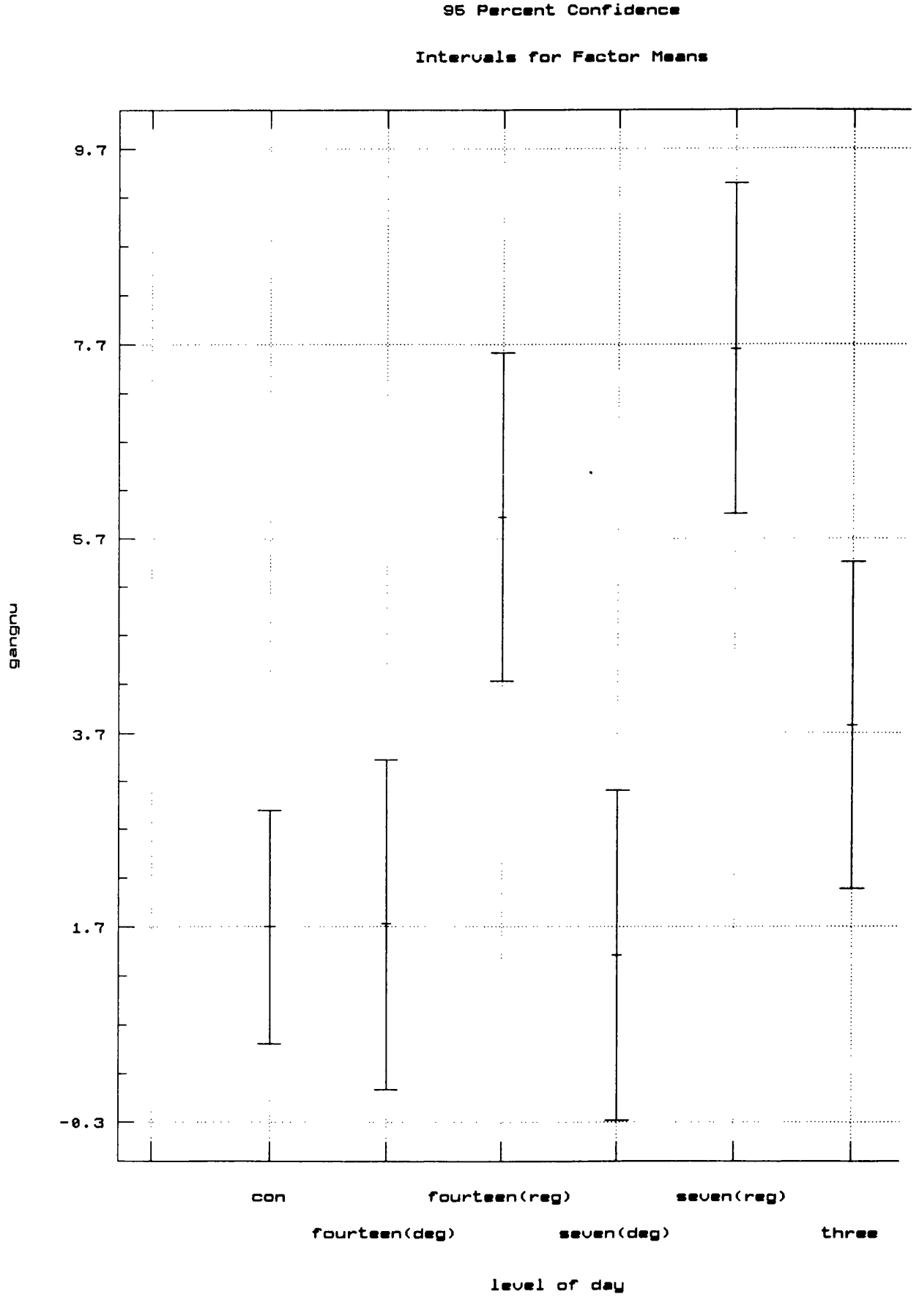
95 Percent Confidence
Intervals for Factor Means
9.7
7.7
5.7
3.7
1.7
-0.3
gangnu
con
fourteen(deg)
fourteen(reg)
seven(deg)
seven(reg)
three
level of day

FIGURE 55:

A graph showing comparison of nucleolar fractional area expressed as a percentage of nuclear area (gangnufr) in control (con), degenerating (deg), regenerating (reg) and chromatolytic (three) ganglion cells three, seven and fourteen days after stretch injury to the optic nerve. All figures show means plus/minus 95% confidence limits.

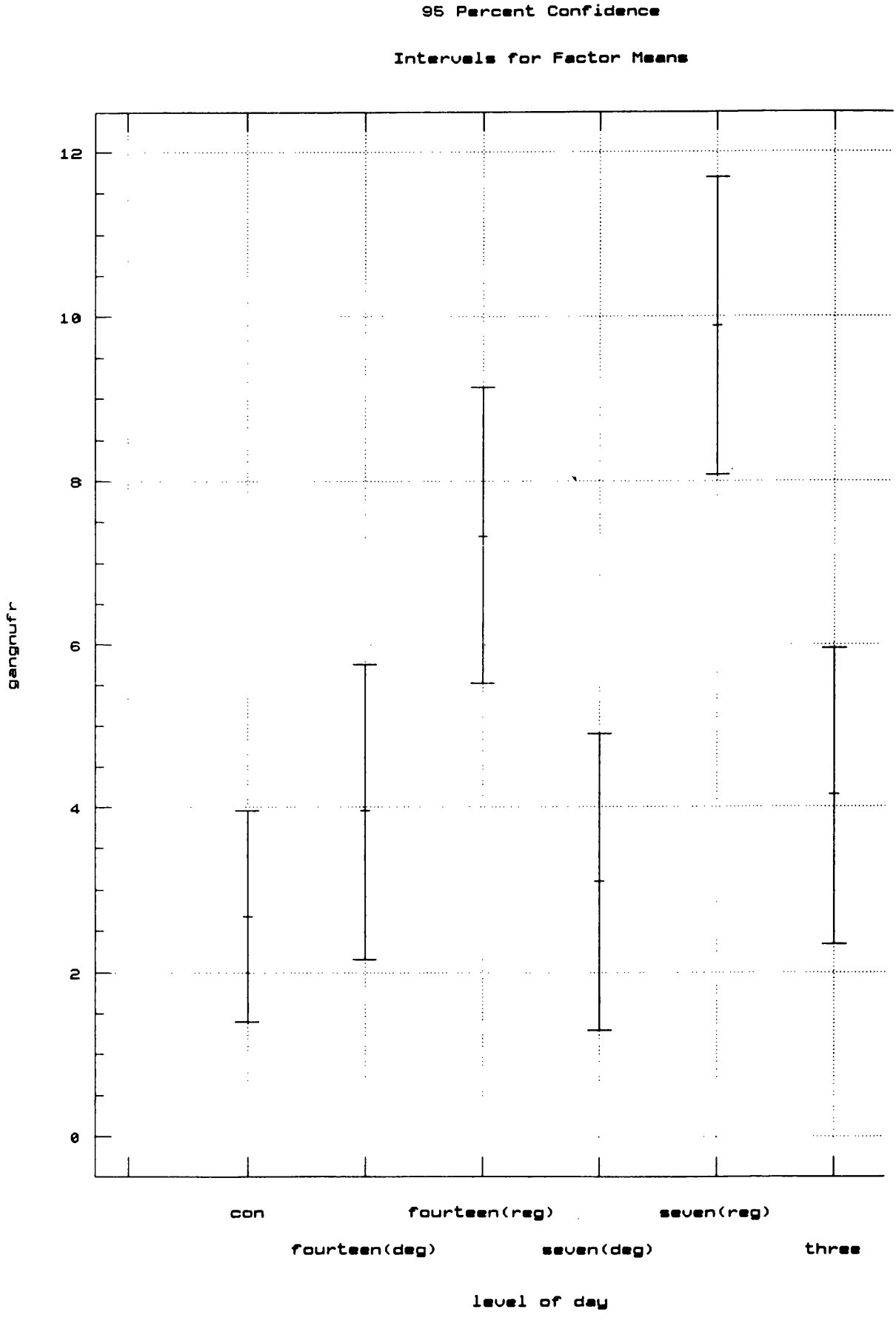
95 Percent Confidence
Intervals for Factor Means
gangnufr
12
10
8
6
4
2
0
con
fourteen(deg)
fourteen(reg)
seven(deg)
seven(reg)
three
level of day

FIGURE 57:

A graph showing comparison of the nuclear cross-sectional area of small neurons (snna) in square micrometers in control eyes and experimental eyes from three, seven and fourteen days survival animals after stretch injury to the optic nerve. All figures show means plus/minus 95% confidence limits.

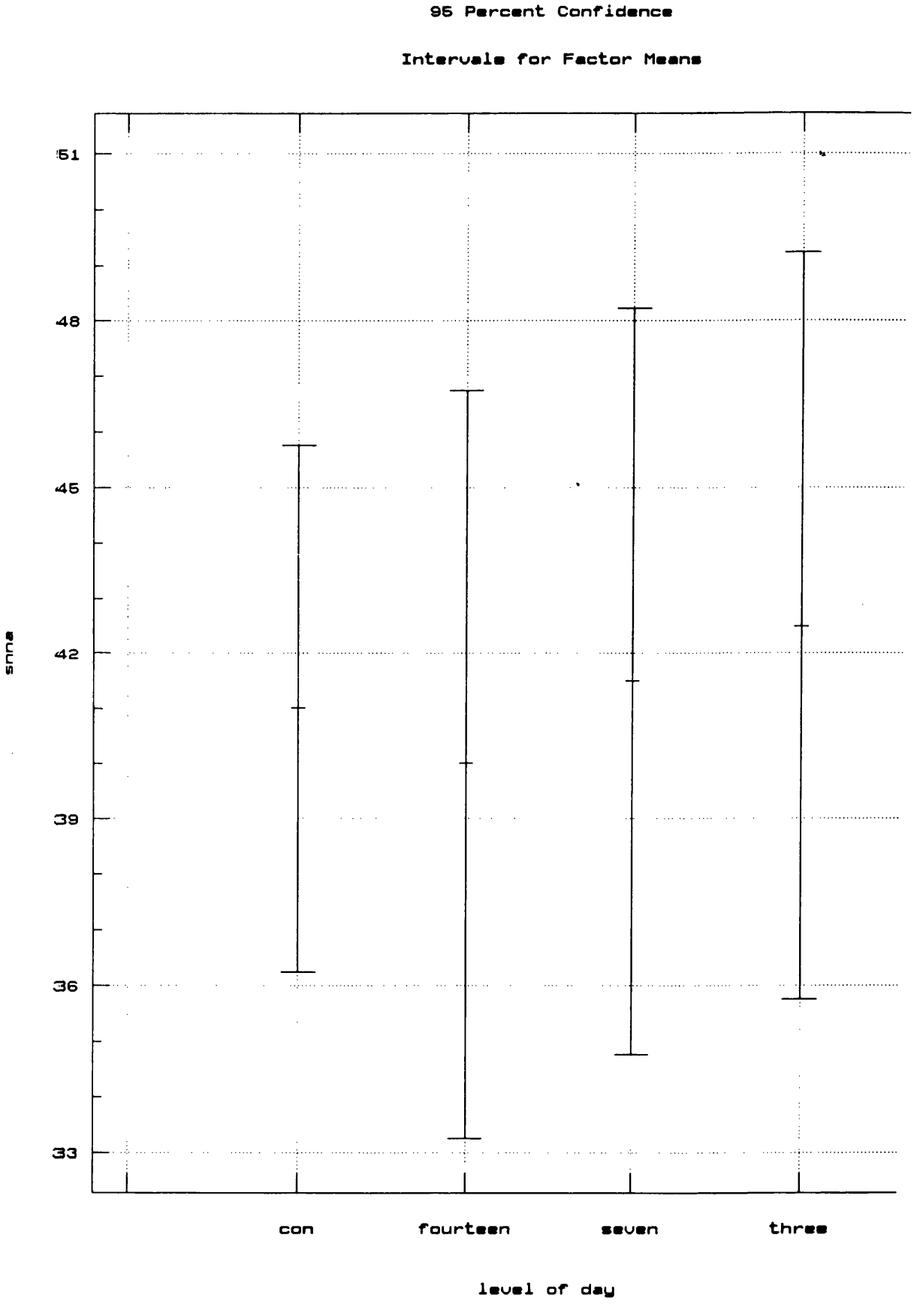
95 Percent Confidence
Intervals for Factor Means
51
48
45
42
39
36
33
means
con
fourteen
seven
three
level of day

FIGURE 58:

A graph showing comparison of the nucleolar cross-sectional area in the nucleus of small neurons (snnu) in square micrometers in control eyes and experimental eyes from three, seven and fourteen days survival animals after stretch injury to the optic nerve. All figures show means plus/minus 95% confidence limits.

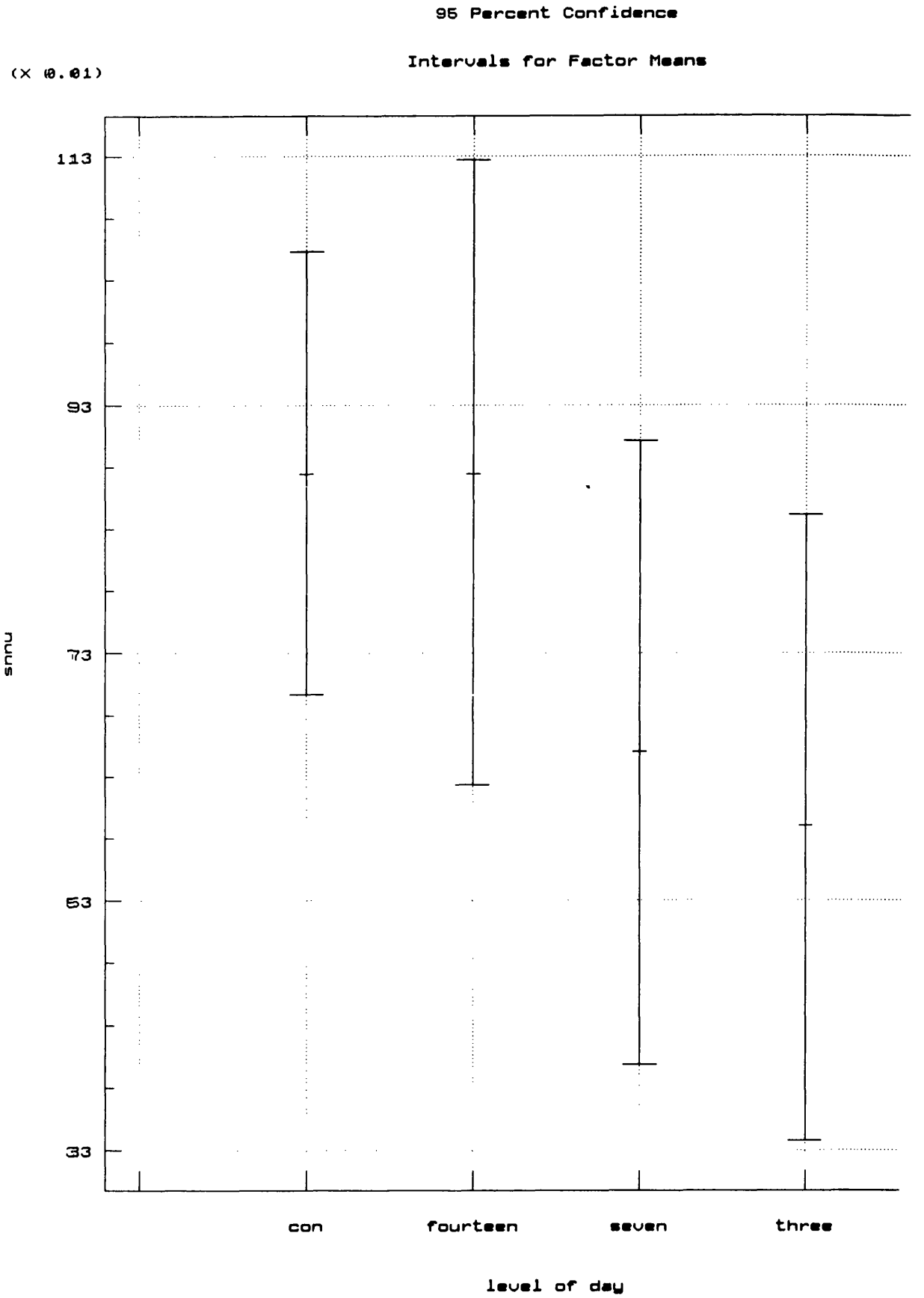
95 Percent Confidence
Intervals for Factor Means
(× 0.01)
113
93
73
53
33
mus
con
fourteen
seven
three
level of day

FIGURE 59:

A graph showing comparison of nucleolar fractional area expressed as a percentage of nuclear area in small neurons (snnufr) in control eyes and experimental eyes from three, seven and fourteen days survival animals after stretch injury to the optic nerve. All figures show means plus/minus 95% confidence limits.